

OPTIMISING THE PRODUCTION PROCESS OF WOOD'S ALLOY END-FRAMES FOR ELECTRON FIELD SHAPING IN RADIOTHERAPY

KARINA RIËTTE HEYDENRYCH (née FOURIE)

Dissertation submitted in fulfilment of the requirements for the degree:

MASTER OF ENGINEERING IN MECHANICAL ENGINEERING

in the

**DEPARTMENT OF MECHANICAL AND MECHATRONICS ENGINEERING
FACULTY OF ENGINEERING, BUILT ENVIRONMENT AND INFORMATION
TECHNOLOGY**

at the

CENTRAL UNIVERSITY OF TECHNOLOGY, FREE STATE

Supervisor: DR JG VAN DER WALT

Co-supervisor: DR FCP DU PLESSIS (UFS)

BLOEMFONTEIN

September 2019

Declaration of Independent Work

I, KARINA RIËTTE HEYDENRYCH, identity number _____ and student number _____, do hereby declare that this research project submitted to the Central University of Technology, Free State (CUT, BFN) for the degree MASTER OF ENGINEERING IN MECHANICAL ENGINEERING, is my own independent work; and complies with the Code of Academic Integrity, as well as other relevant policies, procedures, rules and regulations of the Central University of Technology, Free State, and has not been submitted before to any institution by myself or any other person in fulfilment of the requirements for the attainment of any qualification.

KR Heydenrych
SIGNATURE OF STUDENT

07 September 2019
DATE

Acknowledgements

I would like to acknowledge with gratitude the South African Medical Research Council who made a grant available under the Medical Device Innovation Platform initiative to support this research project.

A special thanks to Prof Herman Vermaak and Dr Gys Jacobs. Their support and action to retain me as part of the CUT team allowed me to finish this study.

I would like to express my gratitude to my supervisor Dr Kobus van der Walt who provided me with a great deal of knowledge, support and assistance throughout my research. Without him this study would not have been accomplished.

To my co-supervisor, Dr Freek du Plessis and his team at the Department of Medical Physics, UFS. Thank you for your help, advice and time taken to process radiation films used in the study and support with the dissertation.

Thank you to Mrs Jenny van Rensburg for reviewing the language of the dissertation and to Dr Jacques Combrinck for the help with the flow simulations, and the motivation to complete my research project.

I would like to thank my parents and my husband for the love, sacrifices, advice and assistance given whenever needed. Their encouragement and motivation in difficult times is much appreciated. Thank you to all my friends, family and colleagues not mentioned for their support and motivation in this endeavour.

Above all, I give thanks to God my Father for His continued empowerment and mercies that eventually saw this study to completion.

Abstract

Skin cancer is commonly treated by means of electron radiation generated by a linear electron accelerator (linac). The radiation applied must be limited or shaped to the size of the cancer-affected area on the patient. This is achieved through applicators that attach to the linac unit, while more precise field shaping is made possible through end-frames that fit into the front end of the applicators.

The end-frames are machined out of high-density metal such as lead or, as in recent years, cast in Wood's alloy. Commercial jigs used to cast the Wood's alloy present various shortcomings in terms of dimensional accuracy of the end-frames, density of the castings and high cost of the jigs.

The aim of this study was to develop a Wood's alloy casting unit that can be made available to local oncology units to produce end-frames that are superior to what can be achieved through commercial jigs. The development and manufacturing of the new casting equipment is described as well as experiments that were performed to evaluate the equipment by comparing end-frames produced to those that were cast in the commercial jig. Results of the experiments show that end-frames cast in the newly developed casting equipment are dimensionally accurate, have consistent high density and can be produced in a short timeframe.

Table of Contents

| | |
|---|----------|
| Declaration of Independent Work | ii |
| Acknowledgements | iii |
| Abstract | iv |
| Table of Contents | v |
| List of Figures | ix |
| List of Abbreviations | xiii |
| List of Units | xiv |
| Chapter 1: Introduction | 1 |
| 1.1 Introduction | 1 |
| 1.2 Problem Statement | 1 |
| 1.3 Aim of the Study | 2 |
| 1.3.1 Objectives | 3 |
| 1.4 Methodology | 4 |
| 1.5 Delimitations of the Study | 5 |
| 1.6 Flowchart | 5 |
| Chapter 2: Skin Cancer and Treatment Thereof | 7 |
| 2.1 Introduction | 7 |
| 2.2 Cancer: An Overview | 7 |
| 2.2.1 Types of Cancer | 8 |
| 2.2.1.1 Location Classification | 8 |
| 2.2.1.2 Histologic Classification | 8 |
| 2.3 Skin | 9 |
| 2.3.1 Hypodermis | 9 |
| 2.3.2 Dermis | 10 |

| | |
|---|-----------|
| 2.3.3 Epidermis | 10 |
| 2.4 Skin Carcinomas | 11 |
| 2.4.1 Types of Skin Carcinoma | 12 |
| 2.4.1.1 Basal Cell Carcinoma | 12 |
| 2.4.1.2 Squamous Cell Carcinoma | 12 |
| 2.4.1.3 Melanoma | 12 |
| 2.5 Treatment of Skin Carcinomas | 13 |
| 2.5.1 Surgery | 13 |
| 2.5.1.1 Excision Surgery | 13 |
| 2.5.1.2 Cryosurgery | 14 |
| 2.5.1.3 Curettage and Electro-cautery | 14 |
| 2.5.1.4 Mohs Micrographic Surgery | 14 |
| 2.5.1.5 Wide Local Excision | 15 |
| 2.5.1.6 Lymph Node Removal | 15 |
| 2.5.2 Chemotherapy | 15 |
| 2.5.3 Immunotherapy | 16 |
| 2.5.4 Photodynamic Therapy | 17 |
| 2.5.5 Radiation Therapy | 17 |
| Chapter 3: Radiation Therapy and Field Shaping | 19 |
| 3.1 Introduction | 19 |
| 3.2 Working Principles of a Linac | 20 |
| 3.3 Radiation Field Collimation | 23 |
| 3.3.1 Multileaf Collimators | 23 |
| 3.3.2 Electron Applicators | 24 |
| 3.4 Fabricating End-frames for Electron Field Shaping | 26 |
| 3.4.1 Lead End-frames | 26 |
| 3.4.2 Wood's Alloy End-frames | 27 |
| Chapter 4: End-frame Casting Jig Development | 32 |
| 4.1 Introduction | 32 |
| 4.2 Preliminary Development of a Casting Jig | 33 |

| | | |
|---|---|-----------|
| 4.2.1 | Material Expansion | 33 |
| 4.2.1.1 | First Jig-Frame Design | 34 |
| 4.2.1.2 | Second Jig-Frame Design | 34 |
| 4.2.2 | Cold Shunts and Shrinkage Cavities | 36 |
| 4.2.2.1 | First Heating/Cooling Block Design | 37 |
| 4.2.2.2 | Second Heating/Cooling Block Design | 37 |
| 4.3 | Optimising the Casting Jig | 40 |
| 4.3.1 | Casting-frames | 40 |
| 4.3.2 | Cooling Base | 42 |
| 4.3.2.1 | Cooling Channels | 42 |
| 4.3.2.2 | Binary Coding | 49 |
| 4.3.2.3 | Casting-frame Location | 49 |
| 4.3.2.4 | Locating Pins | 51 |
| 4.3.3 | Heating and Cooling of Base | 51 |
| 4.3.3.1 | Hot Water Supply | 51 |
| 4.3.3.2 | Cold Water Supply | 52 |
| 4.3.3.3 | Hot-to-Cold-Water Switch | 52 |
| 4.3.4 | Casting Unit | 54 |
| Chapter 5: Evaluation of Cast End-frames | | 58 |
| 5.1 | Introduction | 58 |
| 5.2 | Dimensional Accuracy Comparison | 59 |
| 5.2.1 | Commercial Jig End-frame Expansion Data | 61 |
| 5.2.2 | Newly Developed Jig End-frame Expansion Data | 64 |
| 5.3 | Cooling Rate Comparison | 68 |
| 5.3.1 | Slow Cool in the Commercial and Newly Developed Jig | 69 |
| 5.3.2 | Slow and Fast Cool in Newly Developed Jig | 70 |
| 5.4 | Density Comparison | 71 |
| 5.5 | Cost Comparison | 78 |
| Chapter 6: Conclusion | | 79 |
| 6.1 | Conclusion | 79 |

| | |
|-----------------|------------|
| 6.2 Future Work | 81 |
| References | 83 |
| Appendix A | 92 |
| Appendix B | 96 |
| Appendix C | 100 |
| Appendix D | 104 |
| Appendix E | 108 |
| Appendix F | 117 |
| Appendix G | 125 |
| Appendix H | 128 |
| Appendix I | 129 |

List of Figures

| | |
|---|----|
| Figure 1.1: Flowchart to illustrate the dissertation structure | 6 |
| Figure 2.1: Representation of the layers of the skin [15] | 9 |
| Figure 2.2: Representation of the epidermis, adapted from [18] | 10 |
| Figure 3.1: Block layout of a typical Linac, adapted from [66, p. 43] [67, p. 138] | 20 |
| Figure 3.2: Components within the treatment head for both electron or X-ray treatment mode, adapted from [66, p. 46] [67, p. 142] | 21 |
| Figure 3.3: Elekta™ SL25 linear electron accelerator at the National Hospital | 23 |
| Figure 3.4: Add-on multileaf collimator [78] | 24 |
| Figure 3.5: Elekta electron applicator at the National Hospital | 25 |
| Figure 3.6: Elekta electron applicator from [80] | 25 |
| Figure 3.7: Custom end-frame made for an electron applicator | 25 |
| Figure 3.8: Elekta electron beam shaping jig by Aktina Medical [85] | 27 |
| Figure 3.9: Elekta electron block mould set by RPDinc [86] | 28 |
| Figure 3.10: Siemens electron beam shaping system by Aktina [87] | 28 |
| Figure 3.11: Siemens electron block mould by RPDinc [88] | 28 |
| Figure 3.12: Varian insert frame for electron cone block by RPDinc [89] | 29 |
| Figure 3.13: Casting plate for Varian III electron cone insert frames by RPDinc [90] | 29 |
| Figure 3.14: Creating a polystyrene mould-block with a hot-wire cutter [81] | 29 |
| Figure 3.15: Solidification process [93] | 30 |
| Figure 3.16: Shrinkage cavity [94] | 30 |
| Figure 3.17: Cavities inside a cast Wood's alloy block | 31 |
| Figure 4.1: Schematic representation of development of improved end-frame casting equipment | 33 |
| Figure 4.2: Casting jig with repositionable strips | 34 |
| Figure 4.3: Pin for locating hole | 35 |
| Figure 4.4: Coding system | 35 |
| Figure 4.5: Simple steel cooling block | 37 |
| Figure 4.6: Second block design | 38 |
| Figure 4.7: Casting-jig setup | 38 |

| | |
|---|----|
| Figure 4.8: Infra-red images of cooling of the second block design taken at minute intervals | 39 |
| Figure 4.9: CAD rendering of casting-frame | 41 |
| Figure 4.10: Casting-frame after machining with quick-release clamps | 41 |
| Figure 4.11: Casting-frame kept in place with toggle clamps | 42 |
| Figure 4.12: Final concept of cooling channel layout | 43 |
| Figure 4.13: Bottom, middle and top layers of the final cooling base | 44 |
| Figure 4.14 a & b: Water flow direction through (a) the bottom and (b) the top layer of the base. | 44 |
| Figure 4.15: Direction of water flow in the base | 45 |
| Figure 4.16: Simulated results of the top surface cooling effect | 46 |
| Figure 4.17: Bottom and top layer machined from a 12 mm aluminium sheet | 47 |
| Figure 4.18: Manufactured base layers separated by a rubber gasket | 47 |
| Figure 4.19: IR images of the optimised cooling block at one-minute intervals | 48 |
| Figure 4.20: (a) CAD blank of M8 binary pin and (b) binary pins screwed into base | 49 |
| Figure 4.21: CAD representation of top surface of cooling base | 50 |
| Figure 4.22: CAD representation of casting-frame in position on cooling base | 50 |
| Figure 4.23: Manufactured cooling base with recess on top surface and casting-frame in position | 50 |
| Figure 4.24: Urn and pump | 52 |
| Figure 4.25: Diagram of pipe system for heating and cooling | 53 |
| Figure 4.26: CAD representation of casting unit | 54 |
| Figure 4.27: Manufactured casting unit | 55 |
| Figure 4.28: Jig-frame storage | 55 |
| Figure 4.29: Urn and pump system | 55 |
| Figure 4.30: Melting pot | 56 |
| Figure 4.31: Control panel | 56 |
| Figure 5.1: Flow diagram of experimental work performed | 58 |
| Figure 5.2: Illustration of end-frame border width | 60 |
| Figure 5.3: Jig (a) and end-frame (b) corresponding measurement map | 60 |
| Figure 5.4: Total expansion of all the rubber jig end-frames vs end-frame size | 61 |

| | |
|--|----|
| Figure 5.5: Total expansion vs end-frame border width for the 103 mm x 103 mm jig size. The average end-frame border widths are 17 mm, 37 mm and 52 mm which represent the solid cast | 62 |
| Figure 5.6: Total expansion vs end-frame border width for the 150 mm x 150 mm jig size. The average end-frame border widths are 16 mm, 31 mm and 76 mm which represent the solid cast | 62 |
| Figure 5.7: Total expansion vs end-frame border width for the 200 mm x 200 mm jig size. The average end-frame border widths are 15 mm, 35 mm and 99 mm which represent the solid cast | 63 |
| Figure 5.8: Total expansion of end-frames vs end-frame border width for all three rubber jigs with T indicating border width of end-frames with portals | 64 |
| Figure 5.9: Total expansion of all the new jig end-frames vs end-frame size | 65 |
| Figure 5.10: Total expansion vs end-frame border width for the 90 mm x 90 mm jig size. The average end-frame border widths are 15 mm, 30 mm and 45 mm which represent the solid cast | 66 |
| Figure 5.11: Total expansion vs end-frame border width for the 130 mm x 130 mm jig size. The average end-frame border widths are 20 mm, 30 mm and 65 mm which represent the solid cast | 66 |
| Figure 5.12: Total expansion vs end-frame border width for the 170 mm x 170 mm jig size. The average end-frame border widths are 20 mm, 40 mm and 85 mm which represent the solid cast | 67 |
| Figure 5.13: Total expansion of end-frames vs end-frame border width for all three newly developed jigs with T indicating border width of end-frames with portals | 68 |
| Figure 5.14: Cooling rate comparison between the commercial rubber jig and the new jig | 69 |
| Figure 5.15: Cooling comparison between fast and slow cooling of the new jig | 70 |
| Figure 5.16: Top and bottom surface of an end-frame cast on the commercial jig showing cavities | 72 |
| Figure 5.17: Top and bottom surface of a fast-cooled end-frame cast on the new jig | 72 |

| | |
|--|----|
| Figure 5.18: (a) Four end-frames exposed to electron radiation at isocentre with an applicator attached to unit and (b) settings on the linac during irradiation | 73 |
| Figure 5.19: Four end-frames placed on a Gafchromic film | 74 |
| Figure 5.20: (a) Gafchromic film after exposure to electron radiation and (b) processed film to highlight differences | 74 |
| Figure 5.21: (a) Gafchromic film placed at isocentre with two end-frames to be exposed and (b) settings on the linac during irradiation | 75 |
| Figure 5.22: End-frames sets exposed with the corresponding Gafchromic film and processed image to highlight difference in level of transmission | 77 |

List of Abbreviations

| | |
|--------|--|
| 3D | Three Dimensional |
| Al | Aluminium |
| BCC | Basal cell carcinoma |
| Bi | Bismuth |
| CAD | Computer-aided design |
| Cd | Cadmium |
| CNC | Computer numerical control |
| CUT | Central University of Technology |
| DNA | Deoxyribonucleic acid |
| EBRT | External beam radiation therapy |
| IR | Infra-red |
| Linac | Linear accelerator |
| MeV | Mega-electron-volt |
| MLC | Multileaf collimator |
| MMS | Mohs micrographic surgery |
| Pb | Lead |
| PDT | Photodynamic therapy |
| RF | Radiofrequency |
| RPDinc | Radiation Products Design Incorporated |
| SCC | Squamous cell carcinoma |
| Sn | Tin |
| UV | Ultraviolet |

List of Units

| | |
|--------|------------------------|
| °C | Degree Celsius |
| cm | centimetre |
| dpi | dots per inch |
| Gy/min | Gray per minute |
| kΩ | kilo-ohm |
| keV | kilo-electron-volt |
| kV | kilovolt |
| MeV | Mega-electron-volt |
| Min | Minute |
| mm | millimetre |
| MU | Monitor Unit |
| MV | Megavolt |
| V | Volt |
| W/mK | Watts per meter Kelvin |

Chapter 1: Introduction

1.1 Introduction

Cancer is a harsh reality, but thanks to advances in technology and knowledge gained in this field, the disease is not necessarily considered a death sentence anymore. Many patients now live five years or longer after diagnosis of cancer and experience improvement in the quality of their remaining years. The future in cancer treatment was never more hopeful than now for patients suffering from this much-feared disease. The fields of engineering and radiotherapy are brought together in this multi-disciplinary research project in an attempt to make a contribution towards treatment of this debilitating disease.

1.2 Problem Statement

Superficial cancerous lesions, such as skin cancer, are commonly treated by means of electron radiation in radiotherapy. The radiation field that is applied to the patient must be limited or shaped to the size of the cancer-affected area. This is achieved through different size applicators which attach to the treatment unit's radiation head. To further limit the field size, end-frames that fit into the end of the applicators are used.

End-frames for shaping electron beams in radiotherapy were traditionally manufactured from lead sheet but this was a labour-intensive process. Should these end-frames be damaged by dropping, for example, they were often impossible to repair and had to be reproduced. Most workshops at hospitals were also not equipped to recycle the lead resulting in environmentally unfriendly waste.

End-frames are now commonly manufactured by casting Wood's alloy into commercially available jigs. This technique, however, also presents some problems.

- The jigs are not available locally and have to be imported at high cost.
- The authors were also doubtful about the accuracy of end-frames that could be produced with the commercial jigs considering that rubber is used as a mould to cast the end-frame. Literature and preliminary experiments have shown that the Wood's alloy contracts and then expands while cooling thus affecting the final dimensions of the end-frame.
- After casting the end-frame at room temperature in the commercial jig, the cast frame cools down from its' top surface causing a solidified shell to form. This shell prevents the material from contracting inwards while cooling which leads to voids forming inside the casting. These voids negatively influence the shielding ability of the end-frame.
- Casting into the commercial jig also proves problematic in terms of the Wood's alloy solidifying before the mould is completely filled, especially when large thin frames are cast.

Problems with existing techniques to produce end-frames for electron beam shaping in radiotherapy can be overcome by developing improved end-frame casting equipment. Wood's alloy end-frames can be produced by casting in a custom-designed unit manufactured with locally available equipment and materials.

1.3 Aim of the Study

The aim of this study was to develop equipment for casting Wood's alloy end-frames that are dimensionally accurate, have a consistently high density and

can be produced in a short timeframe at reasonable cost. Radiotherapy departments will benefit from the availability of this equipment to produce end-frames with little effort, while patients will benefit from more effective radiation field shaping.

1.3.1 Objectives

- 1) Perform a literature study on treatment of superficial cancer with a focus on techniques and equipment available for field shaping electron beams in radiation therapy.
- 2) Design and manufacture new equipment for casting Wood's alloy end-frames based on literature and preliminary experiments that were done in this regard. The preliminary experiments included casting Wood's alloy into a solid aluminium frame, casting into a jig with positionable aluminium strips and experimenting with different water-cooling layouts for the jig.

Although each of the design iterations showed improvement on the previous one, there was sufficient justification to design new casting equipment as described in this study based on what was learnt. The following requirements were set for the new equipment:

- a) The casting-jig should limit expansion of the Wood's alloy during cooling to ensure dimensionally accurate end-frames.
- b) Even and fast cooling across the surface of the jig should be ensured in order for the Wood's alloy to cool from the bottom surface upwards to prevent cavities from forming in the alloy while cooling.
- c) A means of heating the casting jig should be provided for to ease the flow of the Wood's alloy while filling the mould.

- d) The equipment should be convenient to use to cast end-frames with little effort.
 - e) The casting equipment should be manufactured using local materials and suppliers to make it more affordable compared to imported commercial casting equipment.
- 3) Evaluate the newly developed Wood's alloy end-frame casting equipment in terms of the following:
- a) Dimensional accuracy of end-frames produced using the newly developed equipment compared to end-frames cast in a commercial jig.
 - b) Cast time comparison between end-frames cast in the newly developed equipment to end-frames cast in a commercial jig.
 - c) Density of the alloy of end-frames cast using the newly developed equipment compared to end-frames cast in a commercial jig.
 - d) Cost of developing the casting equipment compared to importing the commercial casting jig.

1.4 Methodology

The methodology followed in this study was as follows:

- a) Gather information on existing field shaping techniques and equipment for electron radiation in radiotherapy.
- b) Acquire a commercial Wood's alloy casting jig and evaluate this as well as the casting jig that was developed in the preliminary work performed before this study.

- c) Design new casting equipment taking the shortcomings of existing equipment into consideration.
- d) Acquire materials and components to produce the new casting equipment and manufacture with available tools. Compare the manufacturing cost to the cost of acquiring a commercial jig.
- e) Produce Wood's alloy end-frames with the commercial casting jig as well as the new jig and compare in terms of dimensional accuracy, time and density of the alloy.

1.5 Delimitations of the Study

Only Wood's alloy was investigated for the development of the improved end-frame casting equipment as the material is already available in most radiotherapy departments for field shaping of high-energy photon radiation.

1.6 Flowchart

The structure of the dissertation is illustrated with the flowchart in Figure 1.1.

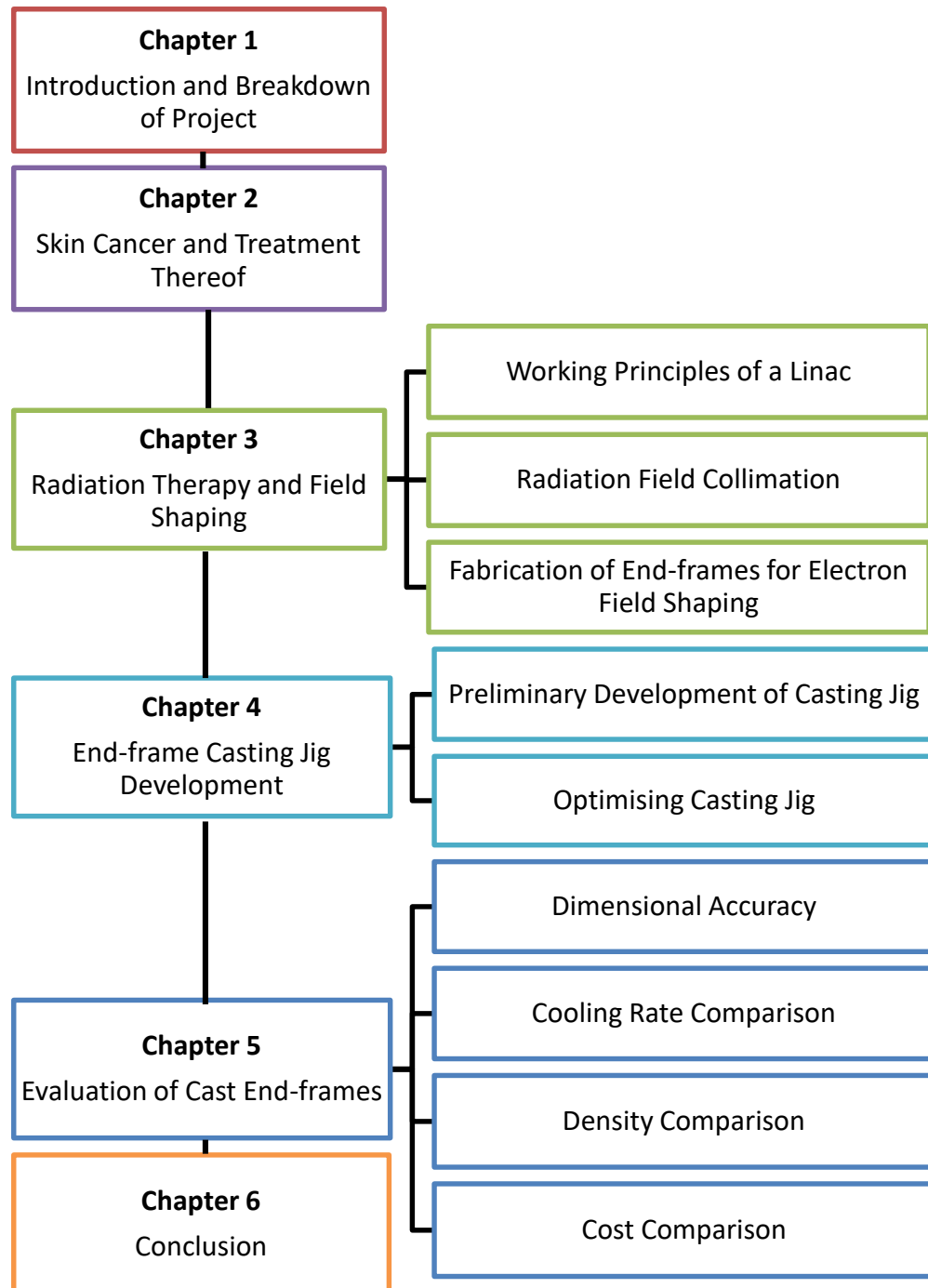


Figure 1.1: Flowchart to illustrate the dissertation structure

Chapter 2: Skin Cancer and Treatment Thereof

2.1 Introduction

Technology for treating cancer has seen great improvement in the past few decades. These days specialists can make use of different technologies to detect, plan and treat cancer with a much higher success rate [1].

Despite this improvement, cancer is still the second most prevalent cause of death, following cardiovascular disease, and the number of new cases diagnosed each year keeps increasing. It is predicted that the number of cases worldwide will nearly double and that South Africa alone will see a 78% increase by 2030 [2] [3].

2.2 Cancer: An Overview

The human body is composed of cells that grow and multiply by dividing of pre-existing cells, a process also known as mitosis. During this process, cells duplicate all of the cellular contents and are subsequently divided into two daughter cells [4]. The rate of mitosis varies for different types of tissue, for example, the epidermis of the skin has to be replaced constantly while cells in the liver can be replaced at a much lower rate [5, p. 279]. Mitosis is a controlled process and it takes place where cells need to be replaced for body functioning, growth and to heal wounds [6, p. 74].

Some cells show an abnormality in this process [7]. The cell growth is not controlled, and unlike healthy cells, continue to grow and divide to form tumours [8, p. 95]. Tumours can be benign or malignant. A benign tumour or non-cancerous growth does not invade nearby tissue or body parts and is seldom life threatening. It can, however, be figure deforming or grow large enough to press on other organs [9, p. 10]. Malignant tumours are made up of cancer cells. These cells can invade and destroy healthy tissue and even spread to

different parts of the body, a process called metastasis. Once a cancer is in the metastatic phase, it becomes harder to treat [9, pp. 11, 21].

2.2.1 Types of Cancer

There are more than 100 types of cancers which can be classified according to location or histologic [10] [7]. The general public are more used to the location classification, while medical professionals prefer the histological term [11].

2.2.1.1 Location Classification

Location classification only requires the place of origin. This, however, is not as accurate as the histological classification as it disregards the type of tissue it is composed of. Some of the familiar places where cancer begins include [12]:

- Skin
- Lungs
- Female breasts
- Prostate
- Colon and rectum
- Cervix and uterus

2.2.1.2 Histologic Classification

In histologic classification, the type of tissue of origin and the place of origin of the cancer has to be considered [11]. All the different cancers can then be grouped in one of five main categories [13].

- Carcinoma – Originates in epithelial tissue like the skin or lining of organs
- Sarcoma – Originates in connective/supportive tissue like bone, cartilage, fat, muscles, blood vessels
- Leukaemia – Originates in blood-forming tissue like bone marrow

- Lymphoma and Myeloma – Originate in immune system cells like lymphoid tissue
- Central Nervous System Cancers – Originate in brain tissues or spinal cord

For the purpose of this study the focus will be narrowed down to carcinomas, more specifically ones that originate in the skin.

2.3 Skin

The skin is the largest organ and covers the whole body, protecting the internal organs, helping temperature regulation and preventing dehydration [14]. It consists of three layers: the hypodermis, dermis and epidermis (Figure 2.1).

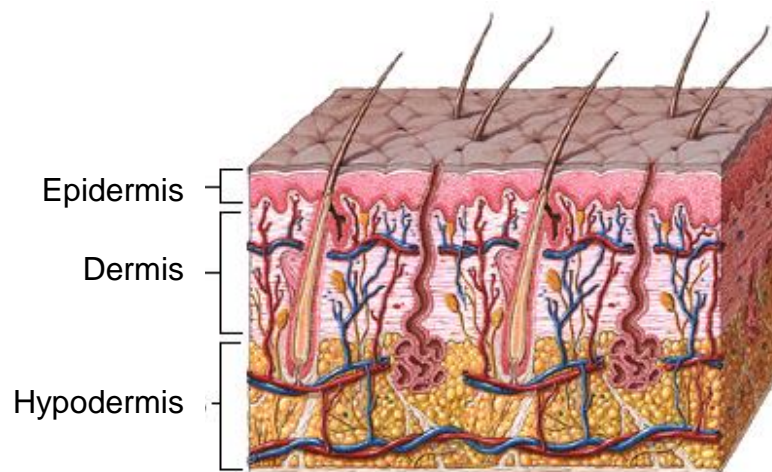


Figure 2.1: Representation of the layers of the skin [15]

2.3.1 Hypodermis

The hypodermis is the fatty layer of the skin that insulates the human body. It consists of fat cells and connective tissue that bond the skin to the muscles underneath and acts as a cushion to protect the internal organs against shock [16, p. 379].

2.3.2 Dermis

The dermis is the thickest of the three layers, making up approximately 90% of the skin's thickness. The hair follicles, lymph vessels, blood vessels, nerves and glands are found in this layer [17, p. 135]. The dermis provides the epidermis with nutrients and stiffness [18].

2.3.3 Epidermis

The epidermis is the outermost layer of the skin and consists of epithelial tissue [19, p. 88]. The layer is responsible for skin colour as well as the toughness of the skin provided by keratin. The thickness varies all over the body with the thinnest at places such as the eyelids and the thickest at the soles [17, p. 130].

The epidermis itself consists of layers (see Figure 2.2). The basal lamina or basal cell layer forms the barrier to the dermis [20, p. 114]. The outermost layer, which is visible, is the stratum corneum and mostly consists of inert or dead cells without nuclei [18]. These cells are filled with keratin and are tough, almost like a horn or a nail, from there the alternative name, horny cell layer [21, p. 354].

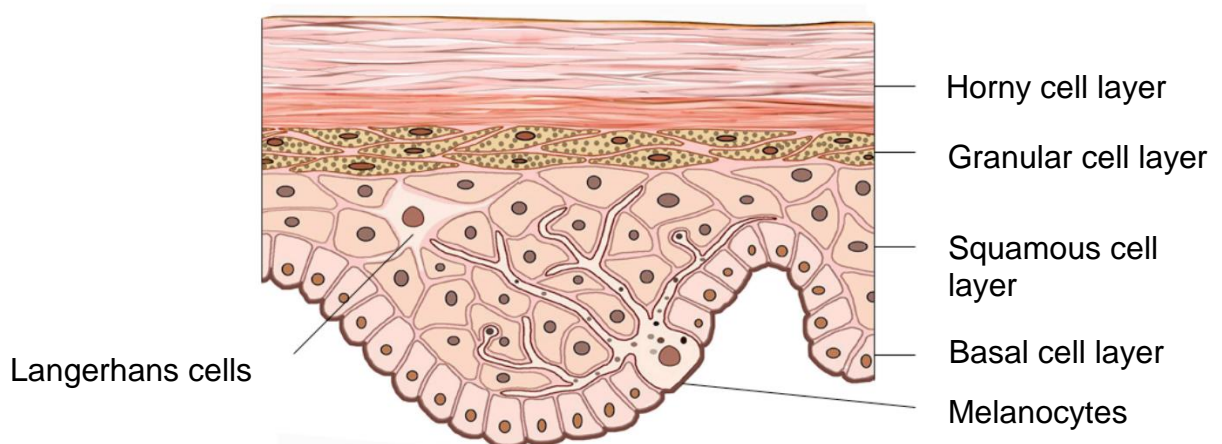


Figure 2.2: Representation of the epidermis, adapted from [18]

The cells in the basal layer are keratinocytes that divide through mitosis to form daughter cells. The daughter keratinocytes gradually progress toward the

surface of the skin, because of the continuous division of the cells in the basal layer, eventually replacing the more superficial cells that are lost or shed. Amongst the basal cells are melanocytes which secrete melanin to the adjacent keratinocytes. Melanin gives the skin its' colour and provide some UV protection [20, p. 116].

The squamous cell layer consists of the daughter keratinocytes. Their cytoplasm starts to shrink and causes the cells to flatten. Some of these cells in the deeper part of the layer can still divide to increase their numbers. Langerhans cells are also found in this layer. These cells detect foreign bodies and stimulate an immune response [17, p. 133] [20, p. 114].

The keratinocytes in the granular cell layer are flat and contain keratohyaline granules which participate in the keratinization of the cells. The nuclei and organelles of the cells disappear and the cells convert to keratin [22, p. 7]. A lipid mixture spreads out over the cell surface which is crucial to retaining water in the body [17, p. 133].

The horny cell layer consists of completely keratinized cells, tightly compacted, providing a barrier to the body [23, p. 7]. The cells are constantly shed and completely replaced approximately every two weeks [21, p. 354].

The migration process of a keratinocyte takes between 15 to 40 days, depending on age of a person, injury to the skin and location [17, p. 133] [18].

2.4 Skin Carcinomas

Carcinoma is cancer that originates in epithelial tissue. The epithelial tissue of the skin is found in the epidermis which is exposed to the elements. The majority of skin cancers are most likely caused by sun exposure. The keratinocyte and melanocyte cells in the epidermis are the origin for three of the most predominant skin cancers [24, p. 8].

2.4.1 Types of Skin Carcinoma

Skin cancers can be broadly classified as either melanoma, arising from melanocytes, or non-melanoma which includes basal cell and squamous cell carcinoma arising from keratinocytes [25, p. 12].

2.4.1.1 Basal Cell Carcinoma

Basal cell carcinoma (BCC) is the most common and accounts for about 80% of skin cancers [26]. It originates in the basal layer of the epidermis where basal cells are found and starts out with a mutation in the cell that causes it to continuously multiply uncontrollably [24, p. 11]. It is the least dangerous, but if left untreated aggressive basal cell cancer can invade and destroy surrounding bone, nerves and muscles. In very rare cases, the cancer can spread to different sites, i.e. metastasize [27, p. 42].

2.4.1.2 Squamous Cell Carcinoma

Squamous cell carcinoma (SCC) originates in the squamous layer. It is the second most common form of skin cancer, where approximately 20% of cases diagnosed are SCC [28, p. 1]. It grows faster than BCC, and is more likely to metastasize. SCC can be cured with early diagnosis and treatment otherwise it can invade surrounding areas and tends to spread to other parts of the body, including internal organs [24] [29, p. 692].

2.4.1.3 Melanoma

Melanoma arises from the pigment cells in the epidermis, the melanocytes. It normally begins in parts of the skin that are exposed to sunlight but can also originate in parts of the nervous system, the eyes and mucous membranes [30]. It accounts for less than 1% of skin cancers but is the most dangerous because of its' tendency to metastasize. Nearly 75% of skin-cancer-related deaths are caused by melanoma [31]. Melanoma can be cured in the *in situ* stage, but the

five-year survival rate decreases to approximately 90% for stage I, 70% for stage II, 25-50% for stage III and 10% for stage IV [32, p. 2] [33, p. 78].

2.5 Treatment of Skin Carcinomas

Standard treatment for skin carcinomas is mainly surgery. However, the treatment option depends on the type, stage, size and location of the cancer as well as the age and health of the patient. In some cases, especially where the cancer is more advanced, treatment could include a combination of extensive surgery, immunotherapy, clinical trial participation and radiation therapy [34]. There are other treatment options that are being tested in clinical trials, but the most common treatment options are the following:

2.5.1 Surgery

Several surgical techniques that can be used for treating skin cancer include excision surgery, cryosurgery, curettage and electro-cautery, Mohs micrographic surgery (MMS), wide local excision surgery and lymph node surgery [35]. It is the first choice of treatment for non-melanoma skin cancers that have not metastasized. In many cases it is successful the first time. It is not uncommon to follow up with a different treatment to make sure there are no cancer cells left behind. A good example of a combination treatment for cancer is where the breast cancer surgical wound is treated postoperatively with radiotherapy [13].

2.5.1.1 Excision Surgery

Excision surgery is usually performed for diagnostic purposes as well as removal of small skin cancers [36, p. 84]. This is done in the doctor's office under local anaesthesia where the cancer and a border of healthy tissue are removed according to recommended excision margin guidelines. The border is then studied under a microscope to ensure that no cancer cells were missed [37].

2.5.1.2 Cryosurgery

Cryosurgery is used to remove small cancers which have not penetrated the skin too deeply. Areas close to organs like the eyes are preferably avoided. The surgery involves liquid nitrogen, carbon dioxide or argon that is sprayed or placed with a cotton swab on the cancer area to freeze it. The tissue in contact dies including the cancerous cells. The area forms a scab which will detach from the skin after about a month [38] [39].

2.5.1.3 Curettage and Electro-cautery

Curettage and electro-cautery are only used on small BCC or SCC and can be done under local anaesthesia. The tumour and border of healthy tissue is scraped out with a spoon-like tool, the curette [40, p. 60]. Then an electrically charged needle device is used in the wound to get rid of any remaining cancer cells and also to control bleeding. This type of surgery can also be applied more than once to make sure that there are no cancer cells left. Complete removal of the lesion cannot be confirmed and the method is therefore used on cancer that has not invaded the dermis [37].

2.5.1.4 Mohs Micrographic Surgery

Mohs micrographic surgery (MMS) is a technique that can be done under local anaesthesia. During treatment, a thin layer of the cancerous lesion is surgically removed and then studied under a microscope. If there are any cancer cells in the dissected layer, the next layer is removed. This layer-by-layer method continues until there are no more cancer cells left. As much as possible of the healthy tissue can therefore be saved, which aids the healing process and minimizes scarring [41, p. 147].

This technique is mostly used on large, aggressive, recurrent or location-sensitive BCC, SCC, certain melanomas and some rare skin cancers, especially if it starts to invade surrounding skin tissue. It is the most definitive treatment but an expensive and time-consuming method, ideal for cases where

the cosmetic outcome is a big factor, for instance, at the nose or eyes. Of all the surgical treatments for skin cancer, this technique has the highest five-year cure rates for both primary and recurring skin cancers [35] [37].

2.5.1.5 Wide Local Excision

Wide local excision is used in places where the border of the tumour is ill-defined, the cancer cells were not removed properly during a previous excision, or if the safety margin was not big enough. The amount of tissue that is removed depends on the type and size of the tumour, where it is located and how much tissue has already been removed. In some cases, where the area is quite large, a skin graft or skin flap can be used to close the wound [24] [40, p. 62] [42].

2.5.1.6 Lymph Node Removal

Lymph node removal is applied as part of a surgical procedure to determine the extent of the cancer. A few cancer cells might be missed during initial staging that can spread and grow new tumours. This type of surgery is generally done with squamous cell cancers and targets the lymph nodes close to the cancer site. It is rarely necessary and can have permanent restrictions on the patient's movement [43, p. 718] [44].

2.5.2 Chemotherapy

Chemotherapy uses anticancer drugs to target cancer cells by inhibiting mechanisms involved in cell division. Several different types of drugs target the cancer cell at different stages of the cell's life cycle. The drugs are effective on certain types of cancers which have a fast growth rate. The side effects can be seen in normal cells that have a naturally fast growth rate such as hair follicles, oral mucous membranes and intestines [43, pp. 76-84] [45, p. 23].

There are different techniques by which chemotherapy can be administered depending on the type, size and location of the cancer and whether it has metastasized. The systematic delivery, where the drug is administered to the body through the bloodstream, either by injection, implants or orally, is generally used once cancer has spread. Regional chemotherapy, where a higher concentrated dose of the drug is administered directly into the blood supply of the cancer, is typically used in locally advanced malignancies with one or two arteries. Topical chemo creams are used to treat area-specific cancers, mostly in the case of actinic keratosis, Bowen's disease and thin basal cell cancers. Skin cancer, however, does not react well to systematic chemo; it is rather used to relieve symptoms or to decrease the size of the tumour before other treatments can be used [25, p. 474] [46, p. 17] [47, p. 464].

2.5.3 Immunotherapy

The aim of immunotherapy is to boost or trigger the immune system to fight the cancer cells. Different approaches can be taken which can be mainly divided into active or passive treatments. During active immunotherapy, the immune system is stimulated to attack tumour cells by using certain cytokines such as interferons and interleukins. These cytokines can be administered directly into the patient's system or by taking the immune cells and enriching them in a laboratory before transferring them back to the patient. Passive immunotherapy enhances the system with antibodies, such as monoclonal antibodies, which are artificial versions of immune system proteins, to fight tumour cells [43, p. 88] [48, pp. 118-124] [49, p. 2].

In skin cancer, immunotherapy is typically used to treat metastatic melanoma when other treatments do not work or are no longer an option [50]. Topical immunotherapy can be used for superficial carcinomas where the patient applies a cream to the cancer area [51]. Immunotherapy is continuously being developed and has already shown improved outcomes in patients. It can also be used as adjuvant treatment to surgery in high-risk cases [52, p. 203] [53, p. 469].

2.5.4 Photodynamic Therapy

Photodynamic therapy (PDT) is a cancer treatment which uses a drug containing photosensitizing agents and a special light, usually with a long wavelength. The drug can be administered by injection into the bloodstream or by applying a cream to the affected area. It accumulates more in cancerous cells than in healthy cells and remains longer in the cancerous cells [54, p. 8]. After a specified time, the area is exposed to the light to activate the drug which reacts with oxygen to form a highly reactive molecular oxygen. This attacks and destroys the cell while damage to healthy tissue is minimal [43, p. 825]. Additionally, the therapy can damage the blood supply to the tumour and warn the immune system to attack the cancerous cells [55, p. 142] [56, p. 75].

The minimally invasive and scar-free wound healing treatment has made PDT a good option in cases where extensive surgery would be required [57, p. 17]. PDT is typically used to treat primary superficial BCCs and SCCs, although the treatment can also be used on other skin cancers and in combination with other treatments such as surgery to prevent recurrence [35] [58, pp. 2,142]. One of the side effects is that a patient could be light sensitive for a while after treatment and should avoid direct sunlight and intense indoor lighting [59, p. 469].

2.5.5 Radiation Therapy

Radiation therapy, or radiotherapy, is where high energy is radiated to the cancer site. This damages the DNA of the cancer cells to such an extent that they can no longer divide and eventually die. The effect of radiation is the same on healthy cells but they heal much faster [55, p. 140] [60, p. 10].

Radiation can be administered through internal, external or systematic radiation. During internal radiation, a radiated needle or capsule is inserted close to or into the tumour. With external radiation, a machine directs high-energy rays into the tumour which is achieved through X-ray, gamma rays or electron radiation.

Systematic radiation is administered through drugs taken orally or intravenously [43, p. 66] [61].

When a patient is to receive external radiotherapy, planning is necessary to determine the doses to be administered. The total radiation dose is usually divided into smaller fractions and administered over a set time with rest periods in between to give the healthy tissue time to recover. The actual treatment takes only a few minutes while the planning and preparation for the treatment takes the most time [43, p. 65] [61, p. 13].

The preferred method used on skin cancers is external radiation and is predominantly used on basal and squamous cell carcinomas although other non-melanoma cancers can also be treated [42]. Radiation therapy is usually an option for skin cancer in cases where the cancer covers a large area, the area is hard to reach with surgery, cosmetic reconstruction will be too complex, such as close to the eyes or nose, or if surgery is not a viable option for the patient. Radiation therapy can also be administered as an adjuvant treatment to surgery to ensure no cancer cells are left behind [29, p. 693] [62, p. 158].

The field of interest of the study is within the external radiotherapy treatment of superficial cancers. More on the process of radiotherapy and how it is only administered to the cancer site is discussed in the next chapter.

Chapter 3: Radiation Therapy and Field Shaping

3.1 Introduction

X-rays were discovered by a German physicist, Wilhelm Roentgen, in 1895 after conducting experiments with a cathode ray tube. He noted the medical potential that his discovery could have and published an article a few days later. Within a few months, radiographs were produced and used in war to detect metal fragments from bullets [29, p. 3].

In 1896, Leopold Freud first reported the use of X-rays to treat diseases of the skin. Dr Charles Leonard observed the value of external beam radiation therapy (EBRT) as a means of cancer treatment in 1903. However, the use of X-rays in medicine was limited because of the high voltage requirement which often resulted in the cathode tubes breaking down. By 1913, improvements on the cathode ray tube, made by Coolidge, ensured more reliable machines working at higher voltages (150 kV) for longer and in 1922 a 200 kV machine was introduced [62, p. 2] [63].

Cobalt-60 EBRT machines were introduced in the 1950s. The machine produced 1.17 MeV and 1.33 MeV gamma rays with a high-activity sealed source. A maximum depth of 5 mm could be achieved and the dose rate of a new source was about 2.5 Gy/min. As a result of source decay, the dose rate decreased and treatment times therefore also increased each month [64] [65, p. 119].

Linear accelerators (Linac) overtook cobalt-60 machines as the dominant provider of EBRT in the 1970s. They generate high-energy electrons and/or photons electrically with energies ranging from 4 to 25 MeV with a greater depth dose depending on the machine (a 6 MV linac has a maximum depth dose of 16 mm). Dose rates of linacs can be modulated from 4 to 10 and more Gy/min. Although cobalt-60 machines are still used in some low-middle-income

countries they have largely been replaced by linacs in radiotherapy departments [64] [65, p. 122].

Since the authors had access to an SL25 linac from Elekta at the Oncology Department at the National Hospital in Bloemfontein, South Africa, all research performed for this study is based on this machine.

3.2 Working Principles of a Linac

Linacs are machines that accelerate electrons to high energy using radio-frequency (RF) waves with the help of multiple components. Figure 3.1 shows a block diagram with all the major components of a typical linac. Although the operation of different manufactures of linacs varies, the basic principle remains the same.

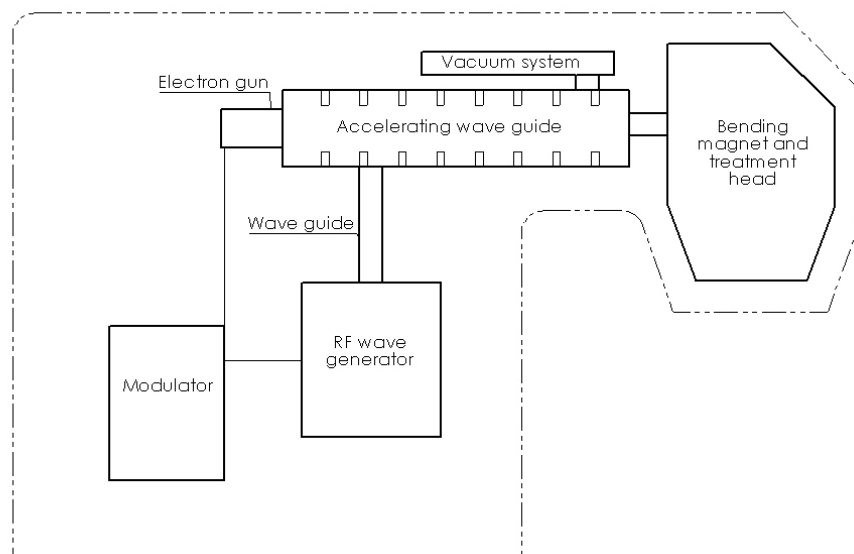


Figure 3.1: Block layout of a typical Linac, adapted from [66, p. 43] [67, p. 138]

Power is supplied to the modulator which delivers direct current pulses simultaneously to the RF wave generator and the electron gun. The RF waves are generated by either a magnetron or a klystron. In Elekta machines this is done by a magnetron [68]. The RF waves are pulsed into the wave guide which transfers it to the accelerating structure. At the same time electrons, produced by the electron gun, are pulse injected into the accelerating structure [66, p. 43].

The accelerating structure consists of discs with different apertures placed inside a tube at different positions. The discs allow the wave and electron velocities to match, while steering- and focusing coils along the structure produce magnetic fields that prevent the electrons from diverging as the acceleration takes place.

The tube is placed under a high vacuum to prevent collisions between electrons and gas particles. As the wave accelerates with the electrons in the electromagnetic field through the tube, the energy of the electrons increases from around 50 keV up to 25 MeV before entering the treatment head (Figure 3.2) [66, p. 43] [69, pp. 136-139].

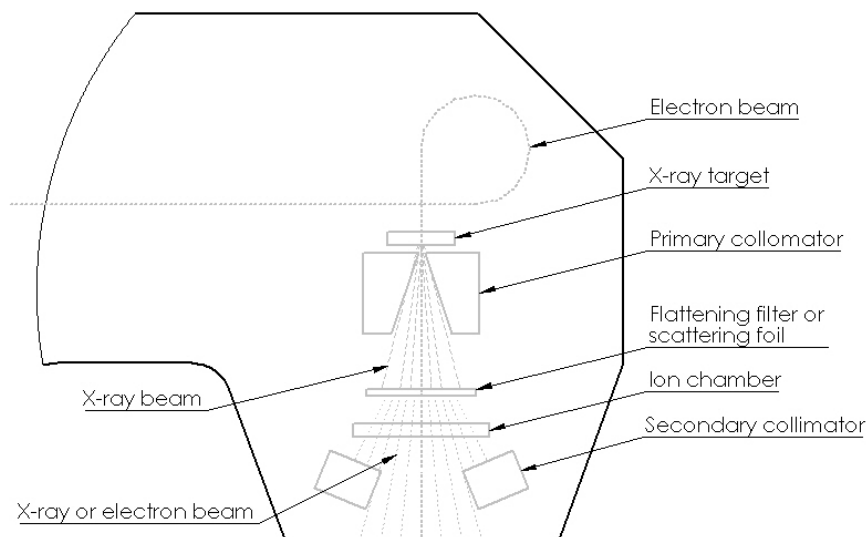


Figure 3.2: Components within the treatment head for both electron or X-ray treatment mode, adapted from [66, p. 46] [67, p. 142]

The electron beam exits the accelerating structure as a thin beam approximately 3 mm in diameter. An evacuated tube transfers the electron beam to the bending transport system where magnets change the direction of travel towards the patient. Some linacs have the capability to deliver both electron and X-ray treatments with a few changes in the treatment head [66, p. 43] [69, p. 144].

To produce photons for X-ray treatments, a target is placed in the path of the electron beam. The X-rays emerging from the target are then shaped by a primary collimator to limit the maximum angle of the beam. Passing the photons through a flattening filter reduces the intensity of radiation, which is the densest at the central axis because of the arrangement of photons, which creates an even-intensity beam. The ion chamber monitors the field symmetry, the dose and dose rate, while the secondary collimators limit the field size to a rectangular shape. Additional collimation can be done with wedges, blocks and multileaf collimators [66, p. 46] [69, p. 140].

In electron mode, the target is retracted and the flattening filter is replaced with a scattering foil to spread the thin electron beam for a uniform treatment field. The secondary collimators are opened to maximum field size to minimize bremsstrahlung contamination of the field. Due to electrons scattering in air, the field must be collimated close to the patient's skin to sharpen the field edges. This is usually done with attachable cones or applicators with different sizes, although the method of collimation varies with manufacturers [66, p. 47] [69, p. 144] [67, p. 142].

Photon or X-ray radiation, as produced by a linac, is used to treat deep-lying tumours in the body. Electron radiation is used to treat superficial tumours as most of the energy is released close to the skin's surface [70, p. 287] [71].

The focus of the study is on electron radiation; more specifically, the collimation of electron radiation beams in Elekta linac machines (Figure 3.3) that are used for the treatment of superficial cancers such as skin cancer.



Figure 3.3: Elekta™ SL25 linear electron accelerator at the National Hospital

3.3 Radiation Field Collimation

During radiation, it is ideal to treat only the cancer-affected area, with minimal exposure of healthy tissue because of the damaging effect radiation has on cells. The less healthy tissue irradiated, the quicker the area can recover since the cancer wound heals through reparative growth of the surrounding healthy tissue after treatment. However, a small amount of healthy tissue surrounding the cancerous area is irradiated for two reasons: to account for body movement which varies on different sites of the body as the patient breathes during treatment and secondly, to eliminate any microspread of cancer cells to the adjacent area [72, p. 206] [73, p. 73].

As stated previously, electrons scatter in air and the treatment field should therefore be collimated close to the target, in this case, the skin [69, p. 145]. There are a few techniques available for the secondary collimation, but the standard for electron treatment is to use applicators [74].

3.3.1 Multileaf Collimators

Multileaf collimators (MLC) are mainly used for proton and photon radiation treatments. They are made of multiple leaves that can move individually to

conform the radiation beam to the shape of the target volume. The MLC can be used in addition to the standard linac collimation system; can replace the standard collimation system to provide all collimation; or replace the standard collimation system with additional shielding (as with Elekta machines) [75, p. 218].

Studies on the use of MLCs for electron therapy have been performed, and found somewhat feasible. Add-on electron MLCs (Figure 3.4) were also developed to decrease the penumbra effect caused by the distance from the collimator to the treatment surface [76] [77].

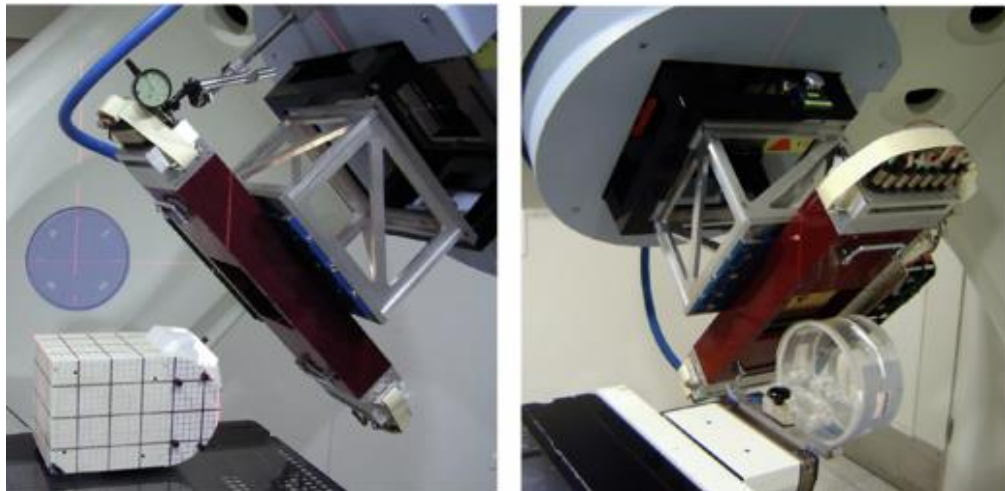


Figure 3.4: Add-on multileaf collimator [78]

3.3.2 Electron Applicators

The conventional technique to shape the electron beam is with a cone or applicator (Figure 3.5). The applicator attaches to the linac head and consists of a series of trimmers made to collimate the electron field. At the end closest to the patient, a cut-out or end-frame made of a high-density material is fitted to further collimate the field. Field sizes range from 5 cm x 5 cm to 25 cm x 25 cm, and the end-frames supplied with the linac usually have a square or round treatment portal. The portals are produced in one-centimetre size increments and chosen to fit the treatment area as closely as possible [79].



Figure 3.5: Elekta electron applicator at the National Hospital



Figure 3.6: Elekta electron applicator from [80]

With Elekta type linacs, the end-frames slide into the end closest to the treatment area of the applicator and are retained by a metal frame and lever mechanism (Figure 3.6). Two locating pins that are mounted in the frame of the applicator and protrude into holes in the end-frame (Figure 3.7) furthermore ensure the correct positioning of the end-frame. To ensure that the correct size end-frame is fitted for each treatment, Elekta linacs use a binary coding system. Four microswitches built into each applicator register the code for the end-frame when inserted.

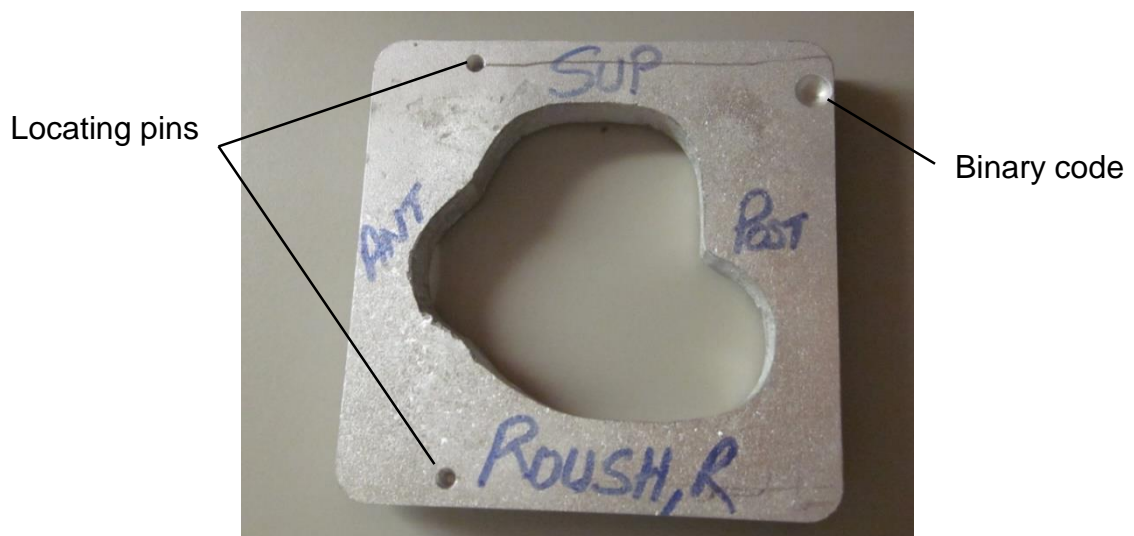


Figure 3.7: Custom end-frame made for an electron applicator

Custom-made end-frames cater for the field sizes between the sizes of the standard applicators and are often made in the hospital where the linac is installed. When the end-frame is fabricated, a binary code is allocated for each frame according to a list of sizes from Elekta by drilling shallow holes in specific locations into the frame, depending on the casting jig. The linac reads the code through microswitches: where a hole corresponds with a switch, the machine reads 1 and if not, it reads 0. A patient's file is logged on the linac system with the specified applicator, end-frame and dosage delivery schedule that the oncologist has worked out [81, p. 84].

3.4 Fabricating End-frames for Electron Field Shaping

3.4.1 Lead End-frames

End-frames were traditionally fabricated from lead, with the thickness in millimetres half the incident energy, i.e. $20 \text{ MeV} = 10 \text{ mm}$ [29, p. 201]. The outer dimensions of the end-frame had to be accurately machined on a milling machine followed by the portal in the centre where the radiation passes through. The sharp corners of the portal had to be filed square after machining. Since the end-frame fitted into the applicator, manufacturing tolerances for outer dimensions could not exceed 0.5 mm. After milling, the positions for the holes of the binary code and locating pins were marked out and carefully drilled before the end-frame was cleaned and spray-painted for safe handling by radiotherapy staff.

Since lead is a soft, malleable material it easily clogs the end-mill cutters used for machining. Therefore, milling had to be done at low speeds with cutting fluid. The lead end-frames damage easily when dropped and must be handled with care. Once damaged beyond repair, the end-frame had to be discarded as most hospital workshops were not equipped to recast lead sheets for producing new end-frames. For the same reason, shavings produced from machining the lead during end-frame production were not recycled which resulted in environmentally unfriendly waste.

3.4.2 Wood's Alloy End-frames

Wood's alloy is now the most commonly used material to fabricate end-frames. Similar to Cerrobend™, Bendalloy™, Pewtalloy, Lipowitz metal, among others, Wood's alloy is a fusible eutectic alloy (single melting point lower than each of the individual materials). It is composed of bismuth, lead, tin and cadmium (approximate 50% Bi, 25% Pb, 12.5% Sn and 12.5% Cd by weight) with a liquidus (completely liquid) melting point that ranges from 70 °C to 78 °C. The thickness required for an end-frame is usually 1.21 times the thickness required for lead, i.e. 12 mm for 20 MeV [82, p. 243] [83] [84]. Because of the low melting point of the material, it can be easily melted in a hospital workshop for casting. If an end-frame is damaged beyond repair it can also be recycled by simply re-melting and re-casting.

Jigs for casting Wood's alloy end-frames are commercially available for Elekta, Siemens and Varian linacs. Suppliers include Aktina Medical, New York, and Radiation Products Design Inc (RPDinc), Minnesota. The suppliers use a similar approach for the jigs for Elekta linacs which consist of a mould plate, a rubber insert and a clamp plate (Figure 3.8) (Figure 3.9). Each applicator frame size has its' own jig. The hole in the rubber insert represents the outer dimensions of the end-frames for the applicators.

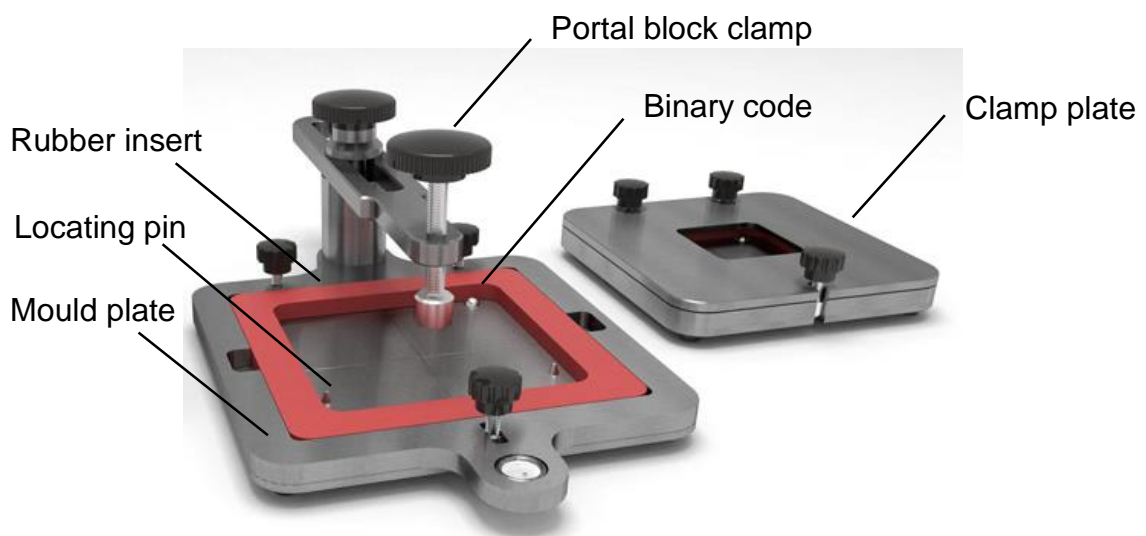


Figure 3.8: Elekta electron beam shaping jig by Aktina Medical [85]

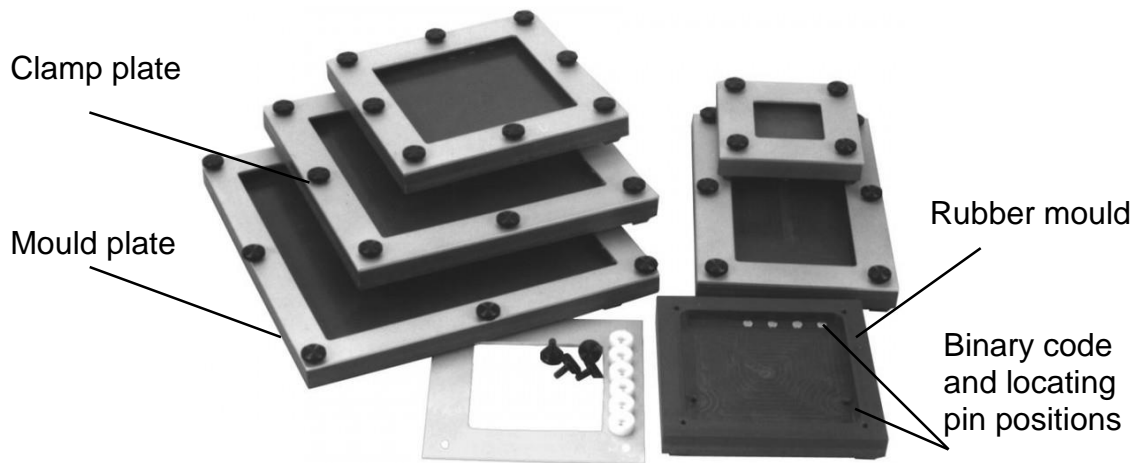


Figure 3.9: Elekta electron block mould set by RPDinc [86]

The Aktina jig for Siemens linacs consists of a plate, open at one end with rubber inserts, one for each applicator size (Figure 3.10), whereas RPDinc supplies a mould for each applicator size (Figure 3.11).



Figure 3.10: Siemens electron beam shaping system by Aktina [87]

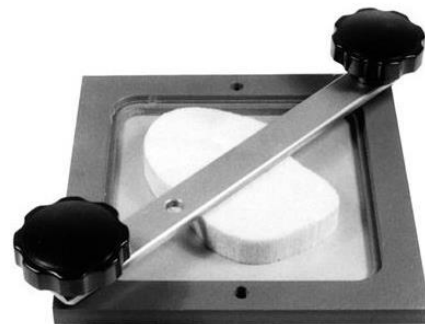


Figure 3.11: Siemens electron block mould by RPDinc [88]

Varian linacs use an aluminium frame (Figure 3.12) that forms the outside of the end-frame, with the main body cast with the alloy. The aluminium frame must be clamped onto a surface, such as the base-plate supplied by RPDinc (Figure 3.13), when casting the Wood's alloy. In this case, the aluminium frame forms part of the end-frame and is not removed as with the other techniques.

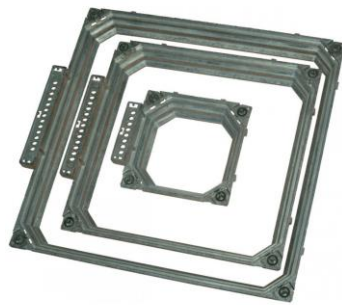


Figure 3.12: Varian insert frame for electron cone block by RPDinc [89]

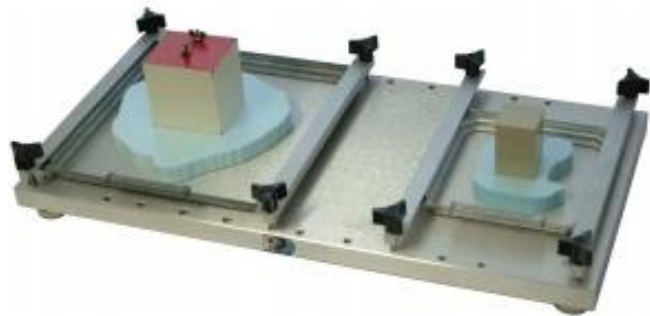


Figure 3.13: Casting plate for Varian III electron cone insert frames by RPDinc [90]

To produce a Wood's alloy end-frame, the following steps should be taken [81, p. 83]:

- Make a template which represents the treatment portal. This can be achieved by an outlined drawing of the intended shape. For patient-specific templates, the shape can be obtained through simulated data or a clinical process [67, p. 174].
- Create a mould-block from the template. This is typically made from expanded polystyrene, cut out with a hot-wire foam cutter (Figure 3.14). Other methods include machining the shape from a medium density fibreboard on a mill or manufacturing the shape with a 3D printer [91].

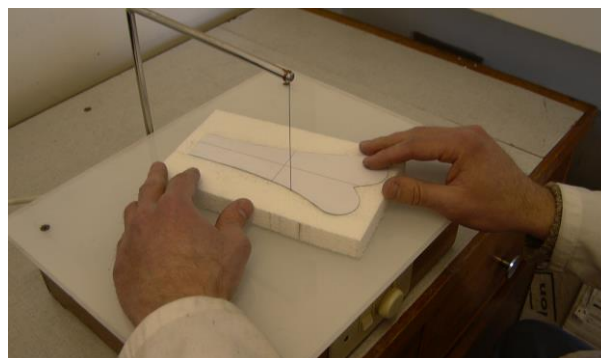


Figure 3.14: Creating a polystyrene mould-block with a hot-wire cutter [81]

- Position the mould-block in the centre of the jig and hold it down with a heavy object or with the clamp that is provided with the jig for this

purpose. Pour molten Wood's alloy in the space between the mould-block and the jig-frame to produce the end-frame and allow to cool down and set.

- Once hardened, the end-frame can be removed from the jig and the mould-block broken or knocked out. Some finishing of the end-frame is required and then painting to ensure safe handling of the material.

Preliminary work with a commercial jig from Aktina Medical showed that casting end-frames with the jig presented a few problems:

- Producing a large end-frame with a large treatment portal results in a thin alloy frame. When casting the Wood's alloy frame, the material solidifies before it completely flows around the polystyrene block causing a cold shunt (proper fusing of metal streams [92]). This is more apparent at low ambient temperatures.
- As the alloy temperature decreases after casting, due to heat transfer to the cooler surroundings, it starts to solidify. This follows the solidification front which is the border between the liquid and solid area, i.e. the outer area will solidify first (Figure 3.15). Most materials reduce in volume as they solidify and attract the inner liquid volume towards the solid front causing internal shrinkage cavities (Figure 3.16).

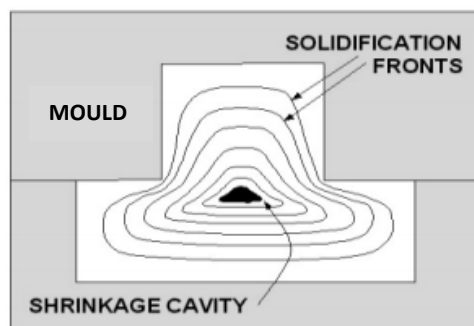


Figure 3.15: Solidification process [93]



Figure 3.16: Shrinkage cavity [94]

The Wood's alloy cast in the jig also solidifies from the top surface as it is exposed to ambient temperature, forming a shell aiding in the formation of cavities inside the casting (Figure 3.17). This is undesired since cavities will reduce the density of the end-frame which is vital to its' shielding ability.

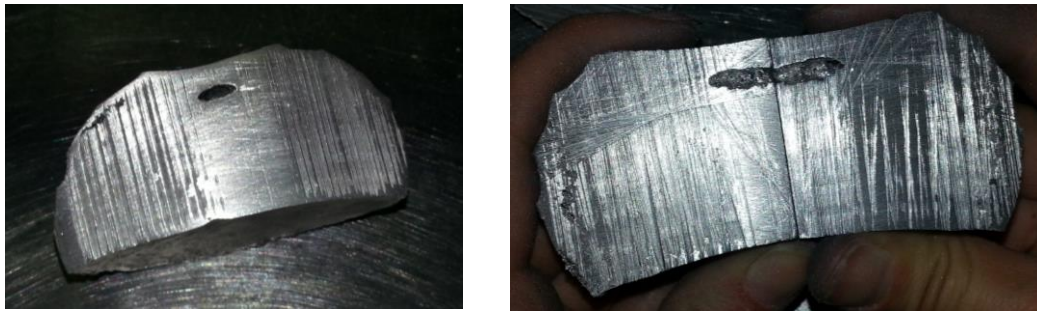


Figure 3.17: Cavities inside a cast Wood's alloy block

- Bismuth is one of the few elements that expands upon freezing, i.e. less dense in solid than in liquid form [95]. Due to the bismuth component in Wood's alloy, it also expands during cooling [96], causing the final dimensions of the end-frame to be slightly larger than the dimensions of the hole in the rubber frame of the Aktina Medical jig.

The extent of expansion also depends on the amount of Wood's alloy in the end-frame, i.e. an end-frame with a smaller treatment portal will expand more than one with a larger treatment portal for the same size end-frame. This is a factor in the accuracy of the outer dimensions which is critical for Elekta-type end-frames, as they slide into the end of the applicator.

- The commercial jigs have to be imported and are expensive to acquire.

Chapter 4: End-frame Casting Jig Development

4.1 Introduction

As stated in the previous chapters, electron radiation is used to treat superficial cancers, typically skin cancer. The electron field should ideally be shaped close to the treatment surface to prevent electron scatter radiating a larger area than intended. This is done with an applicator attached to the head of the linac which trims the field up to the end-frame where final shaping takes place. Wood's alloy, or an equivalent, is already used in radiotherapy departments to cast end-frames with commercially available equipment. However, some problems and areas for improvement were identified on end-frames produced with the equipment as well as with the equipment itself:

- Material expansion, influencing accuracy of dimensions of end-frames
- Cold shunts, weakening the end-frame rigidity
- Shrinkage cavities, reducing shielding ability of the end-frames
- Cost and availability of commercial jigs which must be imported

The aim of this study was to develop improved equipment for casting Wood's alloy end-frames that are dimensionally accurate and have a consistent high density which can be produced in a short timeframe at a reasonable cost. Figure 4.1 illustrates the development of the improved end-frame casting equipment schematically.

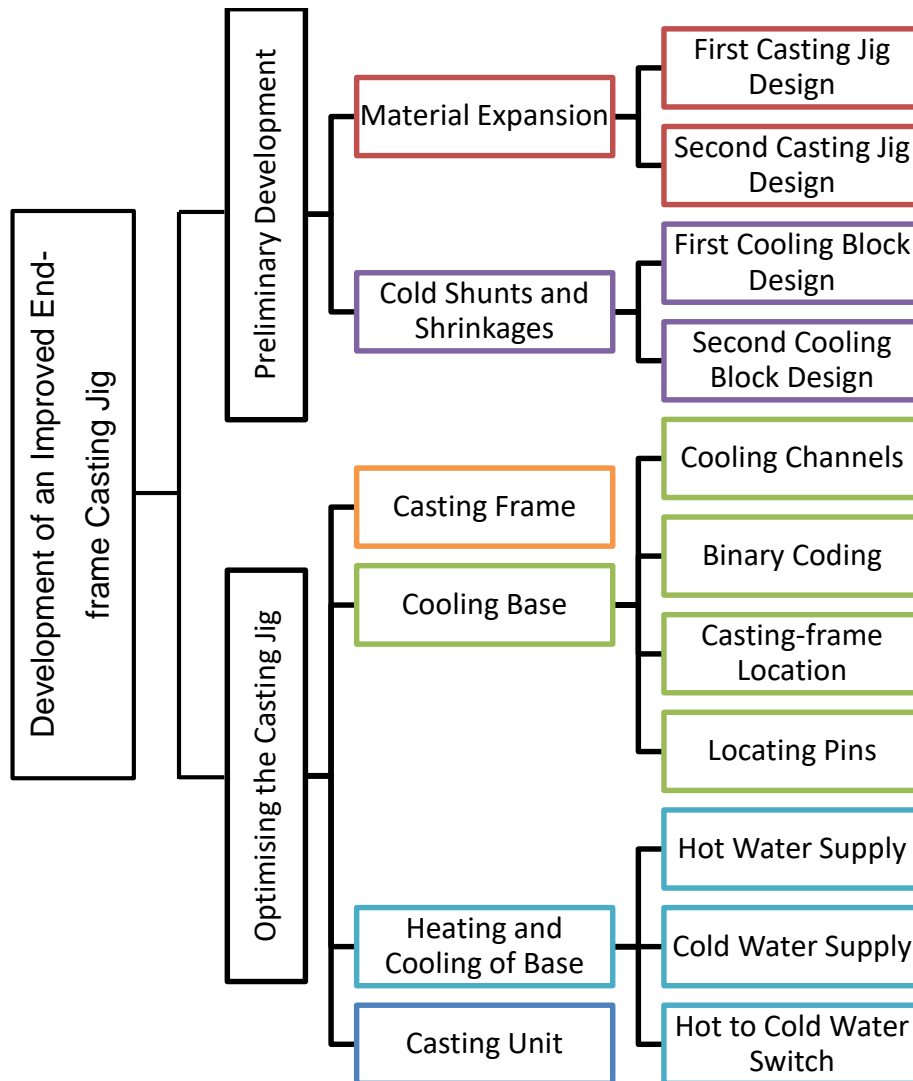


Figure 4.1: Schematic representation of development of improved end-frame casting equipment

4.2 Preliminary Development of a Casting Jig

Each of the identified problems was considered separately and an iterative research process was applied, with each iteration improving on the previous until a feasible solution was found [97].

4.2.1 Material Expansion

As mentioned in Chapter 3, one of the problems experienced with Wood's alloy is the expansion of the material during solidification. The following attempts were made to produce a jig-frame that would counter the expansion.

4.2.1.1 First Jig-Frame Design

The possibility of limiting the expansion by casting the alloy into a solid frame was investigated, as suggested in a paper by Smith [98]. A mould was machined from a 12 mm sheet of aluminium to the desired dimensions for a 10 cm x 10 cm end-frame. To test, an end-frame was cast and allowed to solidify. Once cooled, it was not possible to remove the end-frame from the mould without damaging either because of expansion of the material while cooling. It could therefore be concluded that a solid frame is not the answer to overcome the expansion problem.

4.2.1.2 Second Jig-Frame Design

To overcome the problem experienced with the solid aluminium casting-frame, a second casting-jig was developed. It consisted of a 5 mm steel base-plate with repositionable aluminium strips to provide for all applicator sizes used with Elekta linacs (Figure 4.2). The strips attached to the base-plate with M5 bolts into threaded holes in the base-plate.

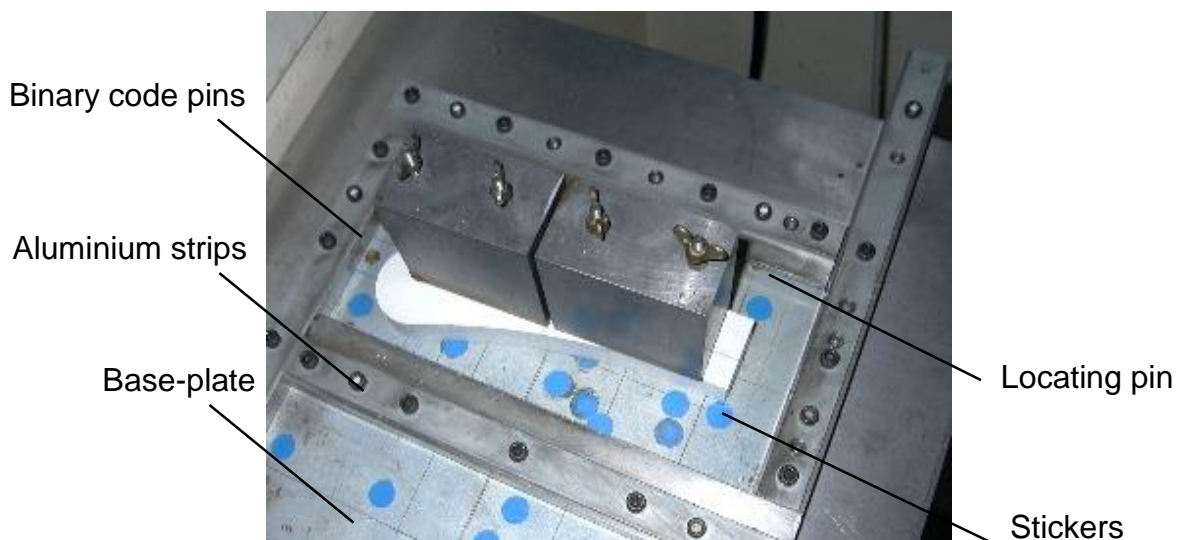


Figure 4.2: Casting jig with repositionable strips

Additional provision was made for the locating- and binary code holes required in the end-frame. Two M3 threaded holes were added on the base-plate for each end-frame size. Pins could then be screwed into these holes to produce

the locating holes in the end-frame when cast (Figure 4.3). These holes corresponded to the locating pins of the applicator.

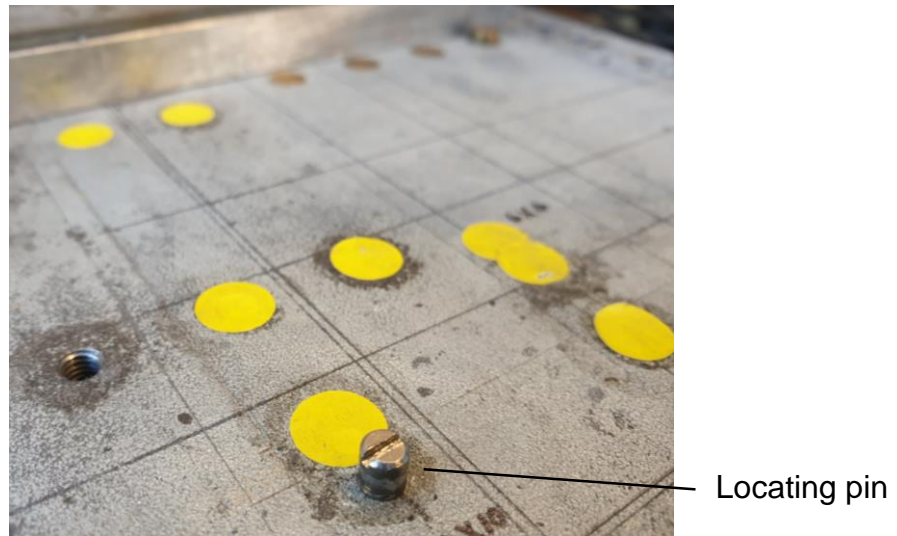


Figure 4.3: Pin for locating hole

The binary code position does not depend on the size of the end-frame and is situated in the top right-hand corner of the back side of the end-frames. Four holes were partially drilled through the base-plate in this position. Removable inserts could then be inserted to either blank off the holes or protrude to produce a hole in the end-frame when cast (Figure 4.4). When the end-frame is fitted into the linac applicator, the binary code holes in the end-frame line up with the four microswitches of the applicator to provide the binary code for end-frame size identification.



Figure 4.4: Coding system

To cast a specific size end-frame, the four aluminium strips had to be positioned and bolted down through the holes provided for that size. The unused holes within the boundary made for other end-frame size strips were closed by means of small round stickers to prevent the molten Wood's alloy from leaking out during casting.

The treatment portal in the end-frame is created from a polystyrene block or high-density fibreboard cut-out, centred on the jig and weighed down by means of lead blocks to prevent it from floating while casting the end-frame. Once cooled, the aluminium strips were loosened, and the end-frame removed for final finishing and painted before use during treatment.

The end-frame expansion was limited with the aluminium strips although it was time consuming to set up the strips by tightening all the bolts and then undoing all again to remove the end-frame after casting.

This jig-frame design, referred to as the second casting-jig, was used in the following experimental setups to solve some of the other problems.

4.2.2 Cold Shunts and Shrinkage Cavities

When casting the Wood's alloy in the casting-jig at room temperature, the alloy solidifies before completely forming the end-frame, causing cold shunts. This is the same problem experienced with the commercial jig, as described in Chapter 3, and is more apparent with thin-framed end-frames. A solution could be to heat the base-plate to the melting point of the Wood's alloy before casting. The molten alloy then has the opportunity to flow around the block forming the treatment portal and thus preventing a cold shunt.

Cooling of the alloy at room temperature also caused the alloy to solidify from its' top surface that is exposed to air, causing shrinkage cavities or voids, as discussed in Chapter 3. These less-dense areas of the end-frames would allow more radiation to pass through during treatment, which is unsatisfactory.

According to literature [99], problems associated with cavities forming in Wood's alloy can be prevented by rapidly cooling the alloy from the bottom upwards. The intention was therefore to manufacture a heating/cooling block on which the casting-jig could be placed. The base-plate could be heated before casting and cooled thereafter.

4.2.2.1 First Heating/Cooling Block Design

The first heating/cooling block attempt consisted of two spaced steel plates with water inlets and outlets (Figure 4.5). The block was sealed around its' periphery to form an enclosed space for the water to flow through.



Figure 4.5: Simple steel cooling block

The second casting-jig was placed on the block and Wood's alloy was cast. Tap water was passed through the block for cooling. It was observed that the Wood's alloy cooled more rapidly using the block but it was also noted that the top surface of the block cooled unevenly. This was caused by air bubbles getting trapped inside the cooling block.

4.2.2.2 Second Heating/Cooling Block Design

A second block was fabricated with the intention to heat and cool the base-plate by circulating hot or cold water through the block. To prevent air bubbles getting trapped inside the block, such as with the first design, it was decided to pass the water through a continuous 8 mm copper pipe bent in the shape of a matrix.

Aluminium was cast around the pipe to form a block with one inlet and one outlet (Figure 4.6).

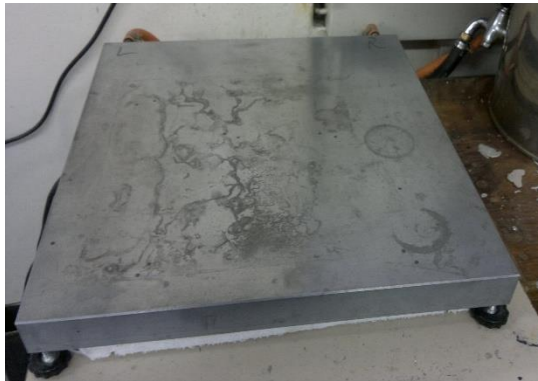


Figure 4.6: Second block design



Figure 4.7: Casting-jig setup

To preheat the block, water was pumped by a small pump from an urn through the block and back to the urn in a closed loop (Figure 4.7). With the second casting-jig placed on the block, it was heated until the desired temperature was reached (melting point of the alloy). Once the Wood's alloy was cast, the casting jig could be cooled by circulating cold tap water through the block.

The second block design was an improvement on the first block but uneven cooling still took place, i.e. from the side where the water entered. This can be visualized through infra-red (IR) images taken at 20-second intervals of the surface of the block with a FLIR E60 camera. Figure 4.8 shows a summary of the images at one-minute intervals while Appendix A shows all the images taken at 20-second intervals. The ambient temperature was 26.4 °C and the cold-water supply temperature was 25.4 °C.

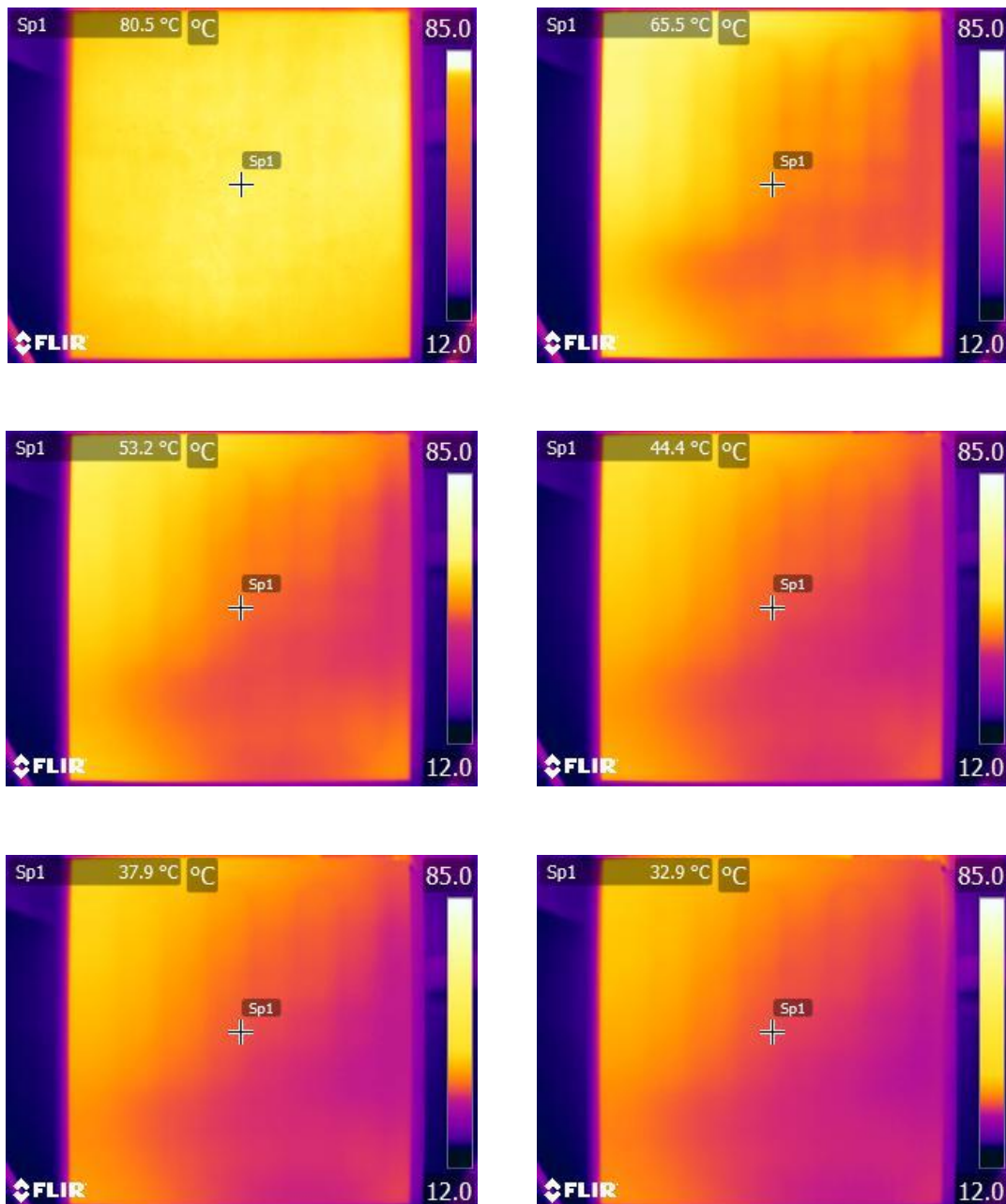


Figure 4.8: Infra-red images of cooling of the second block design taken at minute intervals

The second design of the casting-jig successfully incorporated all features required of Elekta end-frames in the cast product. No additional milling or drilling was required. To produce a Wood's alloy end-frame using the casting technique with the second casting-jig and second cooling block took about one hour compared to roughly five hours in producing a lead end-frame by means of machining operations. However, some areas could still be improved:

- Positioning the strips and fastening the bolts to set up an end-frame size on the jig as well as loosening the bolts to remove the cast frame after cooling was time consuming.
- Covering all unused holes within the cast boundary with stickers proved cumbersome.
- The base-plate warped slightly when heated on the block. This caused a reduced contact area between the base-plate and the cooling block which resulted in uneven heat transfer.
- Uneven cooling of the casting surface resulted in uneven cooling of the end-frame that was produced.

4.3 Optimising the Casting Jig

Taking into consideration the problems associated with the second casting-jig and second heating/cooling block during the preliminary work leading up to the current study, a new casting-jig was designed and fabricated. The intention was to incorporate all the components of the system, such as the casting-jig, cooling block, urn, pump and Wood's alloy melting pot, into a single unit. This unit could then be made available to oncology departments as a solution to easily cast end-frames as required.

4.3.1 Casting-frames

In order to ease the process of configuring the casting-frame for each different end-frame size by using repositionable strips, such as with the second casting-jig design, it was decided to produce a casting-frame for each size commonly used with Elekta linac applicators. The casting-frames were designed to split into two halves along their diagonal corners (Figure 4.9) with the corners extended for clamping purposes. The two halves of the frames were machined

from a 12 mm aluminium sheet and clamps together using quick-release clamps (Figure 4.10).

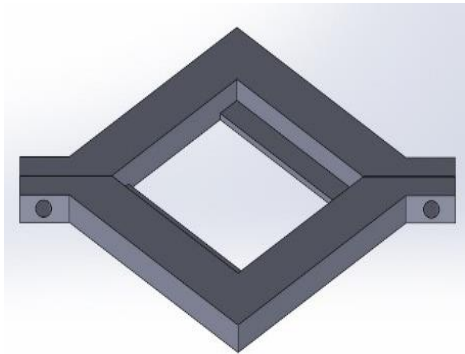


Figure 4.9: CAD rendering of casting-frame

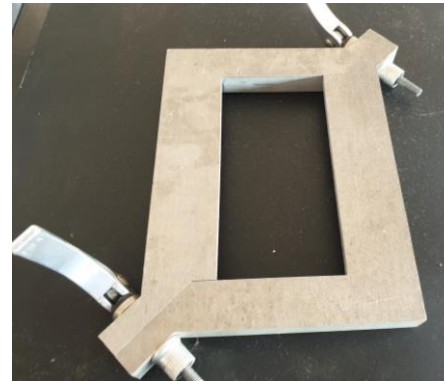


Figure 4.10: Casting-frame after machining with quick-release clamps

To eliminate the problem of the base-plate warping, it was decided to move away from a separate casting-jig and cooling block. All the features of the second casting-jig design, such as pins that are required to form the binary code and locating holes in the end-frames, were incorporated into the top surface of the base of the new casting-jig design. The base of the new design also includes cooling channels to serve the purpose of the cooling block in the second block design. Effective heat transfer can therefore take place between the cast end-frame and the cooling base.

In the new design, toggle-clamps were used to keep the casting frames in position on the cooling base (Figure 4.11). Therefore, it was not necessary to drill holes into the base with bolts to hold the frames down while casting, such as with the second casting-jig design.



Figure 4.11: Casting-frame kept in place with toggle clamps

An adjustable weighted arm was added to the unit to keep the polystyrene cut-out, which represents the treatment portal, in position whilst casting the Wood's alloy.

4.3.2 Cooling Base

Even cooling of the casting surface is important for even solidification of the end-frames. The intention with the new cooling base design was therefore to improve the uneven cooling effects encountered with the second cooling block.

4.3.2.1 Cooling Channels

The layout of the channels inside the base had to be changed to improve on the cooling that was observed with the previous block designs. To save time and material, different cooling channel layouts were designed on a computer-aided design (CAD) program (SolidWorks™). Focus was placed on flow trajectories in the channels to ensure that there was flow in all channels. CAD images of some of the different designs that were considered are shown in Appendix B.

During the first trials of the design phase, some of the channel layouts were eliminated. It was concluded that if the cooling water enters from the side of the block, uneven cooling will take place, such as was experience with the second block design in Section 4.2.2.2. This will result in uneven cooling of the end-frame which is not satisfactory.

With the next designs, the intent was to cool the surface from the centre outwards. The design iterations progressed to a concept of dividing the block in quadrants, each with their own inlet and outlet. The final concept developed into a design which has spiral channels with multiple water inlets and outlets to aid even cooling of the base (Figure 4.12).

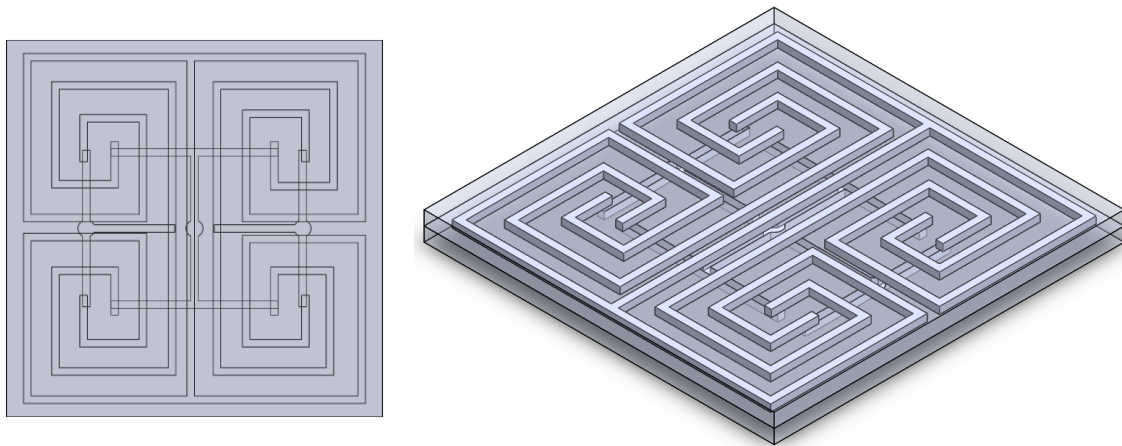


Figure 4.12: Final concept of cooling channel layout

To keep costs to a minimum, it was decided to use conventional manufacturing techniques. The block therefore had to be designed accordingly and was divided into two layers with channels separated with a gasket (Figure 4.13).

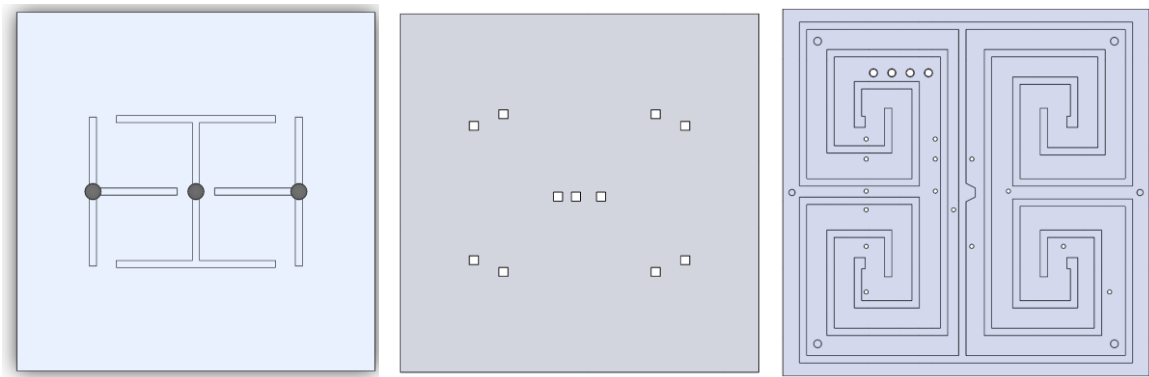


Figure 4.13: Bottom, middle and top layers of the final cooling base

Figure 4.14 illustrates the direction of water through the base. The bottom layer acts as the manifold to the top layer. It has two inlets which diverge to create more inlets to the top layer (indicated with blue). The multiple outlets from the top layer are also converged into one outlet in the centre of the bottom layer (indicated with red).

The quadrant spiral design channels are located in the top layer which heat and cool the top surface of the base. The water flow into the top layer is indicated with blue which turns to pink and then red at outlet to signify the heat transfer of the base to the water while cooling. The direction of flow through the base where the layers are combined is shown in Figure 4.15.

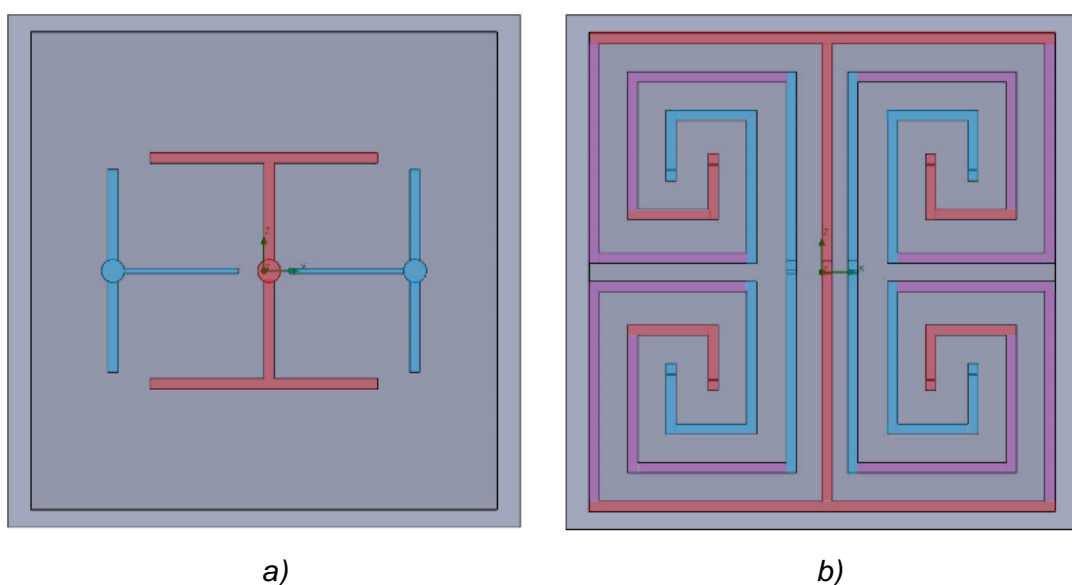


Figure 4.14 a & b: Water flow direction through (a) the bottom and (b) the top layer of the base.

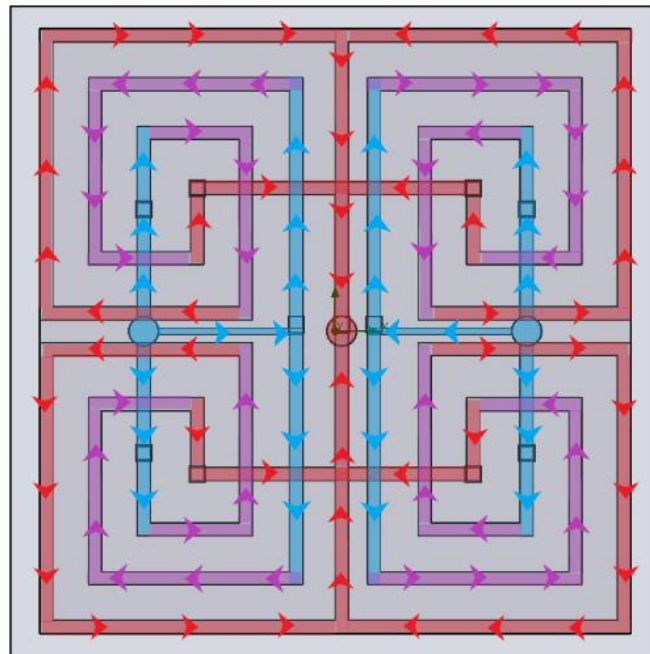


Figure 4.15: Direction of water flow in the base

The final concept was then simulated on Ansys to determine if even cooling of the top surface would take place. Results are shown in Appendix C with the one-minute interval summary shown in Figure 4.16.

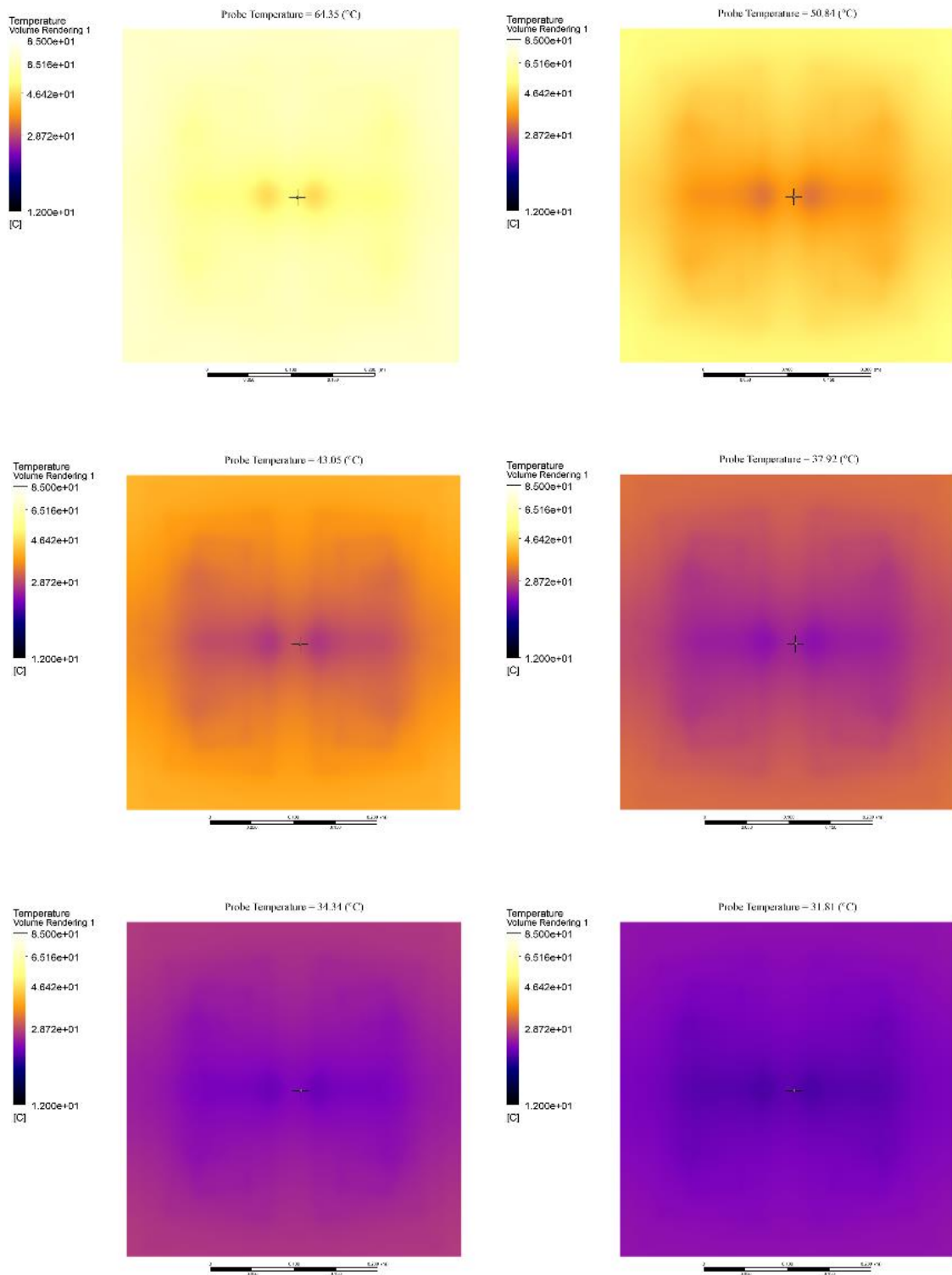


Figure 4.16: Simulated results of the top surface cooling effect

The two layers with channels were machined from a 12 mm aluminium sheet using a Computer Numerical Control (CNC) milling machine (Figure 4.17).

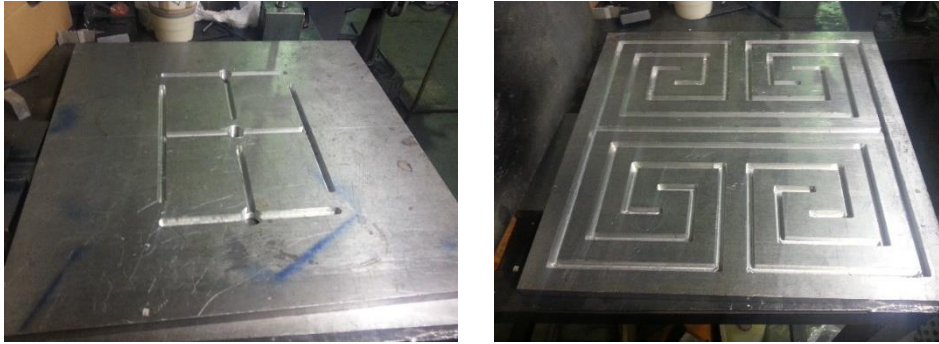


Figure 4.17: Bottom and top layer machined from a 12 mm aluminium sheet

The middle layer or gasket that is used to separate the flow in the channels of the bottom and top layers was made from a 3 mm rubber sheet. Holes were punched out of the rubber sheet to correspond to the in- and outlets of the top layer (Figure 4.18).



Figure 4.18: Manufactured base layers separated by a rubber gasket

Similar to the IR images taken of the second block design, IR images were taken of the optimised cooling base. Figure 4.19 shows a summary of the images at one-minute intervals while Appendix D shows all the images taken at 20-second intervals. The ambient temperature was 26.4 °C and the cold water supply temperature was 25.4 °C.

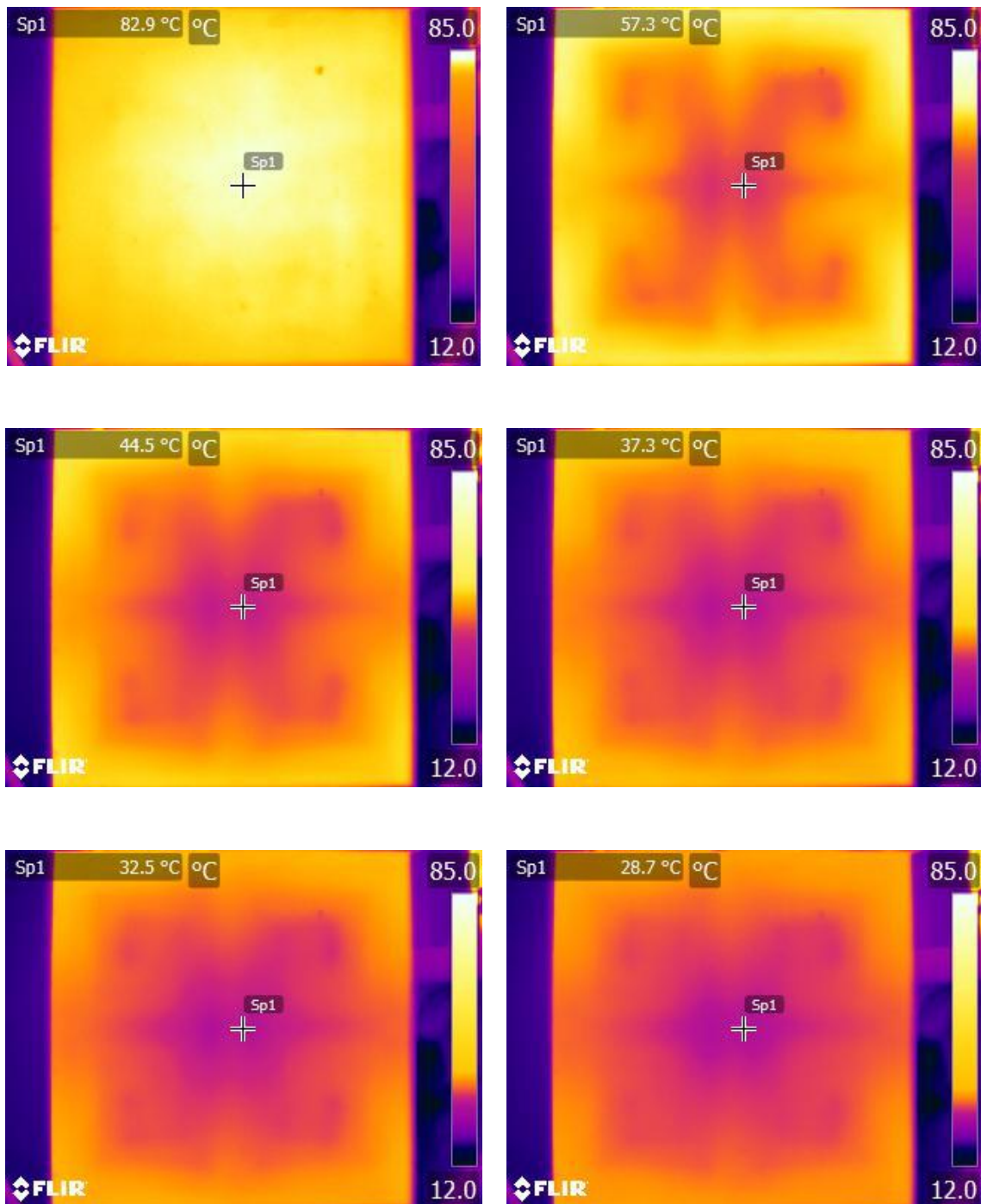


Figure 4.19: IR images of the optimised cooling block at one-minute intervals

The images show a more centred cooling effect with a much less steep temperature gradient across the surface of the jig while cooling compared to the second block design. It furthermore correlates well with the cooling simulation that was performed on Ansys.

4.3.2.2 Binary Coding

Provision was made in the base of the new casting-jig for the pins that are used to create the holes needed in the end-frames for the Elekta applicators' binary coding system. The system reads the binary code from the same top right-hand corner at the same distance, irrespective of the size of the end-frame. Therefore, only four holes were drilled into the cooling base at the appropriate position. The holes were threaded and brass pins, with a slot cut into the top of each, were then screwed into each hole (Figure 4.20).



Figure 4.20: (a) CAD blank of M8 binary pin and (b) binary pins screwed into base

Where a hole is required in the end-frame to represent 1 in the binary coding system, the corresponding pin should be partially unscrewed to stand proud of the surface of the base. The other pins remain flush with the surface of the base and represent 0 in the binary system.

4.3.2.3 Casting-frame Location

Due to the precise position of the binary code pins, the new casting-frames have to be accurately located. This is to ensure that the binary code holes are created at the same position in the top right corner of the cast end-frames. To locate the casting-frame, a recess was milled into the top surface of the cooling block that allowed for all frames to be placed in the same position according to their top right corner against the locating edges (Figure 4.21, Figure 4.22, Figure 4.23).

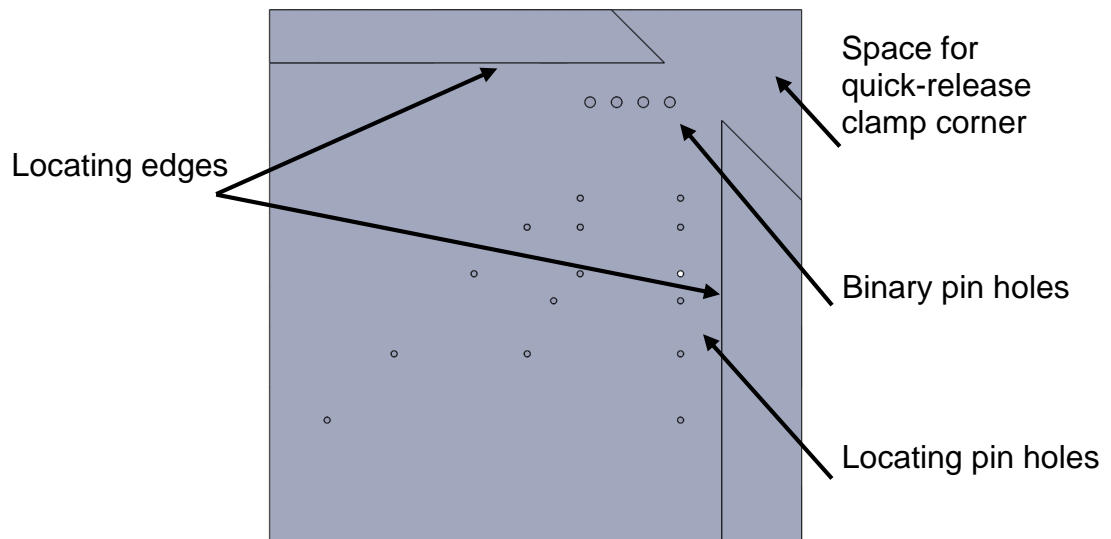


Figure 4.21: CAD representation of top surface of cooling base

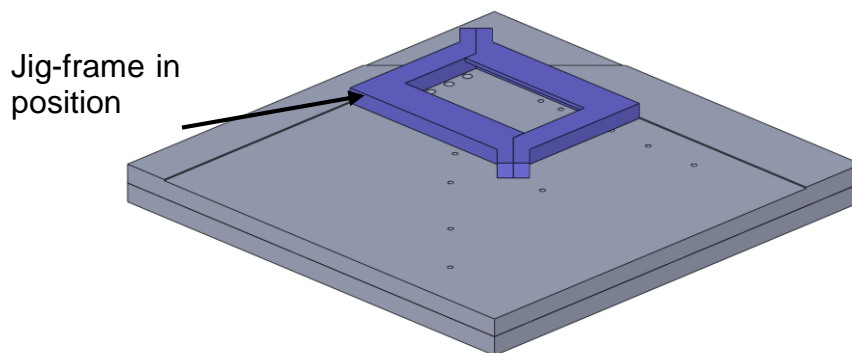


Figure 4.22: CAD representation of casting-frame in position on cooling base

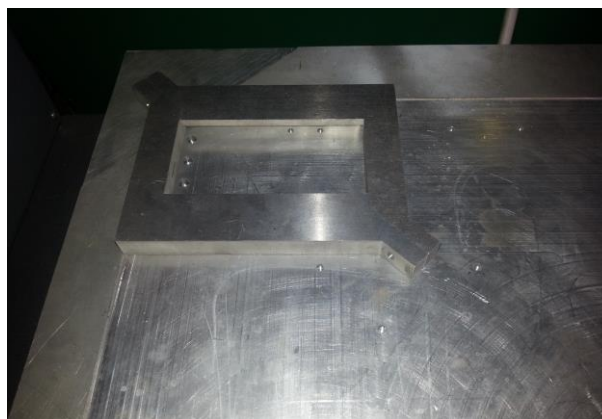


Figure 4.23: Manufactured cooling base with recess on top surface and casting-frame in position

4.3.2.4 Locating Pins

Lastly, provision was also made for locating holes required in Elekta linac end-frames. A similar approach was taken to that used for the binary code. When a specific size end-frame had to be cast, the locating pins for that end-frame were partially unscrewed to stand proud of the surface of the base and thus create the locating holes in the end-frame. Locating pins not required remain flush and thus close the hole made in the base.

Great care had to be taken in the design of the cooling base for the coding system and locating holes not to coincide with the cooling channels that were milled into the first layer of the base. This would have caused the screws to obstruct the flow of water in the channels as well as water to leak out of the screw holes.

4.3.3 Heating and Cooling of Base

To heat or cool the base, hot or cold water is pumped through the system. Most oncology departments have readily available tap water which can be used for cooling, but heated water had to be supplied by a different source. Since the same channels are used for either hot or cold water, the change between supply also had to be considered.

4.3.3.1 Hot Water Supply

The hot water to be used to heat the base must have a higher temperature than the melting point of the cast alloy (80 °C) to account for heat loss. The water should therefore be close to boiling point. To achieve this, it was decided to use a hot water urn. The hot water is then pumped with a circulation pump to the base through an insulated pipe system (Figure 4.24). It then flows through the channels and back to the urn to form a closed loop. This will ensure that the water level in the urn remain relative constant and only has to be topped up due to loss because of evaporation.



Figure 4.24: Urn and pump

4.3.3.2 Cold Water Supply

To cool the base, it was decided to use the local water supply from a tap. The supply is under normal municipal pressure which is sufficient for the water to flow through the channels. One end of a hose connects to the tap and the other end to a T-connection that connects to the channel system. The water is then discarded from the base through a pipe to a sink or other means. A heat exchanger can however be included in the cabinet to cool the water in a closed-loop system at a later stage.

4.3.3.3 Hot-to-Cold-Water Switch

The hot and cold water use the same inlets and outlet of the base, thus the system had to be adapted to account for this, as explained with reference to Figure 4.25. The flow of water is controlled by normally closed solenoid valves (opens when powered), one at inlet and two at outlet. The operator can easily switch between hot or cold water circulation from a control panel mounted on the cabinet. To supply hot water, a switch must be flipped which will activate the pump, cut the power to the cold inlet and outlet solenoids and power the hot

water outlet solenoid. This creates a closed-loop flow from the urn, through the pump and base and back to the urn.

To change to the cold water supply, the switch is flipped to the opposite side. This cuts the power supply to the pump and hot outlet solenoid and simultaneously supplies power to the cold inlet and outlet solenoids, opening the valves. The pressure of the tap water then forces the cold water through the base. To prevent the cold water from flowing through the pump to the urn, a one-way valve was installed in the hot water pipeline.

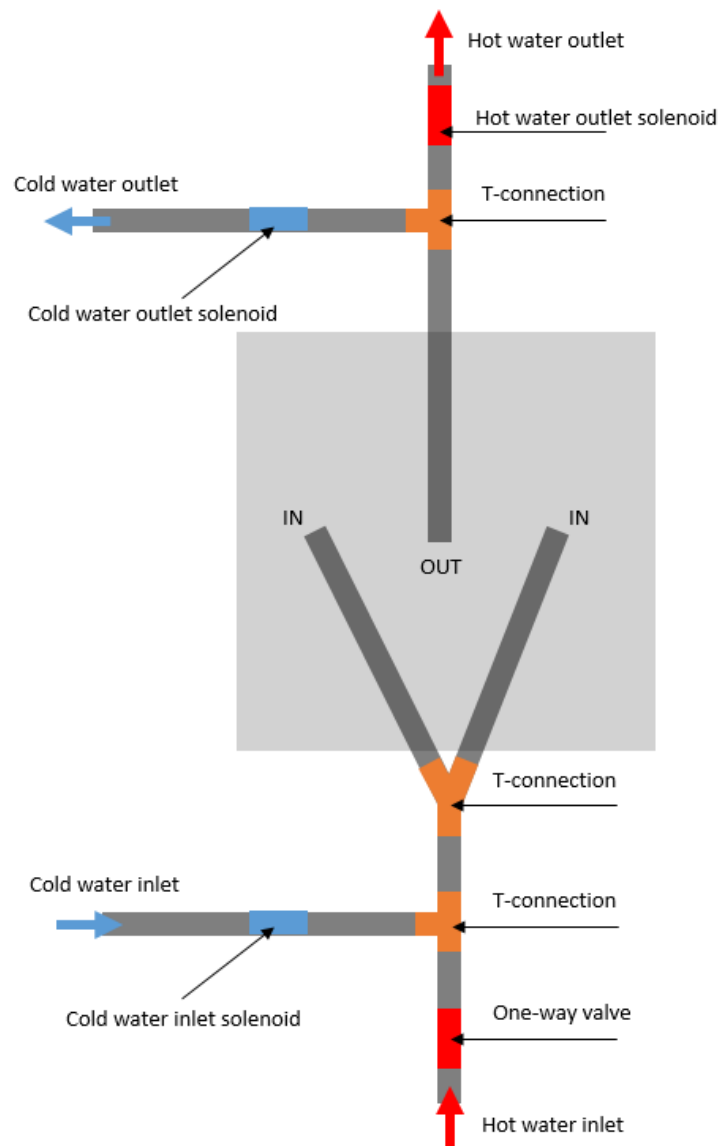


Figure 4.25: Diagram of pipe system for heating and cooling

4.3.4 Casting Unit

A cabinet was designed to incorporate all parts of the new casting equipment, (Figure 4.26) and manufactured (Figure 4.27). The intent was to provide a place for the casting-jig, urn and pump system, Wood's alloy melting pot, storage for casting-frames and manufactured end-frames or new alloy stock in a single unit.

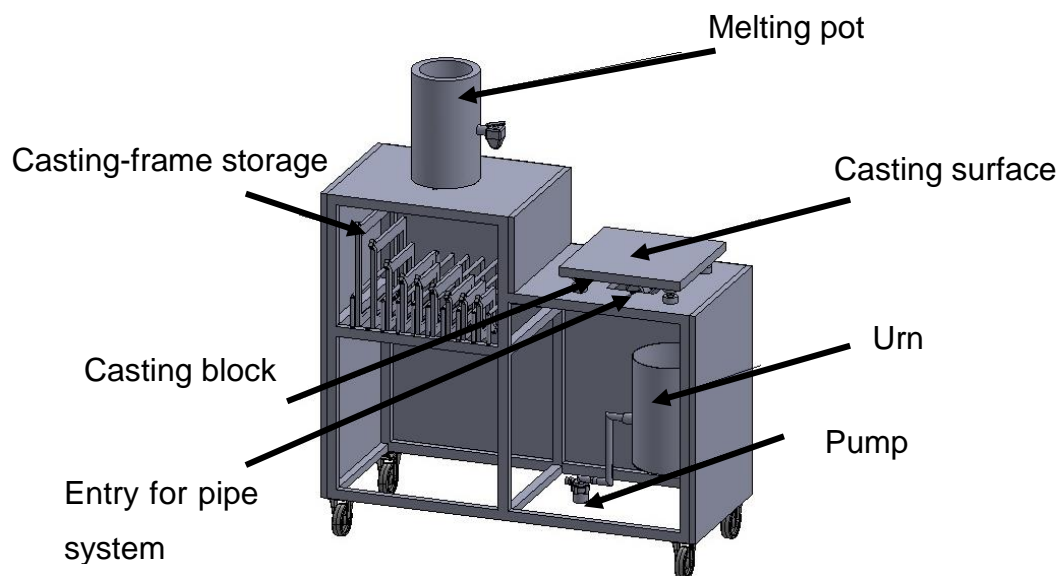


Figure 4.26: CAD representation of casting unit

The frame of the cabinet was manufactured from 25 mm x 25 mm steel tubing clad with steel-sheet panels. The cabinet was powder coated to ensure a durable finish. Three doors mounted on the front provide access to the inside of the cabinet. The cabinet is mounted on lockable castor wheels for ease of movement.



Figure 4.27: Manufactured casting unit

Provision was made for storing the different size casting-frames inside the cabinet which is accessible through the top door on the left (Figure 4.28). The bottom left door provides access to additional space that can be used to store manufactured end-frames. The urn is behind the right-hand door and is positioned below the casting unit with the pump and pipe system (Figure 4.29). A transformer had to be added to reduce the standard electricity supply for the 12 V pump.



Figure 4.28: Jig-frame storage



Figure 4.29: Urn and pump system

The melting pot (Figure 4.30) for the Wood's alloy was placed behind the control panel, next to and above the casting jig to easily cast end-frames. There are two lights on the control panel (Figure 4.31): one to indicate power to the

unit, and the other to indicate power to the urn. The urn temperature control was moved to the control panel for ease of access. Lastly, switches were added to control the pump system.



Figure 4.30: Melting pot



Figure 4.31: Control panel

All parts and material for the casting unit were locally sourced excluding the melting pot which was already available at the hospital. Commercial alloy melting pots are available internationally although alternatives can be made with local material/items.

The process to produce a Wood's alloy end-frame with the new equipment is as follows (some steps are interchangeable):

- Make a template which represents the treatment portal.
- Create a mould-block from the template, either using expanded polystyrene, or medium-density fibreboard.
- Select the desired casting frame size and position the frame on the cooling base against the locating edge. Clamp the frame down with the toggle clamps.
- Unscrew the required binary and locating pins.

- Position the mould-block in the centre of the casting frame and hold it down with the weighted arm.
- Switch on the unit to heat the base to the melting point temperature of the alloy. Care should be taken as the base will be too hot to touch.
- Once the temperature has been reached, molten Wood's alloy can be poured in the space between the mould-block and the casting-frame.
- After casting, the unit can be switched to cooling mode to cool the cast in order for it to set.
- The end-frame can be removed from the jig and the mould-block broken or knocked out once the alloy hardens and the temperature is below 44 °C. Removal of the end-frame entails lifting the weighted arm and lifting the casting-frame from the base. Release the quick-release clamps and remove the end-frame from the casting-frame.
- The end-frames should be painted to ensure safe handling of the material.

Chapter 5: Evaluation of Cast End-frames

5.1 Introduction

This chapter describes the experimental work that was performed to evaluate the Wood's alloy end-frames that were produced using the newly developed casting equipment, as described in Chapter 4. The evaluation was performed by comparing the produced end-frames to those that were cast in a commercially available jig which was available to the author from Aktina Medical. Although the commercial jig is meant for casting end-frames for Siemens linacs instead of Elekta linacs, which this study focusses on, the principle of operation remains the same. The layout of experimental work performed in this chapter is graphically shown through a flow diagram in Figure 5.1

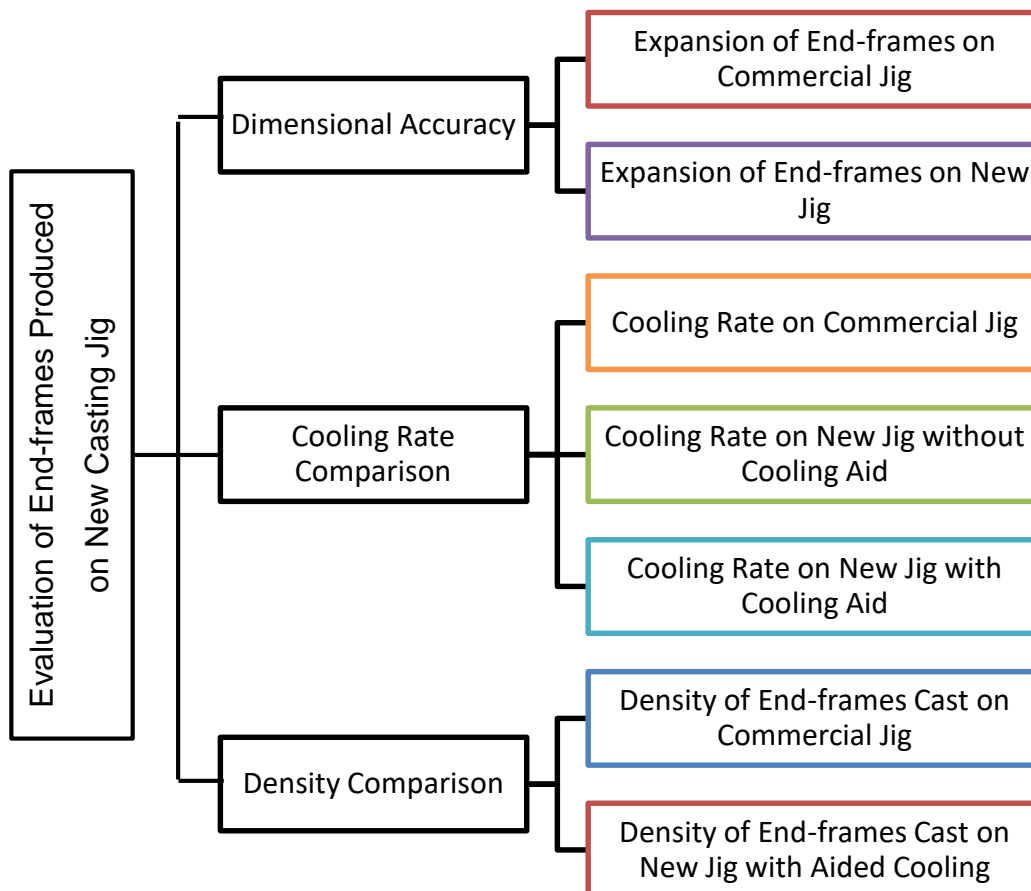


Figure 5.1: Flow diagram of experimental work performed

5.2 Dimensional Accuracy Comparison

As mentioned in Section 3.4.2, Wood's alloy undergoes contraction and expansion in its' transformation from a liquid to a solid while cooling. The expansion results in end-frames with dimensions larger than intended if not limited by the frame into which the alloy is cast. To determine if the end-frames cast into the newly developed casting jig are an improvement on end-frames cast in a commercial jig in terms of dimensional accuracy, the following experiment was conducted.

Three end-frame sizes were selected for both the commercial jig as well as the newly developed jig (small, medium and large). Since Siemens and Elekta applicators are not exactly the same size, the dimensions of the end-frames were also not the same. The Siemens applicator frame sizes selected were: 103 mm x 103 mm, 150 mm x 150 mm and 200 mm x 200 mm. The Elekta applicator frame sizes selected were 90 mm x 90 mm, 130 mm x 130 mm and 170 mm x 170 mm.

For each jig size, end-frames were cast with two different portal sizes as well as a solid end-frame. The portals were formed using blocks of medium-density fibreboard which were machined on a CNC milling machine to specified dimensions.

The portal sizes were selected in order to create an end-frame border thickness (Figure 5.2) that was approximately the same for the two types of jigs (one in the range of 15 mm and another in the range of 35 mm). This was to see if the size of the treatment portal in the end-frame has an influence on the expansion of the Wood's alloy.

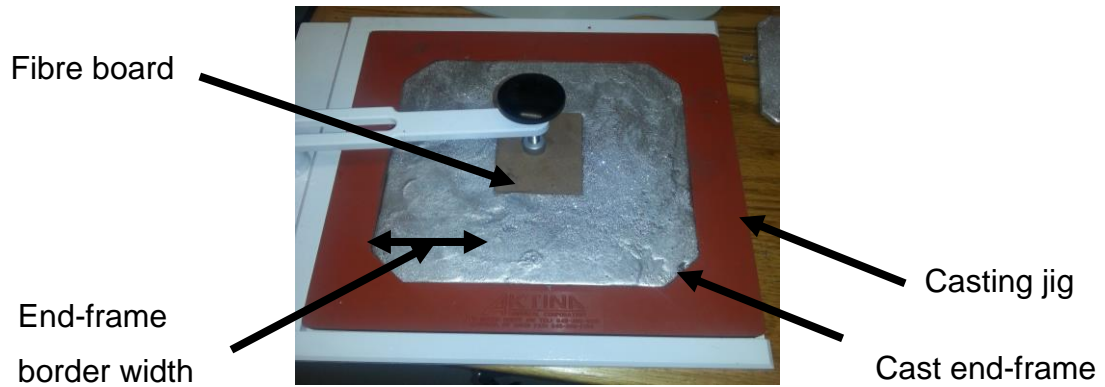


Figure 5.2: Illustration of end-frame border width

For each size, a solid end-frame was also cast to determine if the frame would expand more with the maximum volume of alloy cast.

The end-frames were cast for all three selected sizes on the commercial and newly developed casting jigs with the different treatment portal sizes. Both set-ups were allowed to cool slowly at room temperature to establish similar conditions for the expansion experiment. The test was also repeated on the new jig with fast cooling, but no difference was found when compared to the slow-cool data.

The jigs were measured, as indicated in Figure 5.3, before each cast. The corresponding dimensions were then measured on the end-frame to determine the total expansion. All dimensions were measured using Mitutoyo (up to 15 cm) and Kennedy (up to 30 cm) digital Vernier callipers and tabulated in Appendix E.

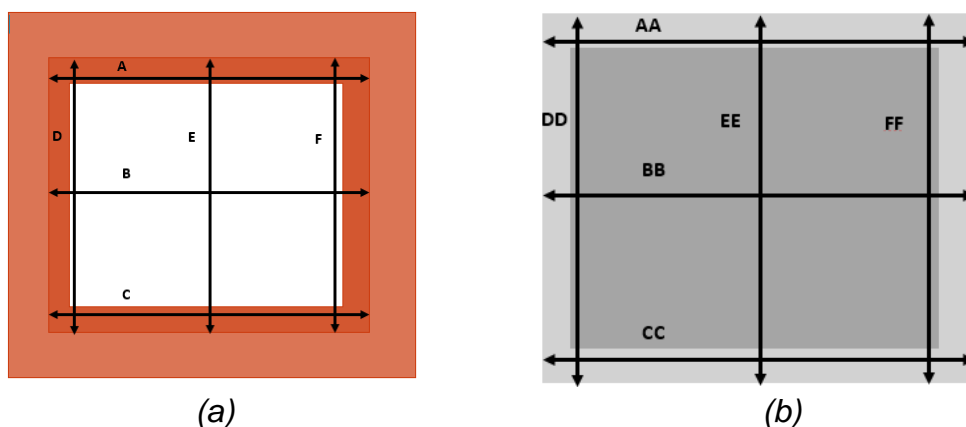


Figure 5.3: Jig (a) and end-frame (b) corresponding measurement map

The tabulated results were summarized in graphs of the total expansion against the end-frame size and end-frame border width as indicated in Figure 5.4. A total expansion/reduction tolerance of 0.5 mm is considered acceptable and is indicated with a coloured band on the graphs.

5.2.1 Commercial Jig End-frame Expansion Data

As stated, the commercial jig used for the experiment is for Siemens applicators supplied by Aktina Medical, as described in Section 3.4.2. The jig consists of rubber inserts with the same outer dimensions and each with a different size hole for the cast area (Figure 3.10).

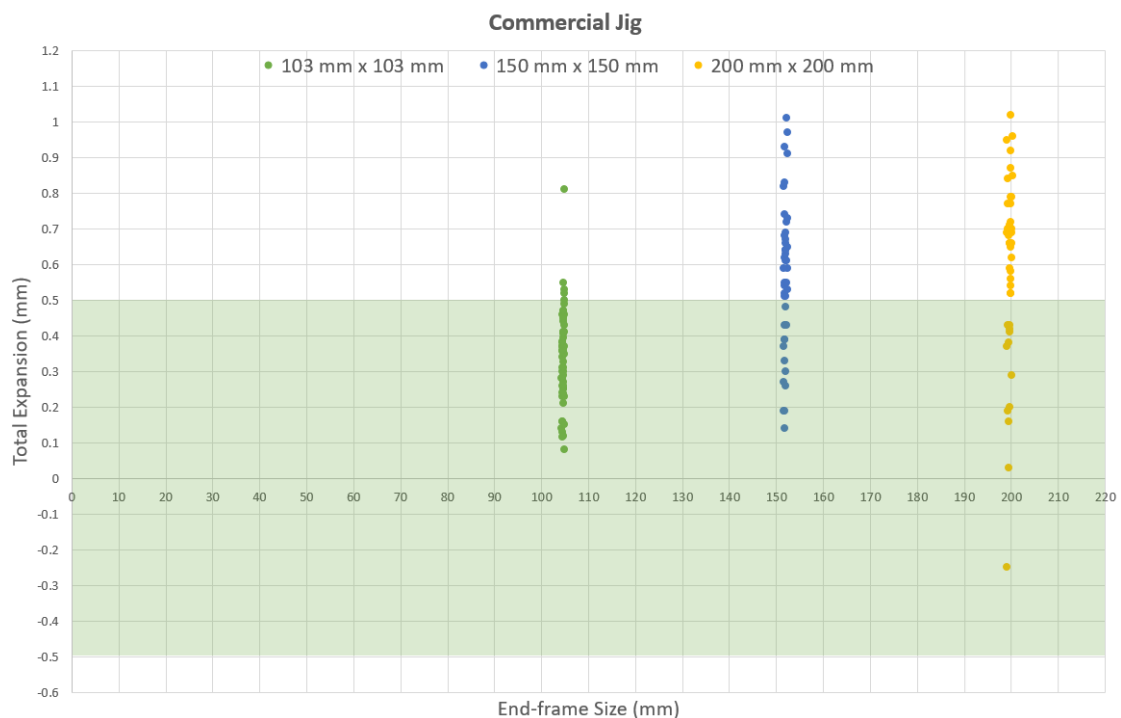


Figure 5.4: Total expansion of all the rubber jig end-frames vs end-frame size

By comparing all the cast frame results of total expansion against the end-frame sizes in Figure 5.4, it can be concluded that the smaller (103 mm x 103 mm) end-frame expands less than the bigger end-frames as the cluster of data points are closer to the acceptable range. This could be ascribed to the border width of the rubber jig which is substantial and possibly limits further expansion. There is, however, no trend to be observed as the frames sizes are increased (150 mm x 150 mm and 200 mm x 200 mm).

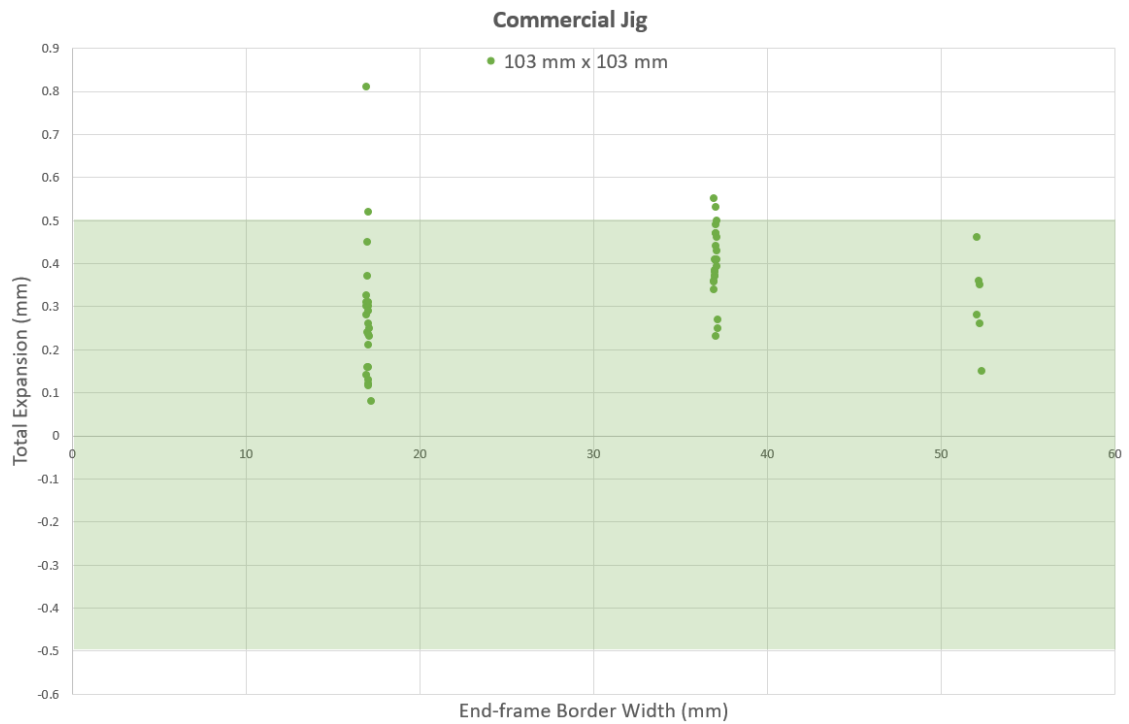


Figure 5.5: Total expansion vs end-frame border width for the 103 mm x 103 mm jig size. The average end-frame border widths are 17 mm, 37 mm and 52 mm which represent the solid cast

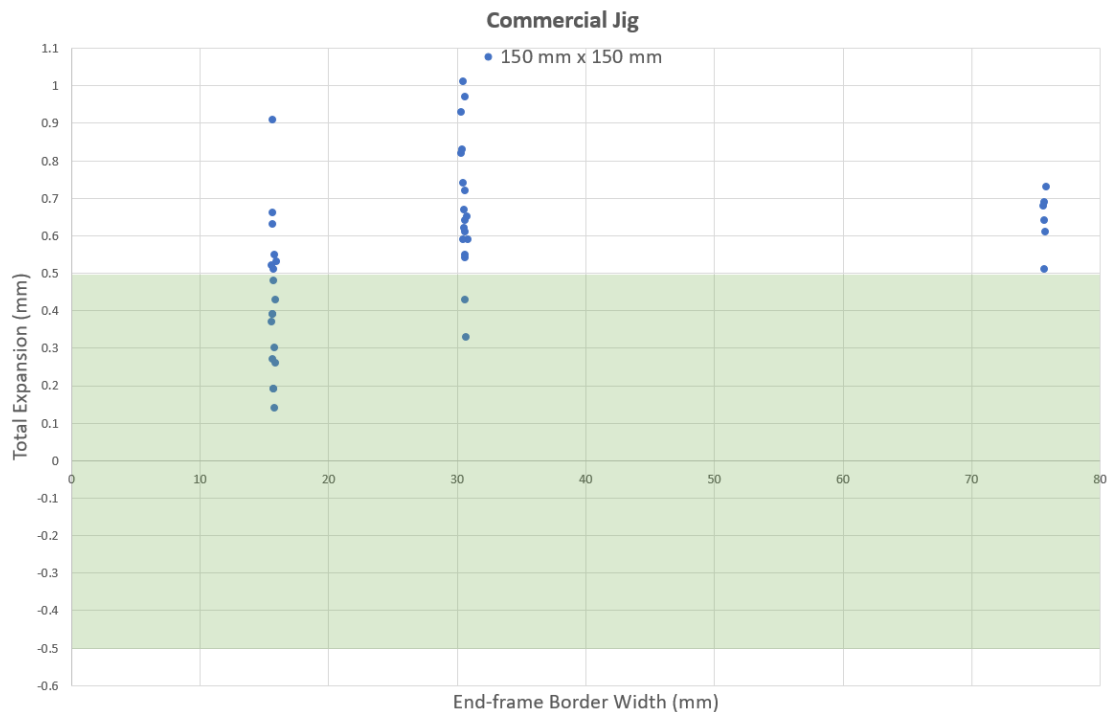


Figure 5.6: Total expansion vs end-frame border width for the 150 mm x 150 mm jig size. The average end-frame border widths are 16 mm, 31 mm and 76 mm which represent the solid cast

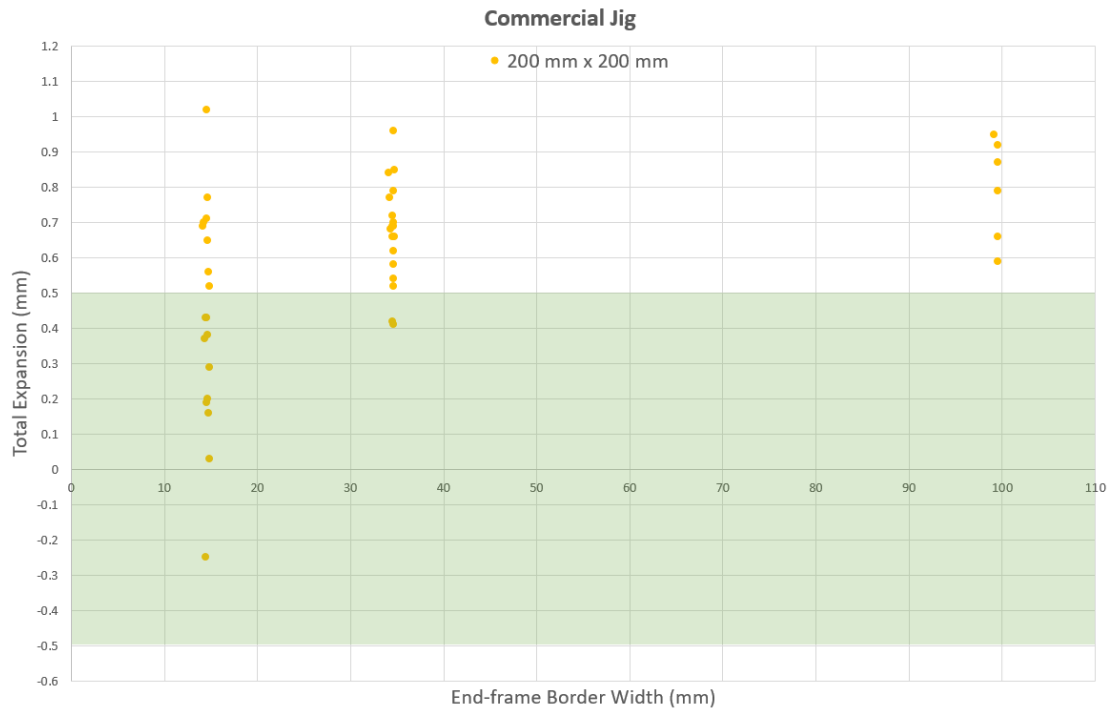


Figure 5.7: Total expansion vs end-frame border width for the 200 mm x 200 mm jig size. The average end-frame border widths are 15 mm, 35 mm and 99 mm which represent the solid cast

From Figure 5.5, Figure 5.6 and Figure 5.7 no clear pattern can be deduced to determine what the influence of the end-frame border width on the total expansion of the end-frames is. It can be observed that the clusters of data points are spaced closer to the acceptable range with the thinner end-frame border width, but the solid cast does not expand considerably more compared to the frames with portals.

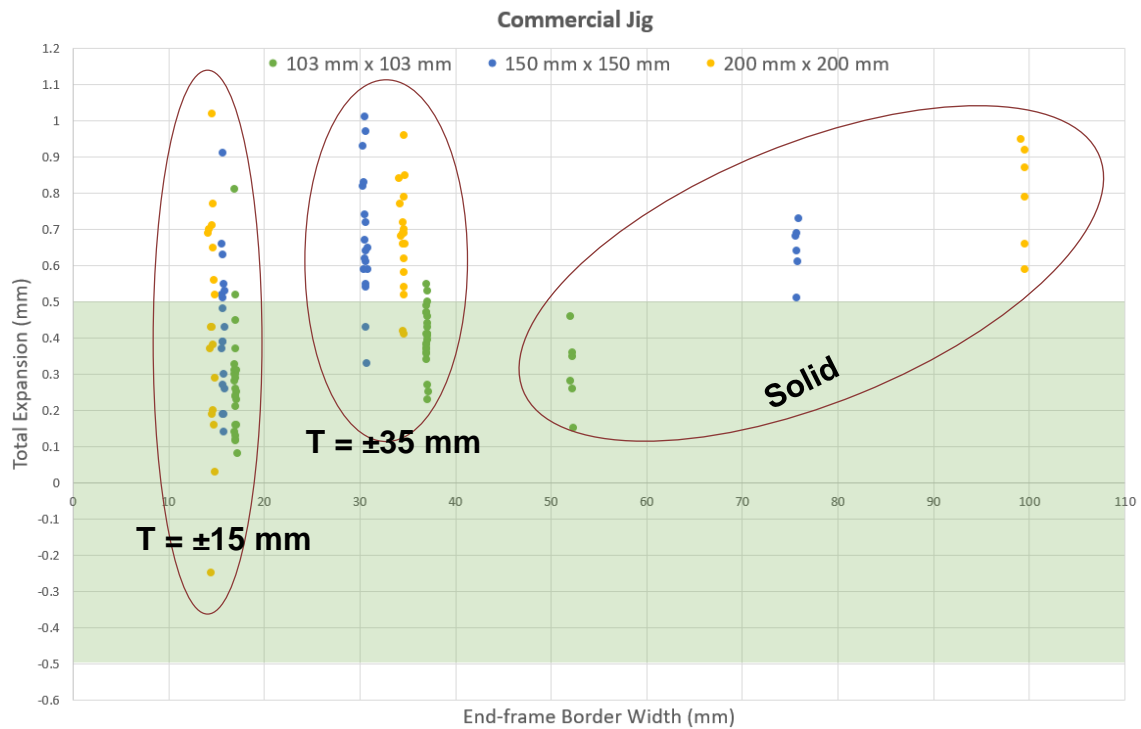


Figure 5.8: Total expansion of end-frames vs end-frame border width for all three rubber jigs with T indicating border width of end-frames with portals

From Figure 5.8 it can be observed that expansion-data point clusters of the solid castings increase almost linearly as the jig sizes increase. This was originally expected since the larger jigs will have more material expanding as the alloy solidifies. However, the same conclusion cannot be drawn for the end-frames with portals. It can be observed that the total point clusters are moving upward, away from the acceptable range of the end-frames as the border width increases, but there is no clear pattern.

5.2.2 Newly Developed Jig End-frame Expansion Data

The cast frames described in Section 4.3.1 were used to determine if there is less expansion of end-frames produced with the newly developed casting jig compared to the commercial jig. The aim was to select available sizes as close as possible to the sizes used for the commercial jig, although this was not quite possible.

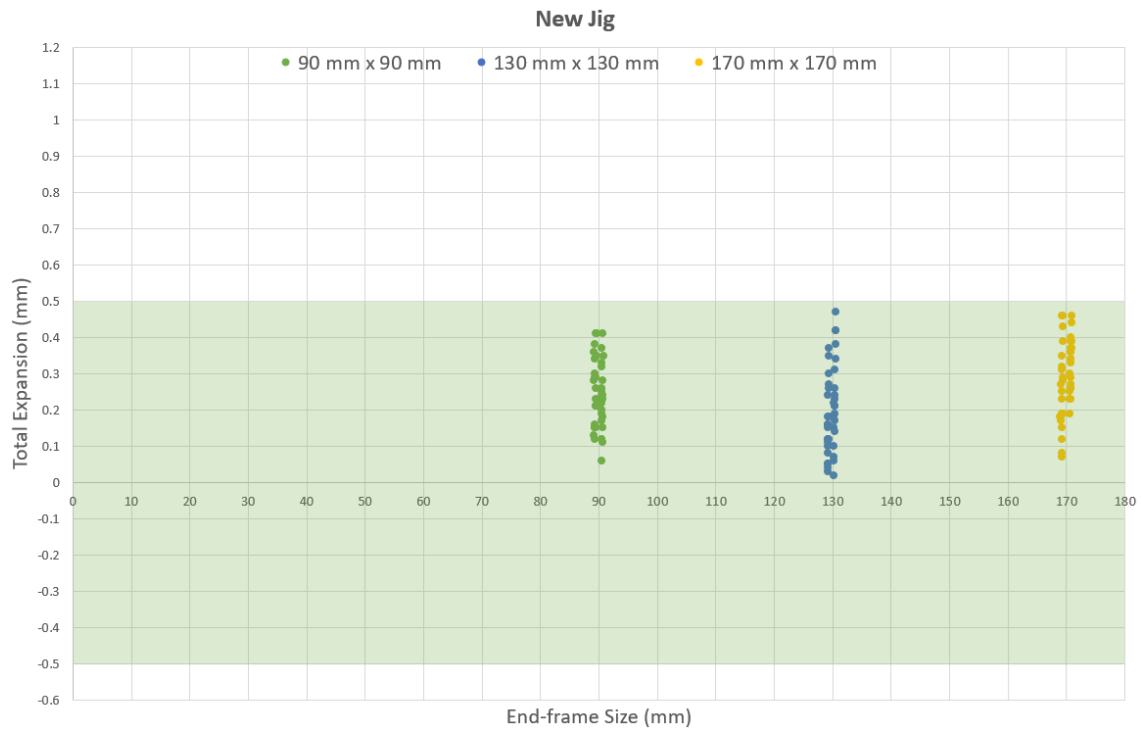


Figure 5.9: Total expansion of all the new jig end-frames vs end-frame size

In an analysis of the graph in Figure 5.9, it can be seen that the total expansion of the end-frames is within the acceptable range. There is, however, still some expansion occurring with the newly developed jig. This could be ascribed to the quick-release clamps used to hold the corners of the frame together. The mechanisms of the clamps are spring loaded and may account for some play if a force is applied by the expanding Wood's alloy. The cluster of expansion-data points does not show a clear pattern to indicate an increase in terms of end-frame sizes.



Figure 5.10: Total expansion vs end-frame border width for the 90 mm x 90 mm jig size. The average end-frame border widths are 15 mm, 30 mm and 45 mm which represent the solid cast

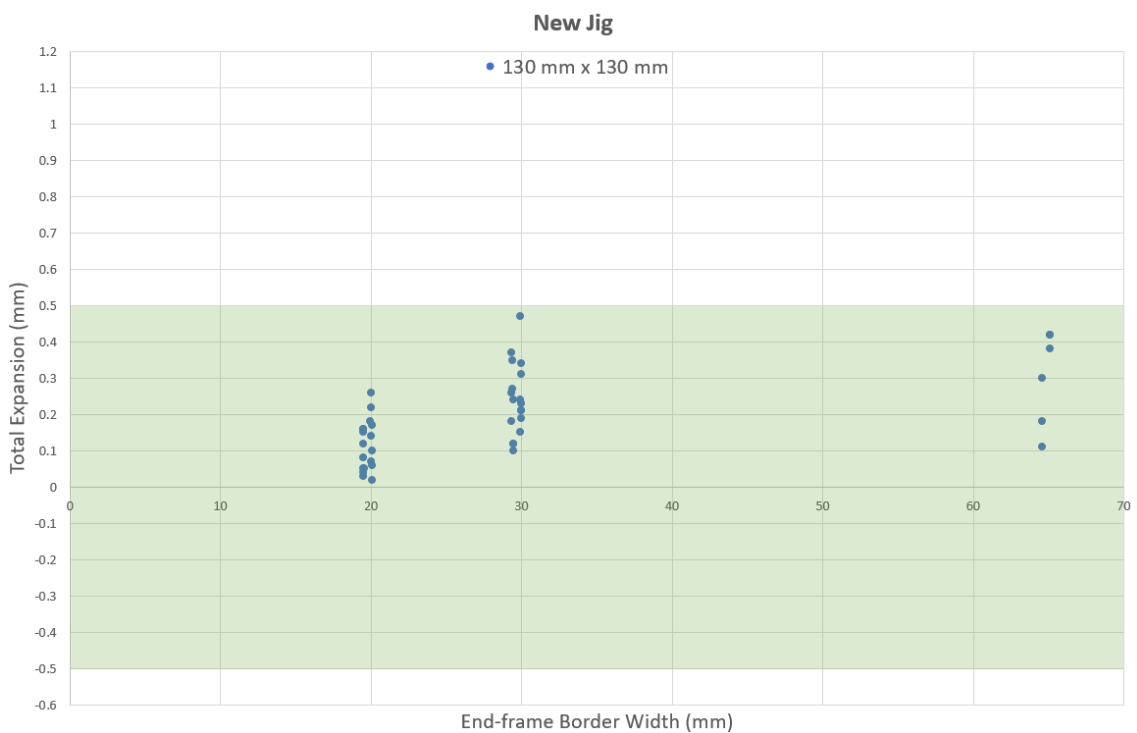


Figure 5.11: Total expansion vs end-frame border width for the 130 mm x 130 mm jig size. The average end-frame border widths are 20 mm, 30 mm and 65 mm which represent the solid cast

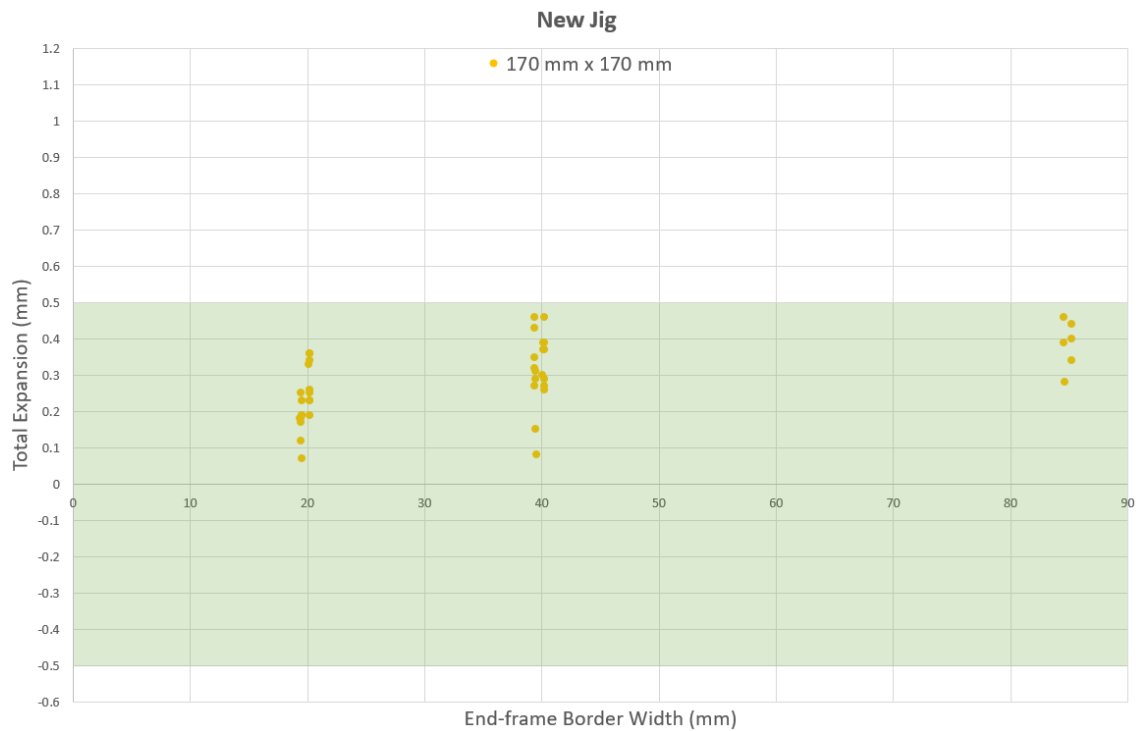


Figure 5.12: Total expansion vs end-frame border width for the 170 mm x 170 mm jig size. The average end-frame border widths are 20 mm, 40 mm and 85 mm which represent the solid cast

From Figure 5.10 it is noted that there is no clear increase in expansion associated with the increase in end-frame border width. In Figure 5.11 and Figure 5.12 however, the data point clusters can be seen to increase slightly with the increase in end-frame border width. Yet the solid casts do not expand considerably more compared to the frames with portals.

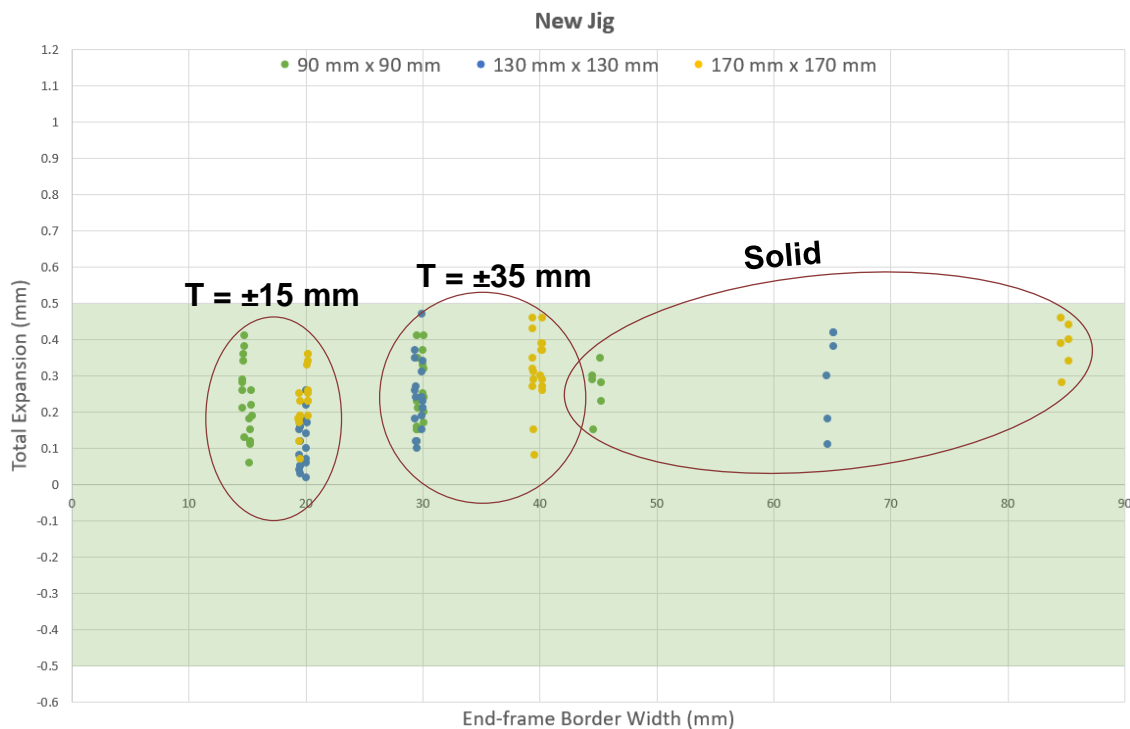


Figure 5.13: Total expansion of end-frames vs end-frame border width for all three newly developed jigs with T indicating border width of end-frames with portals

From Figure 5.13 it can be observed that expansion-data point clusters of the solid castings increase slightly, almost linearly, as the jig sizes increase. This could be ascribed to the amount of alloy expanding while solidifying which places more tension on the clamped corners. For the end-frames with portals, the total data point cluster seems to be moving upward, away from the origin line, though there is no clear pattern.

5.3 Cooling Rate Comparison

To determine if the newly developed jig saves time in the production of end-frames, the rate of cooling of Wood's alloy for both the commercial and newly developed jig was measured. The experiment was conducted as follows:

A thermistor with a resistance of 10 k Ω was inserted into a thin-walled aluminium sleeve with heat transfer paste to ensure effective heat conduction to the thermistor. The thermistor was connected to an NI-USB 6009 data

acquisition unit from National Instruments. The data acquisition unit was in turn connected to a laptop which ran a programme written in LabView to log the temperatures measured by the thermistor.

5.3.1 Slow Cool in the Commercial and Newly Developed Jig

Solid end-frames of 10 cm x 10 cm size were cast in the commercial jig and the newly developed jig, respectively. As soon as the Wood's alloy was cast, the tip of the sleeve with the thermistor was submerged in the molten alloy. The alloy was then allowed to solidify slowly at room temperature (21.5 °C) with no additional cooling supplied. Each second a new temperature measurement was logged. Results from the measurements are tabulated in Appendix F and summarized in the following graph shown in Figure 5.14.



Figure 5.14: Cooling rate comparison between the commercial rubber jig and the new jig

Comparing the slow-cooling method on the newly developed jig to the commercial rubber jig, one can see that the new jig cools down faster by nearly 23 minutes. This can be ascribed to the thermal conductivity of the aluminum

frame (205 W/mK), whereas the rubber frame's thermal conductivity (0.17 - 0.3 W/mK) is much lower [100] [101].

5.3.2 Slow and Fast Cool in Newly Developed Jig

The experiment was also repeated for the newly developed jig with the cooling of the base surface switched on once the aluminum sleeve was inserted. Results are shown tabulated in Appendix F and summarized in the graph shown in Figure 5.15.

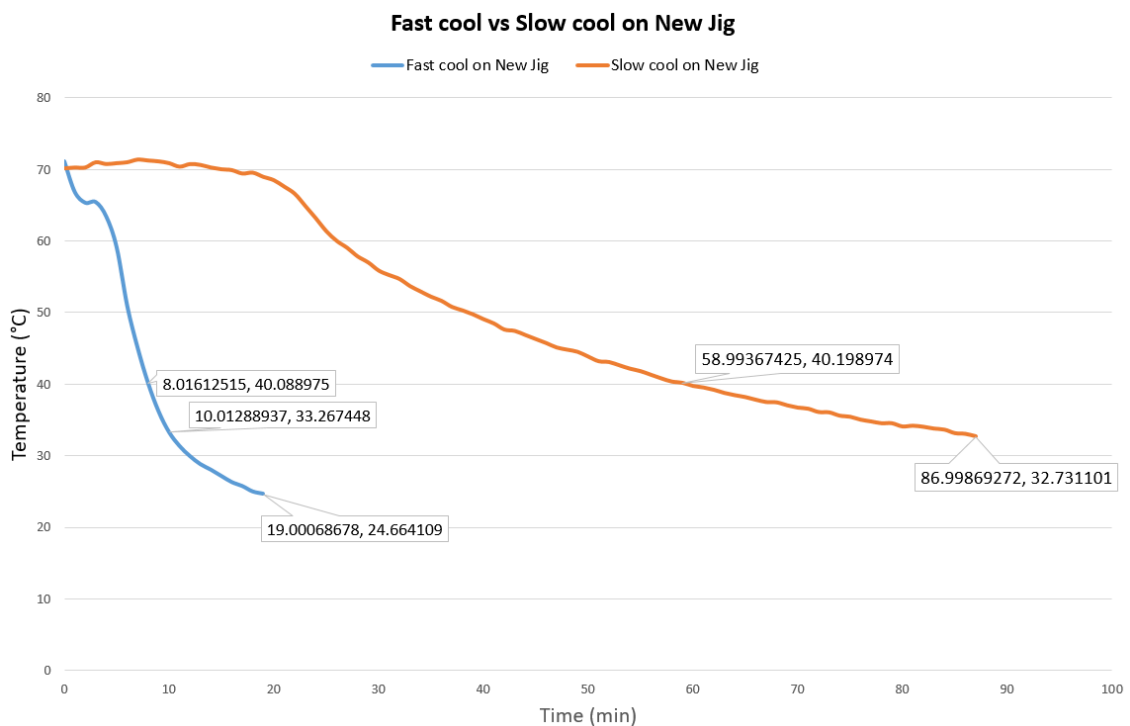


Figure 5.15: Cooling comparison between fast and slow cooling of the new jig

The graph clearly shows that the fast-cool method considerably reduces the casting time of the end-frames compared to the slow-cool method on the cooling base with the new jig. Safe surface touch temperatures are below 44 °C [102] and the frames could be removed once this temperature was reached.

Two callouts at 40 °C were added on the graph to indicate the time when one can remove the end-frames. The end-frame on the fast-cooled jig can be

removed after 8 minutes of cooling compared to nearly 60 minutes of cooling without cooling aid.

5.4 Density Comparison

As was discussed in Section 3.4.2, cavities form in the Wood's alloy end-frames when slow cooled. The cavities in the end-frames will decrease the overall shielding of the end-frame at that position and should be avoided. The solution created and discussed in Section 4.3.2 with the newly developed jig, is to cool the cast end-frame from the bottom with a cooling base.

To see if the newly developed jig improves on the density of the cast end-frames, the following experiment was conducted. Three 10 cm x 10 cm end-frames were cast on the commercial (Aktina) and newly developed jigs each. The commercial jig castings were left to cool at room temperature and the newly developed jig castings were fast cooled. For this experiment, treatment portals were not included in the end-frames to increase visibility of any cavities that may have formed.

The top surfaces of the cast end-frames were subsequently machined on a CNC milling machine to a thickness of 12 mm. A uniform thickness was required in order to perform density comparisons between the different castings.

An initial inspection on the end-frames cast on the commercial Aktina jig showed shallow cavities on the bottom surfaces (see Appendix G). Some of the cavities inside the end-frames were exposed during machining (Figure 5.16).



Figure 5.16: Top and bottom surface of an end-frame cast on the commercial jig showing cavities

The end-frames cast on the newly developed jig with aided cooling had no apparent cavities on the bottom surfaces other than the holes required for the binary coding system and locating pins. There were also no cavities evident on the machined side of the end-frames (Figure 5.17).



Figure 5.17: Top and bottom surface of a fast-cooled end-frame cast on the new jig

In addition to the obvious cavities on the surface of the end-frames, there may be hidden cavities inside the castings. A means to determine this is to investigate how effectively the end-frames shield radiation. Radiation passing through areas of the end-frames would indicate lower density and thus porosity or cavities. The six end-frames were taken to the Oncology Department at the

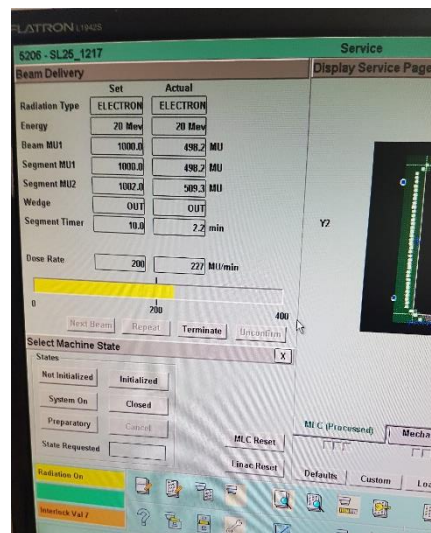
National Hospital in Bloemfontein where they were tested on an Elekta SL25 linac.

Gafchromic film was used for the experiment which changes colour when exposed to ionizing radiation. The film does not require development such as is required with conventional X-ray films.

The height of the Elekta SL25 linac's table was adjusted to isocentre which is one metre from the source of radiation in the machine's treatment head. A sheet of Gafchromic film was placed on the table and four of the Wood's alloy castings placed on top of it; two of the slow-cooled-, and two of the fast-cooled end-frames (Figure 5.19). An electron energy of 20 MeV was selected on the linac and the film was exposed at 1 000 MU (Figure 5.18). The end-frames were exposed in sets to save on film used.



(a)



(b)

Figure 5.18: (a) Four end-frames exposed to electron radiation at isocentre with an applicator attached to unit and (b) settings on the linac during irradiation

To use the electron radiation option of the linac, an applicator must be attached to the treatment head (Figure 5.18). For the experiment, the largest available electron applicator (25 cm x 25 cm) was used with no end-frame placed in the applicator end.



Figure 5.19: Four end-frames placed on a Gafchromic film

Because of the high density of the Wood's alloy, not much of a colour change took place on the film even when a larger radiation dose was applied (Figure 5.20 and Appendix H). This was expected since 12 mm is sufficient to shield the electron radiation at 20 MeV, as was shown in Section 3.4.2.

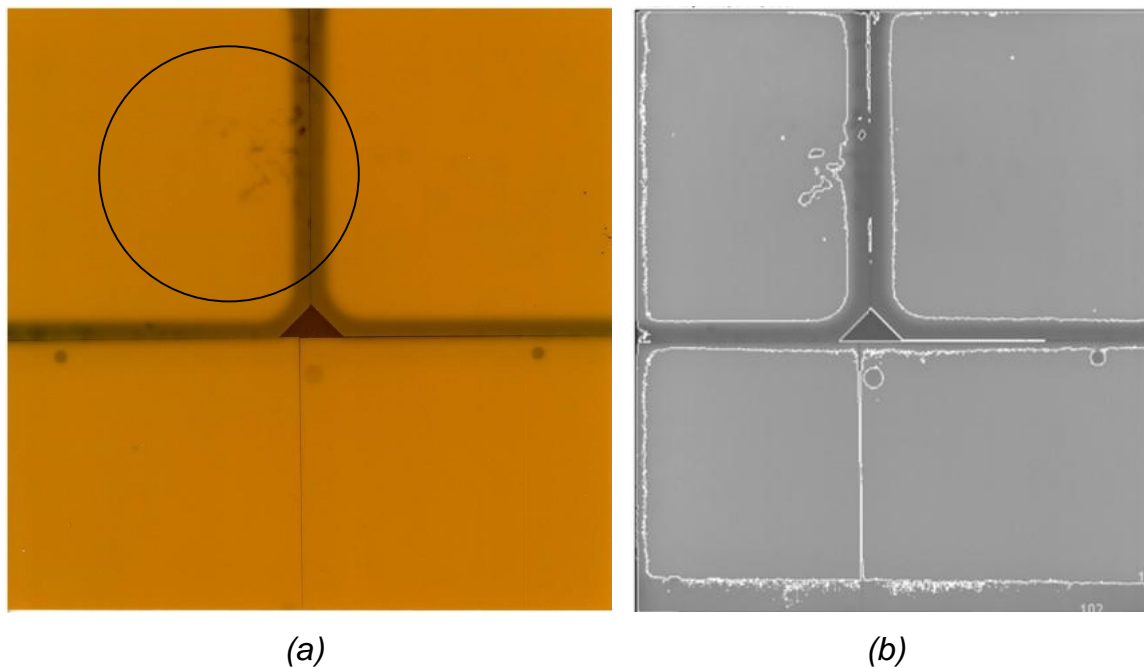


Figure 5.20: (a) Gafchromic film after exposure to electron radiation and (b) processed film to highlight differences

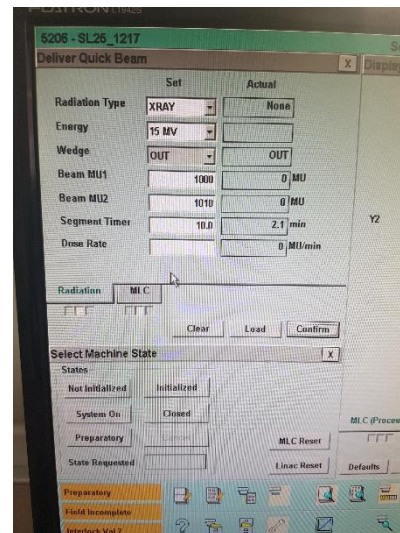
The effect on the edge of the Aktina end-frames that did not have a 12 mm thickness can be clearly seen on the film. In Figure 5.20 (a), some darker spots can also be seen on the film where the shielding of the slow-cooled end-frames was not sufficient, thus indicating cavities inside the end-frame. The circular dark spots on the fast-cooled end-frames are due to the locating and binary holes in the end-frame.

The films were scanned on an Epson desktop scanner set at 600 dpi. and processed with ImageJ where the differences were highlighted using the Glasbey lookup table. The highlighted areas indicate a difference in shielding ability, as shown in Figure 5.20 (b).

It was decided to switch to photon radiation which has a higher energy to penetrate the Wood's alloy to better show irregularities in the density of the castings. 15 MV was selected on the linac and a new sheet of Gafchromic film was exposed at 1 000 MU for each set (Figure 5.21). The end-frames were exposed in sets of two, one slow cooled and one fast cooled. This was repeated for all six castings (Figure 5.22 (a), (d), (g)).



(a)



(b)

Figure 5.21: (a) Gafchromic film placed at isocentre with two end-frames to be exposed and (b) settings on the linac during irradiation

The photon radiation had a more pronounced discolouration of the film. All the films were scanned on the Epson desktop scanner set at 600 dpi. Due to the reflectiveness of the films, some light-coloured marks are visible on the images which can be attributed to the scanning process (Figure 5.22 (b), (e), (h) and Appendix I).

The photon irradiated images were also processed on ImageJ to highlight changes in shielding ability better than what can be illustrated with the film itself (Figure 5.22 (c), (f), (i)).

Each of the slow-cooled frames does show some dark spots which indicate higher transmission than the rest of the frame. This was also seen on the thinner edge of the slow-cooled frames and the binary and locating pins of the fast-cooled frames. The position of the cavities inside the end-frames are not the same for each end-frame, and there is no apparent way to tell if and where cavities will occur in the slow-cooled end-frames.

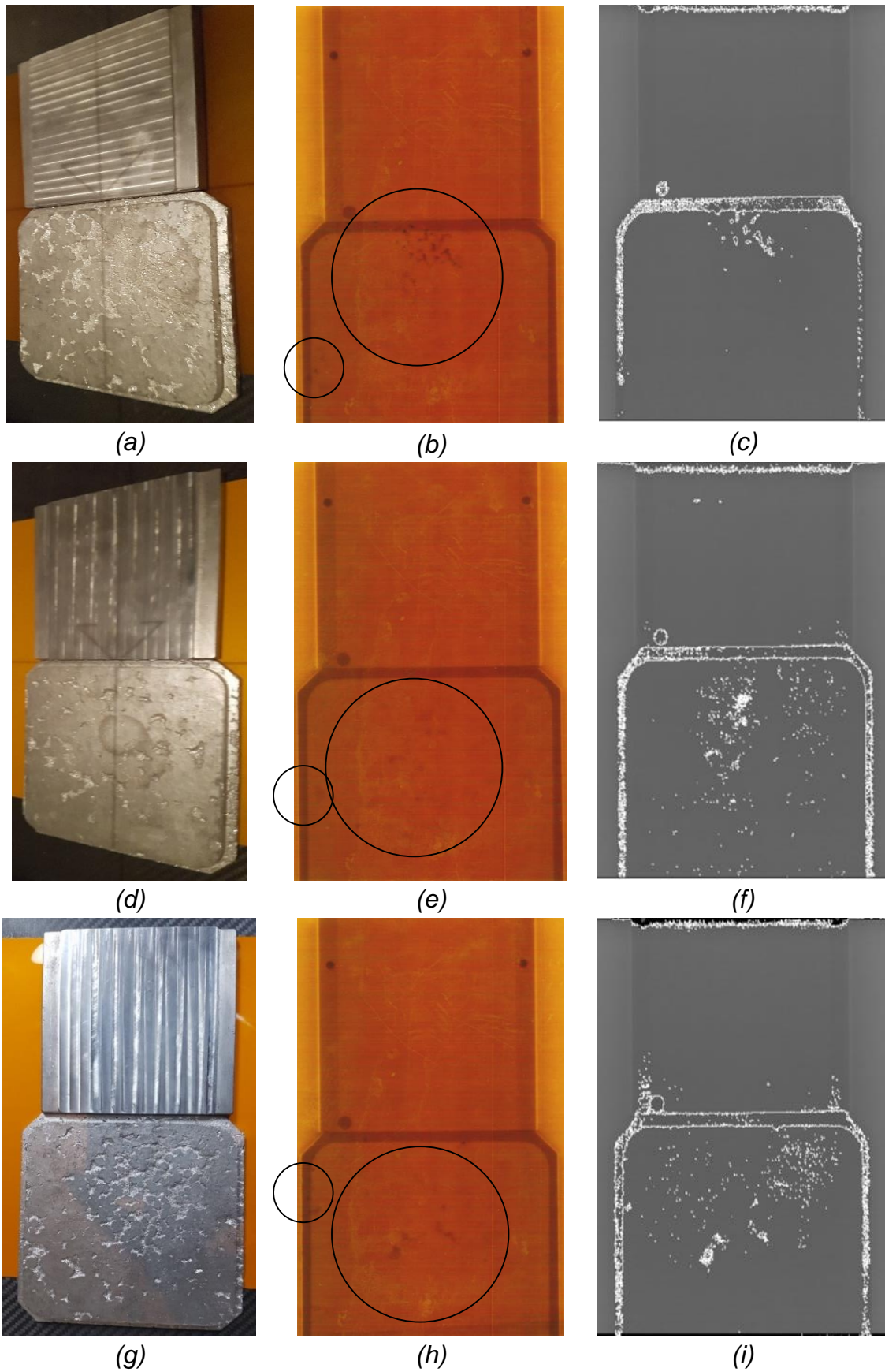


Figure 5.22: End-frames sets exposed with the corresponding Gauchromic film and processed image to highlight difference in level of transmission

The purpose of this experiment was not to quantify the amount of radiation that passes through the cavities in the end-frames but merely to indicate that there is uneven density across the slow-cooled end-frames which may result in radiation transmission.

5.5 Cost Comparison

At the time of submission, the only quote received for commercial casting equipment was from RDPinc. The items quoted were for Varian Linacs and Siemens Linacs only. A summary of the billed items are as follows:

| | |
|---|-------------|
| Plate for Varian III Electron Cone Insert Frames | R 18 203.00 |
| Varian III Insert Frame for Electron Cone Block (3 sizes) | R 5 602.00 |
| Siemens Primus Electron Block Mould (5 sizes) | R 37 711.00 |
| Shipping + wire transfer | R 26 746.00 |

A quote for the newly developed casting unit was sourced from a local product developer, Product Development and Technology Station (PDTs). The costs are summarized below:

| | |
|--|-------------|
| Aluminium Cooling Base | R 10 600.00 |
| Aluminium Casting Frames (5 sizes) | R 14 500.00 |
| Casting Unit (Without Base and Frames) | R 4 920.00 |

Total: R 30 020.00

Chapter 6: Conclusion

6.1 Conclusion

The aim of this study was to develop equipment for casting Wood's alloy end-frames that are an improvement on end-frames that can be produced through commercially available equipment in terms of dimensional accuracy, density, time and cost. To achieve this aim, three objectives were set which focussed on a literature overview, development of new casting equipment and testing of end-frames produced through the casting equipment, respectively. Specific requirements for the development and testing of the equipment were set under Objectives 2 and 3 (Section 1.3.1).

In order to meet Objective 1, a comprehensive literature overview on skin cancer and different treatment techniques are presented in Chapter 2. Chapter 3 focusses on radiation therapy and techniques developed to shape electron radiation fields. It was concluded from this chapter that various shortcomings exist in the production of electron field shaping end-frames using commercially available casting-jigs.

In Chapter 4, design iterations one and two of preliminary work that was done in the development of a new casting-jig is presented together with methods of cooling the jig. This led to the development of the casting-jig that forms the focus of this study.

A requirement set for the new casting-jig (Objective 2a) was to limit the expansion of the Wood's alloy while solidifying. This was addressed by producing aluminium casting-frames which limit expansion of the Wood's alloy more effectively compared to the rubber-frames that are used in commercial casting-jigs.

Objectives 2a and 2b require even cooling across the base of the new casting-jig to ensure that no cavities form in the end-frame while the Wood's alloy solidifies, as well as a means of heating the base to ease the flow of the alloy while casting. This was achieved through the design of a base with channels which was divided into four quadrants with multiple inlets and outlets to ensure even cooling when cold water is pumped through the channels. The same channels can provide heating of the base if hot water is pumped through the channels.

Even cooling of the base was first demonstrated by simulating the CAD model on Ansys. Once the base was manufactured, IR images were taken at regular time intervals while cooling. The simulated results and IR images correspond well with differences ascribed to items such as screws that hold the layers of the base together that were not considered in the CAD model.

The new casting equipment developed for this study include the casting-jig with cooling base, pot for melting the Wood's alloy and urn for heating the water, all in one unit. Provision was made for the binary code as well as locating pins required for Elekta-type end-frames with no additional machining required to finish the products. End-frames can therefore be conveniently produced with the equipment which satisfies this requirement, as stated under Objective 2c.

Determining the dimensional accuracy of end-frames produced was required under Objective 3a. This was performed by comparing end-frames produced in the new casting equipment to end-frames produced in a commercial casting jig using measurements with a digital Vernier calliper. The end-frames produced in the new casting jig performed consistently better compared to those produced in the commercial jig and were able to meet the 0.5 mm tolerance set for Elekta-type end-frames.

Casting time (Objective 3b) was compared between end-frames cast in the new and commercial jigs using measurements with a thermistor connected to a data acquisition unit and data logger. The Wood's alloy in the new casting jig cooled to a safe-to-remove temperature of 40 °C within eight minutes while the same

was only possible after 70 minutes for the commercial jig. End-frames can, therefore, be produced significantly faster using the newly developed equipment compared to the commercially available jig.

In comparing the densities (Objective 3c) of end-frames produced by means of the commercial and new casting equipment, the new equipment performed significantly better. Shallow cavities were obvious on the bottom of end-frames produced in the commercial casting jig. These cavities were also found to extend to the top surface of the castings in some cases when the top surface of the end-frames was machined level.

Gafchromic films taken when the end-frames were exposed to photon radiation on an Elekta LS25 linac also indicated cavities inside the castings. None of the cavities were evident on the surface or inside end-frames produced through rapid cooling using the new casting equipment. The consistently high density of the end-frames produced using the new equipment will ensure effective shielding for electron field shaping purposes.

A cost comparison (Objective 3d) between the new equipment and the commercial casting jig shows that the cost of the complete casting unit is about the same as an imported commercial jig. However, if the import cost is included, the commercial jigs are more expensive.

Considering the comparisons between the commercial and new casting equipment described above, all the objectives set for the new end-frame casting equipment have been met and the aim of this study has therefore also been achieved.

6.2 Future Work

Although substantially more even cooling could be achieved in the new casting-jig base compared to previous cooling blocks, as described in Section 4.3.2.1, this can still be improved upon. Future work will focus on further simulations

using Ansys to find an even better layout of cooling channels inside the casting-jig base. The depth of the channels inside the base can, for example, be varied for more even cooling across the surface.

The casting-frames developed for the new casting-jig can be improved upon since the current frames allow for some play in the quick-release clamps which causes an increase in dimensions of the end-frames when the Wood's alloy expands while cooling. A different method needs to be found to hold the two halves of the clamps together while still being easy to release.

References

- [1] D. Mutter, G. Bouras and J. Marescaux, "Digital Technologies and Quality Improvement in Cancer Surgery", *European Journal of Surgical Oncology: The Journal of the European Society of Surgical Oncology and the British Association of Surgical Oncology*, vol. 31, no. 6, pp. 689-694, 2005.
- [2] M. Kulendran et al., "Global Cancer Burden and Sustainable Health Development", *Lancet*, vol. 9865, no. 381, pp. 427-9, 2013.
- [3] F. Bray et al., "Global Cancer Transitions According to the Human Development Index (2008-2030): A Population-based Study", *The Lancet. Oncology*, vol. 13, no. 8, pp. 790-801, 2012.
- [4] Y. Imoto et al., "The Cell Cycle, Including the Mitotic Cycle and Organelle", *Journal of Electron Microscopy*, vol. 60, no. 1, pp. 117-136, 2011.
- [5] R. Milo and R. Phillips, *Cell Biology by the Numbers*, New York: Garland Science, 2015.
- [6] M. Kent, *Advanced Biology*, New York: Oxford, 2000.
- [7] P. Crosta, "Medical News Today", 24 November 2015. [Online]. Available: <http://www.medicalnewstoday.com/info/cancer-oncology>. [Accessed 30 June 2017].
- [8] D. Kimura, *Cell Growth Processes: New Research*, New York: Nova Science, 2008.
- [9] L. M. Franks and N. M. Teich, *Cellular and Molecular Biology of Cancer*, New York: Oxford University Press, 2003.
- [10] SEER, "SEER Training: Cancer Classification", National Institutes of Health, [Online]. Available: <http://training.seer.cancer.gov/disease/categories/classification.html>. [Accessed 08 January 2015].
- [11] SEER, "SEER Training: Cancer Types by Site", [Online]. Available: <https://training.seer.cancer.gov/disease/categories/site.html>. [Accessed 5

- July 2017].
- [12] American Institute for Cancer Research, "World Cancer Research Fund International", [Online]. Available: <http://www.wcrf.org/int/cancer-facts-figures/worldwide-data>. [Accessed 05 July 2017].
- [13] P. W. Nee, *The Key Facts on Cancer Types*, vol. 2, Boston: MedicalCenter.com, 2013.
- [14] E. McLafferty, C. Hendry and A. Farlay, "The Integumentary System: Anatomy, Physiology and Function of Skin", *Nursing Standard*, vol. 27, no. 3, pp. 35-42, 2012.
- [15] G. A. Starkebaum, "MeclinePlus", [Online]. Available: <http://www.nlm.nih.gov/medlineplus/ency/imagepages/8912.htm>. [Accessed 6 July 2017].
- [16] R. Narayan, *Biomedical Materials*, New York: Springer, 2009.
- [17] K. S. Saladin, *Human Anatomy*, New York: McGraw-Hill, 2007.
- [18] DermNet NZ, "Principles of Dermatological Practice", [Online]. Available: <https://www.dermnetnz.org/cme/principles/structure-of-the-epidermis/>. [Accessed 22 January 2015].
- [19] J. J. Davis, *Essentials of Medical Terminology*, New York: Cengage, 2008.
- [20] F. H. Martini, *Anatomy and Physiology*, Singapore: Pearson, 2007.
- [21] C. Turkington and J. S. Dover, *The Encyclopedia of Skin and Skin Disorders*, 3rd ed., New York: Facts on File, 2007.
- [22] C. Hinrichsen, *Organ Histology: A Student's Guide*, Singapore: World Scientific, 1997.
- [23] W. H. Burgdorf et al., *Dermatopathology*, New York: Springer-Verlag, 1984.
- [24] T. Slevin, *Sun, Skin and Health*, Collingwood: CSIRO, 2014.
- [25] D. S. Rigel, *Cancer of the skin*, Utah: Elsevier, 2011.
- [26] A. Krilaviciute, I. Vincerzevskiene and G. Smailyte, "Basal Cell Skin Cancer and the Risk of Second Primary Cancers", *Anal of Epidemiology*, vol. 26, no. 7, pp. 511-514, 2016.

- [27] C. Goldsmith, *Skin Cancer*, Minneapolis: Lerner, 2011.
- [28] J. Reichrath, *Molecular Mechanisms of Basal Cell and Squamous Cell Carcinomas*, New York: Springer, 2006.
- [29] E. C. Halperin, C. A. Perez and L. W. Brady, *Perez and Brady's Principles and Practice of Radiation Oncology*, Philadelphia: Lippincott, 2008.
- [30] L. Nathanson, *Current Research and Clinical Management of Melanoma*, New York: Springer, 1993.
- [31] R. Prasad and S. K. Katiyar, "Green Tea Polyphenols Inhibit the Growth and Induce Death of Melanoma Cells by Initiating DNA Damage and Inhibition of Class I Histone Deacetylases", in *AACR Annual Meetings*, San Diego, 2014.
- [32] M. J. Murphy, *Diagnostic and Prognostic Biomarkers and Therapeutic Targets in Melanoma*, London: Springer, 2012.
- [33] J. A. Bishop and M. Gore, *Melanoma: Critical Debates*, Oxford: Blackwell Science, 2002.
- [34] M. Simões, J. J. Sousa and A. A. Pais, "Skin Cancer and New Treatment Perspectives: A Review", *Cancer Letters*, vol. 357, no. 1, pp. 8-42, 2015.
- [35] S. Chummun and N. R. McLean, "The Management of Malignant Skin Cancers", *Surgery*, 2017.
- [36] A. Baldi, P. Pasquali and E. P. Spugnini, *Skin Cancer: A Practical Approach*, New York: Springer, 2014.
- [37] D. L. Stulberg, B. Crandell and R. Fawcett, "Diagnosis and Treatment of Basal Cell and Squamous Cell Carcinomas", *American Family Physician*, vol. 70, no. 8, pp. 1481-1488, 2004.
- [38] B. Krans, "Cryosurgery", Healthline, 16 December 2015. [Online]. Available: <http://www.healthline.com/health/cryosurgery#overview1>. [Accessed 11 August 2017].
- [39] C. M. Scott, G. F. Graham and R. R. Lubritz, "Recovery", in *Dermatological Cryosurgery and Cryotherapy*, London, Springer, 2016, pp. 219-220.

- [40] W. I. Lane and L. Comac, *The Skin Cancer Answer*, New York: Avery, 1999.
- [41] D. F. MacFarlane, *Skin Cancer Management: A Practical Approach*, London: Springer, 2010.
- [42] E. Craythorne and F. Al-Niami, "Skin Cancer", *Medicine*, vol. 45, no. 7, pp. 431 - 434, 2017.
- [43] A. H. Ko, M. Dollinger and E. H. Resenbaum, *Everyone's Guide to Cancer Therapy: How Cancer is Diagnosed, Treated and Managed Day to Day*, Kansas City: Andrews McMeel, 2008.
- [44] Perlmutter Cancer Center, "Surgical Procedures for Basal & Squamous Cell Skin Cancers", NYU Langone Hospitals, [Online]. Available: <http://nyulangone.org/conditions/basal-squamous-cell-skin-cancers-in-adults/treatments/surgical-procedures-for-basal-squamous-cell-skin-cancers>. [Accessed 20 July 2017].
- [45] M. C. Perry, *The Chemotherapy Source Book*, Philadelphia: Lippincott Williams & Wilkins, 2008.
- [46] K. R. Aigner and F. O. Stephens, *Induction Chemotherapy: Systemic and locoregional*, Berlin: Springer, 2016.
- [47] D. S. Rigel, *Cancer of the Skin*, Utah: Elsevier, 2011.
- [48] J. C. Westman, *The Cancer Solution*, Bloomington: Archway, 2015.
- [49] N. Rezaei, *Cancer Immunology*, London: Springer, 2015.
- [50] M. R. Girotti et al., "No Longer an Untreatable Disease: How Targeted and Immunotherapies have Changed the Management of Melanoma Patients", *Molecular Oncology*, vol. 8, no. 6, pp. 1140-1158, 2014.
- [51] V. Lazareth, "Management of Non-melanoma Skin Cancer", *Seminars in Oncology Nursing*, vol. 29, no. 3, pp. 182-194, 2013.
- [52] R. C. Rees, *Tumor Immunology and Immunotherapy*, Glasgow: Oxford University Press, 2014.
- [53] R. A. Swartz, *Skin Cancer: Recognition and management*, Massachusetts: Blackwell, 2008.
- [54] T. Patrice, *Photodynamic Therapy*, Cambridge: The Royal Society of

- Chemistry, 2003.
- [55] The Brown Reference Group, Diseases and Disorders; Volume 1, New York: Marshal Cavendish, 2008.
- [56] V. L. Heinz, Skin Cancer: New Research, New York: Nova Science, 2007.
- [57] R. Pottier et al., Photodynamic Therapy with ALA: A Clinical Handbook, Cambridge: Royal Society of Chemistry, 2006.
- [58] M. H. Gold, Photodynamic Therapy in Dermatology, New York: Springer, 2011.
- [59] R. K. Pandey, D. Kessel and T. J. Dougherty, Handbook of Photodynamic Therapy: Updates on Recent Applications of Porphyrin-based Compounds, Singapore: Word Scientific, 2016.
- [60] S. Levitt et al., Technical Basis of Radiation Therapy; Practical Clinical Applications, New York: Springer, 2012.
- [61] National Institutes of Health, Radiation Therapy and You: A Guide to Self-help During Cancer Treatment, US Department of Health and Human Services, 2000.
- [62] A. B. Cognetta and W. M. Mendenhall, Radiation Therapy for Skin Cancer, New York: Springer, 2013.
- [63] A. B. Reed, "The History of Radiation Use in Medicine", *Journal of Vascular Surgery*, vol. 53, no. 1, pp. 3S-5S, 2011.
- [64] B. J. Healy et al., "Cobalt-60 Machines and Medical Linear Accelerators: Competing Technologies for External Beam Radiotherapy", *Clinical Oncology*, vol. 29, no. 2, pp. 110-115, 2017.
- [65] National Research Council, "Radiation Source Use and Replacement: Abbreviated Version", The National Academies Press, Washington DC, 2008.
- [66] F. M. Khan, The Physics of Radiation Therapy, Philadelphia: Lippincott Williams & Wilkins, 2003.
- [67] C. M. Washington and D. T. Leaver, Principles and Practice of Radiation Therapy, St. Louis: Elsevier, 2016.

- [68] Radiology Oncology Systems, “Elekta Linear Accelerator Comparison Chart”, Radiology Oncology Systems, 2018. [Online]. Available: <https://www.oncologysystems.com/radiation-therapy/linear-accelerators/elekta-linear-accelerator-comparison-chart.php>. [Accessed 14 February 2018].
- [69] P. Cherry and A. Duxbury, *Practical Radiotherapy, Physics and Equipment*, Oxford: Blackwell Publishing, 2009.
- [70] D. B. Evans, P. W. Pisters and J. L. Abbruzzese, *Pancreatic Cancer*, New York: Springer-Verlag, 2002.
- [71] E. Shinohara, “Radiation Therapy: Which Type is Right for Me”, OncoLink, 05 March 2018. [Online]. Available: <https://www.oncolink.org/cancer-treatment/radiation/introduction-to-radiation-therapy/radiation-therapy-which-type-is-right-for-me>. [Accessed 22 March 2018].
- [72] V. Gregoire, P. Scalliet and K. K. Ang, *Clinical Target Volumes in Conformal and Intensity Modulated Radiation Therapy*, New York: Springer, 2004.
- [73] J. Tobias and D. Hochhauser, *Cancer and its Management*, Chichester: Wiley Blackwell, 2015.
- [74] S. O. Inyang and A. C. Chamberlain, “O.18 - Design and optimization of Dual Electron Multileaf Collimator”, *National Congress of the South African Association of Physicists in Medicine and Biology*, vol. 31, no. 53, p. S5, 2015.
- [75] P. Mayles, A. Nahum and J. Rosenwald, *Handbook of Radiotherapy Physics: Theory and Practice*, New York: Taylor & Francis, 2007.
- [76] Mueller S et al., “Electron Beam Collimation with a Photon MLC for Standard Electron Treatments”, *Phys. Med. Biol.*, vol. 63, no. 2, 2018.
- [77] T. Vatanen, E. Traneus and T. Lahtinen, “Comparison of Conventional Inserts and an Add-on Electron MLC for Chest Wall Irradiation of Left-sided Breast Cancer”, *Acta Oncologica*, vol. 48, no. 3, pp. 446-451, 2009.
- [78] T. Gauer et al., “Characterization of an Add-on Multileaf Collimator for

- Electron Beam Therapy”, *Phys. Med. Biol.*, vol. 53, no. 4, 2008.
- [79] W. Strydom, W. Parker and W. Olivares, “Electron Beams: Physical and Clinical Aspects”, in *Radiation Oncology Physics: A Handbook for Teachers and Students*, Vienna, International Atomic Energy Agency, 2005, pp. 273-299.
- [80] Oncology Parts, “Elekta Products”, [Online]. Available: <https://www.oncologyparts.com/collections/elekta/products/45133954001>. [Accessed 20 November 2018].
- [81] J. G. van der Walt, *Radiation Field Shaping Through Low Temperature Thermal-Spray in Radiotherapy*, Bloemfontein, 2009.
- [82] F. M. Khan, *The Physics of Radiation Therapy*, Philadelphia: Lippincott Williams & Wilkins, 2010.
- [83] Belmont Metals, “WOODS Metal, 158-169 F, 70-76 C Low Melting Alloy”, [Online]. Available: <https://www.belmontmetals.com/product/woods-metal/>. [Accessed 28 November 2018].
- [84] Reade International Corp., “Wood's Metal Alloy”, [Online]. Available: <https://www.reade.com/products/wood-s-metal-alloy>. [Accessed 28 November 2018].
- [85] Aktina Medical, “Electron Beam Shaping System for Elekta”, [Online]. Available: <http://www.aktina.com/product/electron-beam-shaping-system-for-elekta-beam-modulator/>. [Accessed 29 November 2018].
- [86] Radiation Products Design, Inc., “Elekta Electron Block Mold Set”, [Online]. Available: <https://www.rpdinc.com/elekta-electron-block-mold-set-5set-4411.html>. [Accessed 29 November 2018].
- [87] Aktina Medical, “Siemens Electron Beam Shaping System”, [Online]. Available: <http://www.aktina.com/product/siemens-electron-beam-shaping-system/>. [Accessed 29 November 2018].
- [88] Radiation Products Design, Inc., “Siemens Primus Electron Block Mold”, [Online]. Available: <https://www.rpdinc.com/siemens-electron-block-mold-4300.html>. [Accessed 29 November 2018].
- [89] Radiation Products Design, Inc., “Varian III with MLC, Insert Frame for Electron Cone Block”, [Online]. Available: <https://www.rpdinc.com/varian->

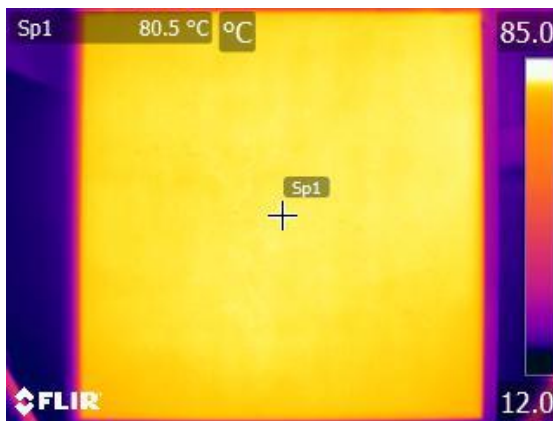
- electron-cone-block-frame-4385.html. [Accessed 29 November 2018].
- [90] Radiation Products Design, Inc., “Cooling Plate for Varian III Electron Cone Insert Frames”, [Online]. Available: <https://www.rpdinc.com/cooling-plate-for-varian-iii-electron-cone-insert-frames-8715.html>. [Accessed 29 November 2018].
- [91] S. Michiels et al., “Production of Patient-Specific Electron Beam Aperture Cutouts Using a Low-Cost, Multi-Purpose 3D Printer”, *Journal of Applied Clinical Medical Physics*, vol. 19, no. 5, pp. 1-5, 2018.
- [92] R. Rajkolhe and J. G. Khan, “Defects, Causes and Their Remedies in Casting Process: A Review”, *International Journal of Research in Advent Technology*, vol. 2, no. 3, pp. 375-383, 2014.
- [93] C. M. Choudharai, B. E. Narkhedeb and S. K. Mahajanc, “Methoding and Simulation of LM 6 Sand Casting for Defect Minimization with its Experimental Validation”, *Procedia Engineering*, vol. 97, pp. 1145-1154, 2014.
- [94] S. Priyadarsini, S. Pattnaik and M. K. Sutar, “Defects in Casting, their Causes and Remedial Measures: A Review”, *International Journal of Computer & Mathematical Sciences*, vol. 6, no. 11, pp. 228-234, 2017.
- [95] C. Stoll, “Facts About Bismuth”, Live Science, 20 11 2017. [Online]. Available: <https://www.livescience.com/39451-bismuth.html>. [Accessed 11 December 2018].
- [96] Metaconcept Groupe, “CERRO® ALLOYS”, [Online]. Available: <https://uk.metaconceptgroupe.com/produits/cerro-alloys/>. [Accessed 11 December 2018].
- [97] M. Denscombe, *Good Research Guide: For Small-scale Social Research Projects*, 4th ed., Berkshire, GBR: Open University Press, 2010.
- [98] P. B. Smith, “Irregular-shaped Fields in Electron Radiotherapy”, *The British Journal of Radiology*, vol. 64, no. 762, p. 561, 1991.
- [99] D. Dea and E. San Luis, “Casting of Electron Field Defining Apertures: Casting with the Metal Mold Kits”, *Medical Dosimetry*, vol. 13, no. 3, pp. 149-151, 1988.
- [100] C. R. Nave, “Thermal Conductivity”, Hyperphysics, 2016. [Online].

Available: <http://hyperphysics.phy-astr.gsu.edu/hbase/Tables/thrcn.html>.
[Accessed 31 May 2019].

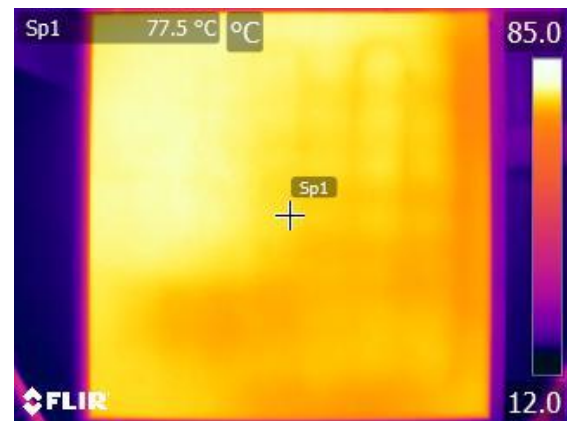
- [101] CLEAR, “Comfortable Low Energy ARchitecture”, [Online]. Available: https://www.new-learn.info/packages/clear/thermal/buildings/building_fabric/properties/conductivity.html. [Accessed 31 May 2019].
- [102] ASTM Committee, “Standard Guide for Heated System Surface Conditions That Produce Contact Burn Injuries”, in *ASTM Standards C 1055 - 99*, vol. 04, Conshohocken, American Society for Testing and Materials, 1999.

Appendix A

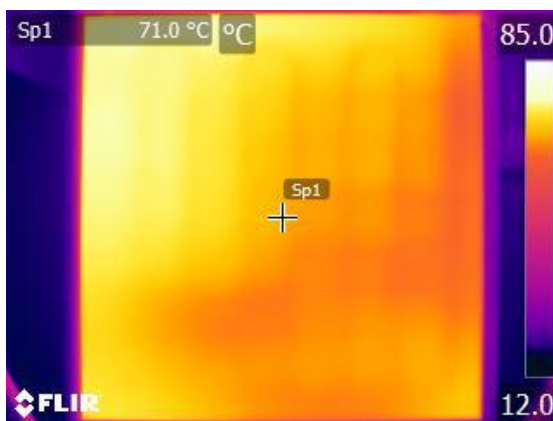
Infra-Red (IR) images of the second block design, taken at 20-second intervals with a FLIR E60 camera during cooling of the block.



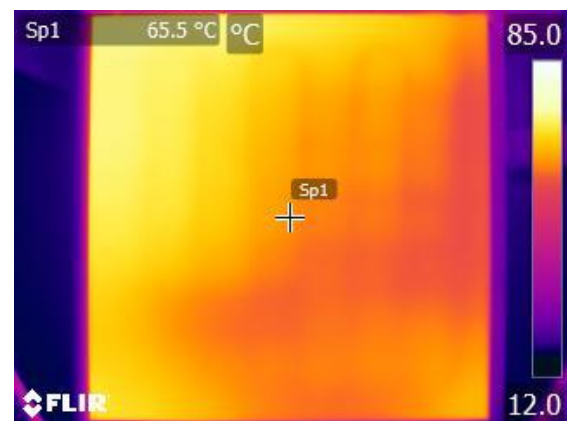
Time = 0 s; Temp = 80.5 °C



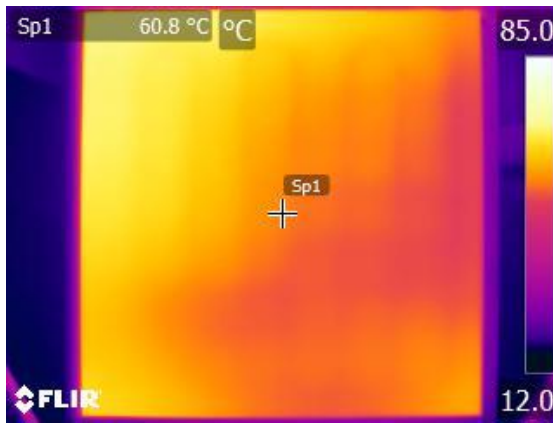
Time = 20 s; Temp = 77.5 °C



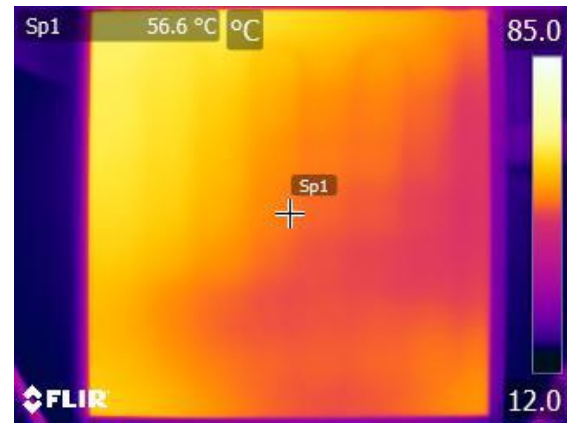
Time = 40 s; Temp = 71.0 °C



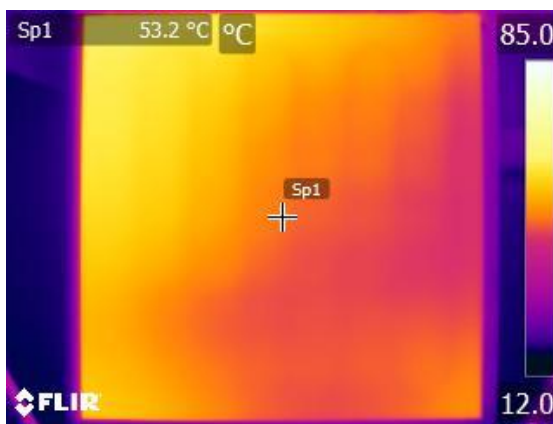
Time = 60 s; Temp = 65.5 °C



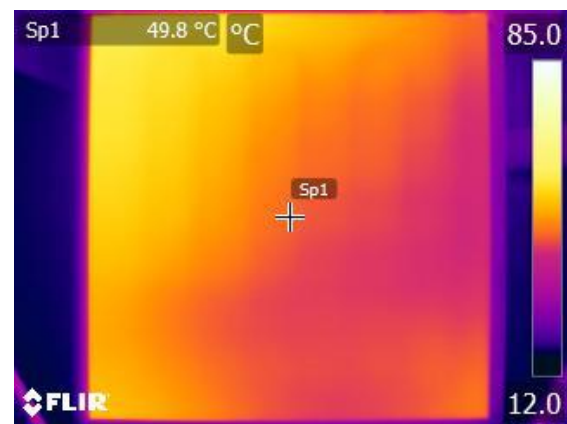
Time = 80 s; Temp = 60.8 °C



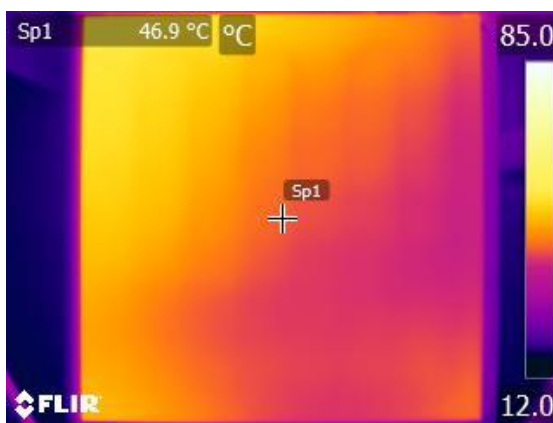
Time = 100 s; Temp = 56.6 °C



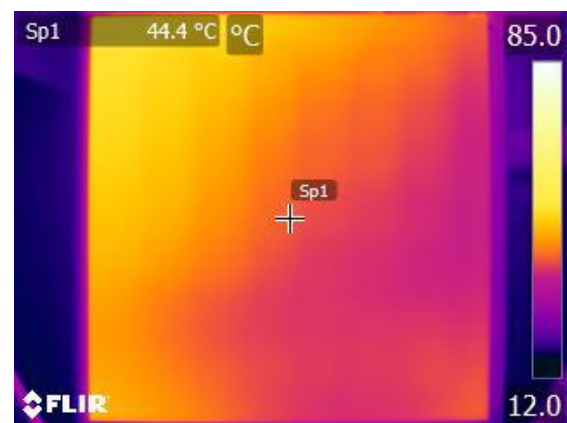
Time = 120 s; Temp = 53.2 °C



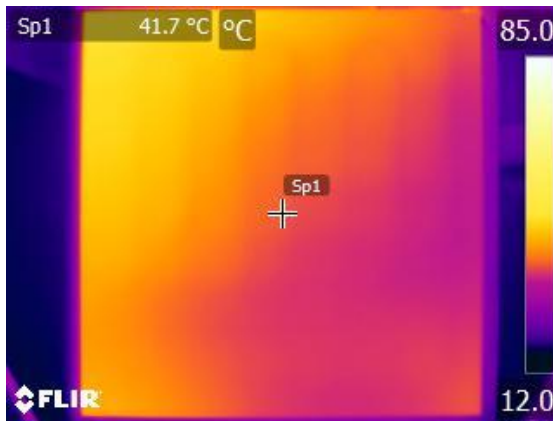
Time = 140 s; Temp = 49.8 °C



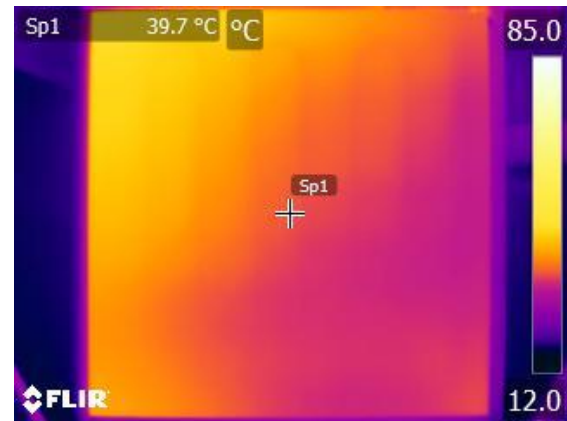
Time = 160 s; Temp = 46.9 °C



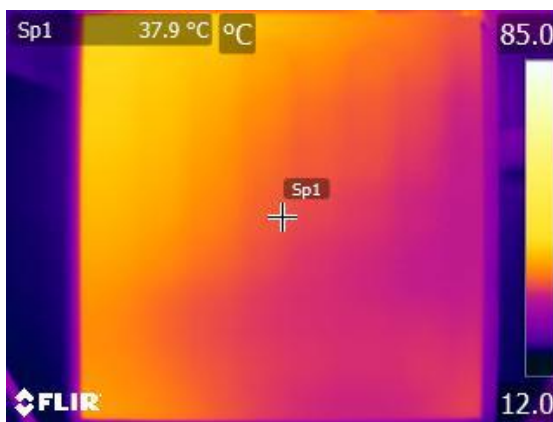
Time = 180 s; Temp = 44.4 °C



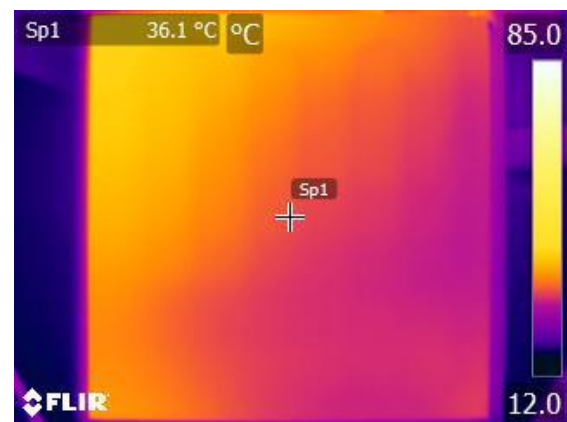
Time = 200 s; Temp = 41.7 °C



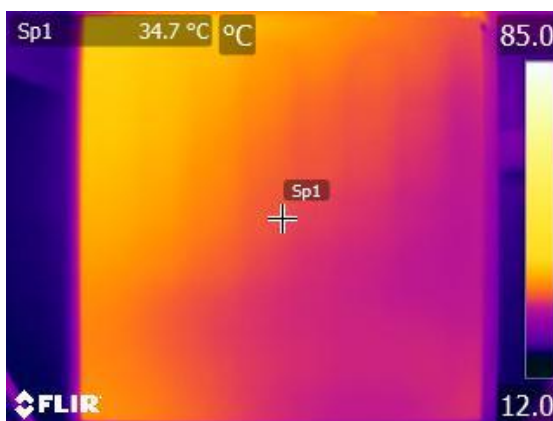
Time = 220 s; Temp = 39.7 °C



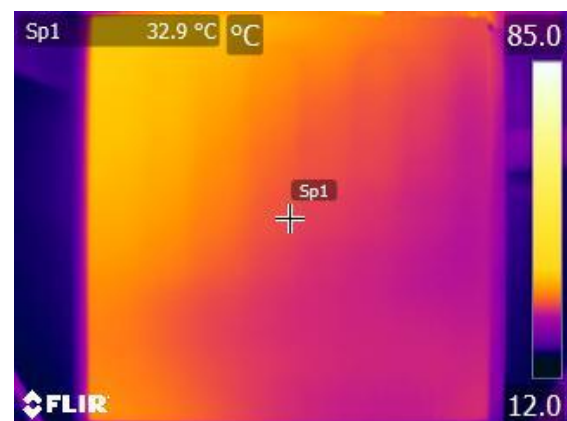
Time = 240 s; Temp = 37.9 °C



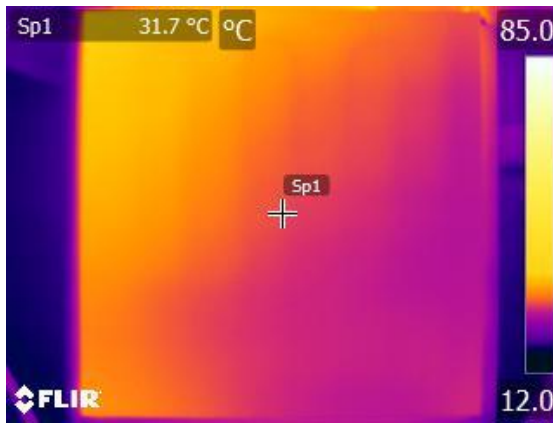
Time = 260 s; Temp = 36.1 °C



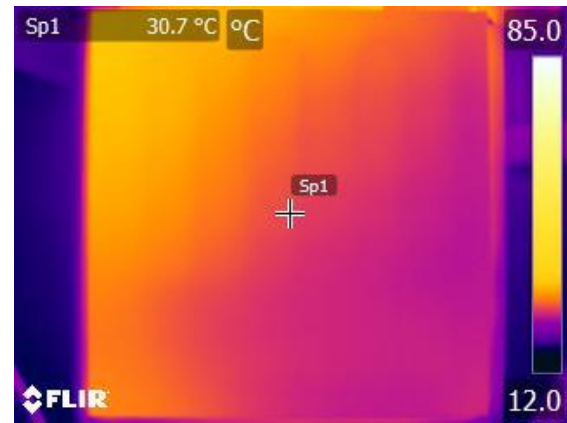
Time = 280 s; Temp = 34.7 °C



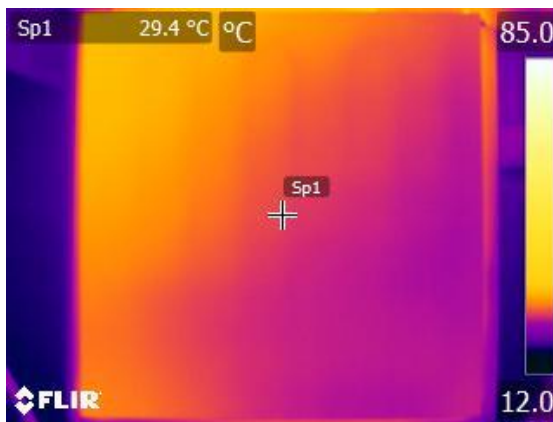
Time = 300 s; Temp = 32.9 °C



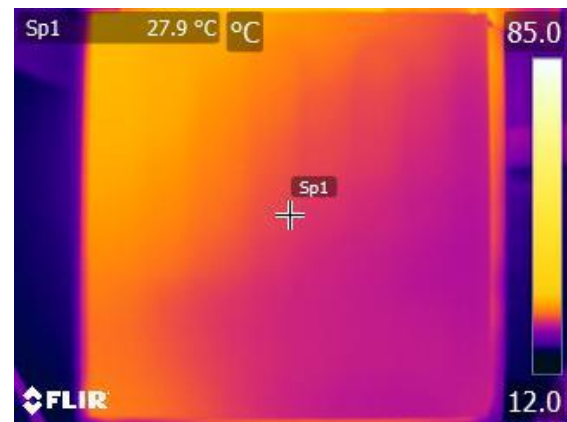
Time = 320 s; Temp = 31.7 °C



Time = 340 s; Temp = 30.7 °C



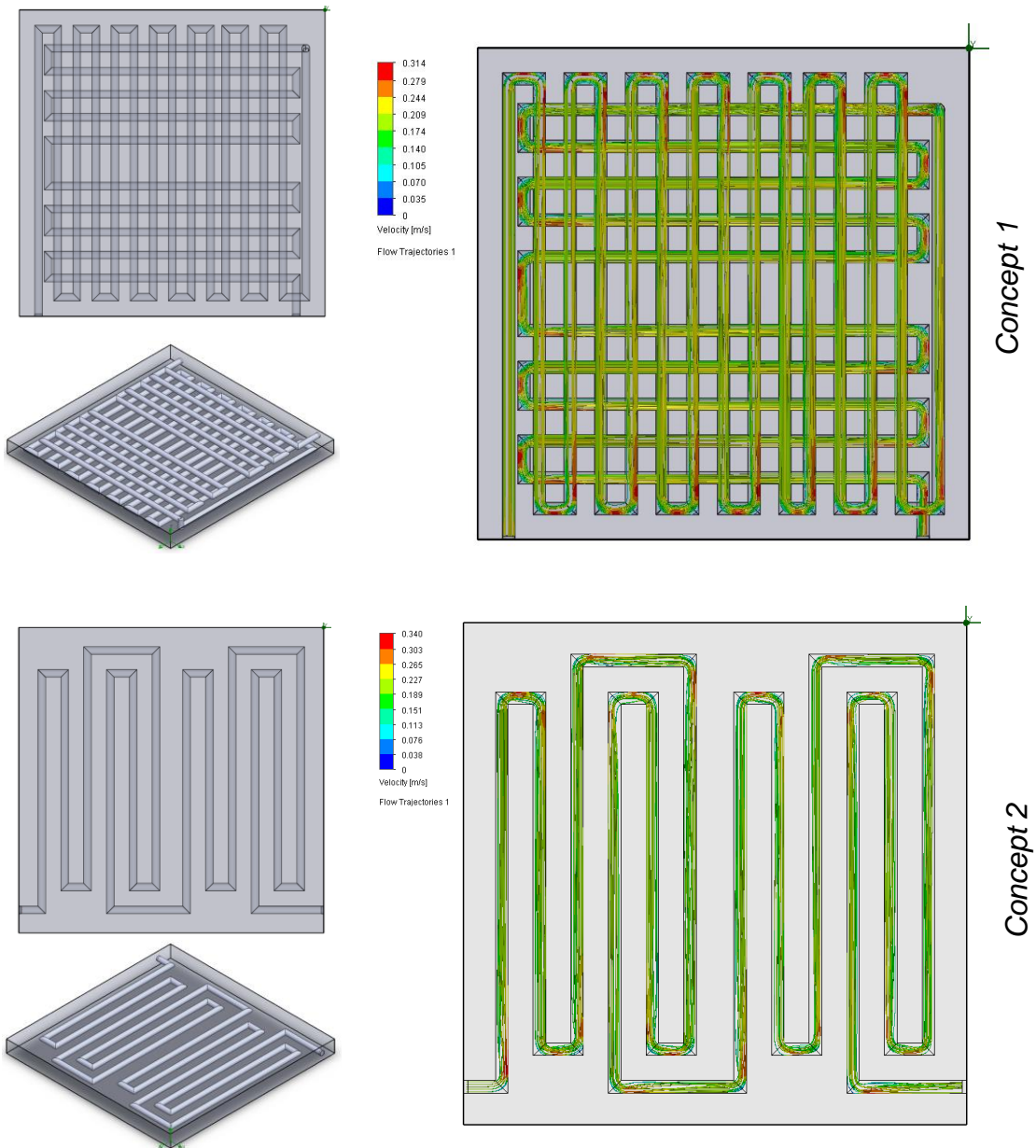
Time = 360 s; Temp = 29.4 °C

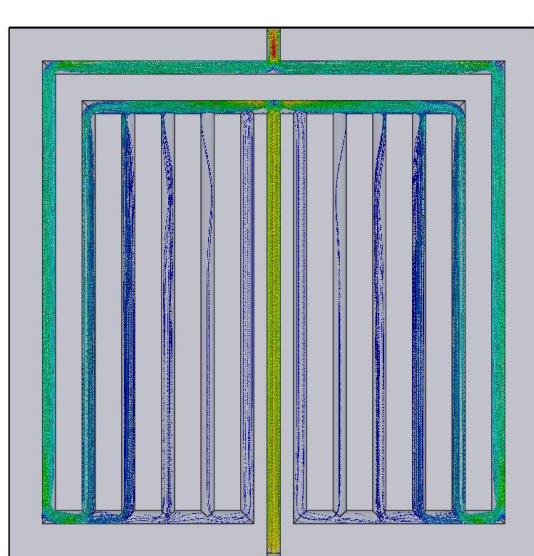
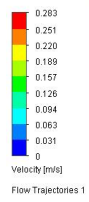
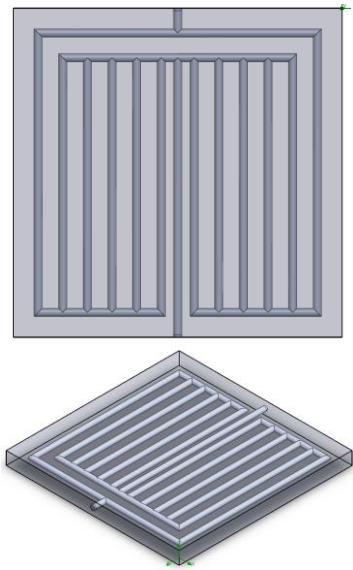


Time = 380 s; Temp = 27.9 °C

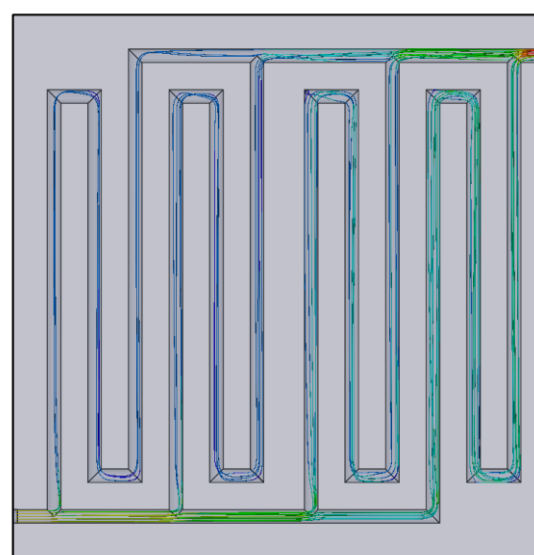
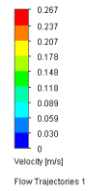
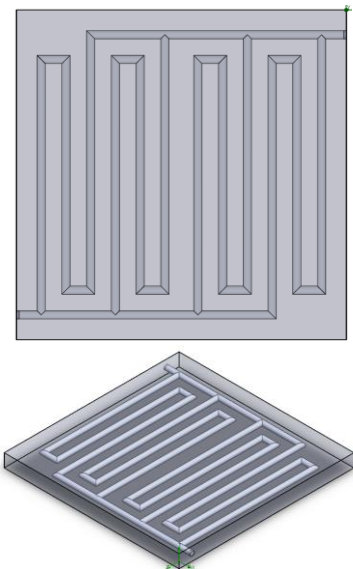
Appendix B

Channel layouts designed on SolidWorks™ to optimise the cooling base with flow simulation through the channels.

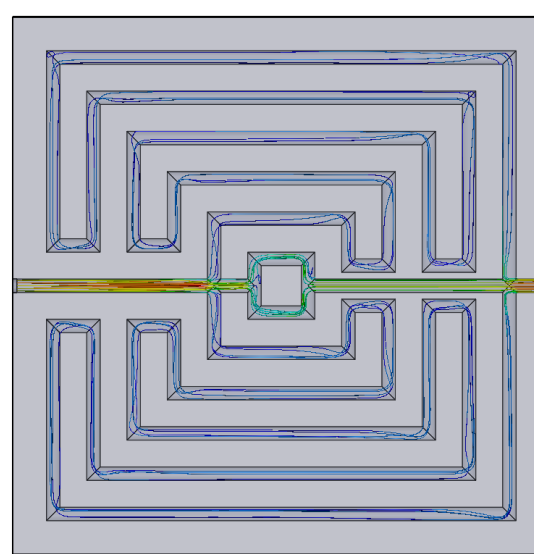
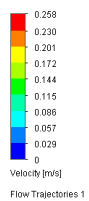
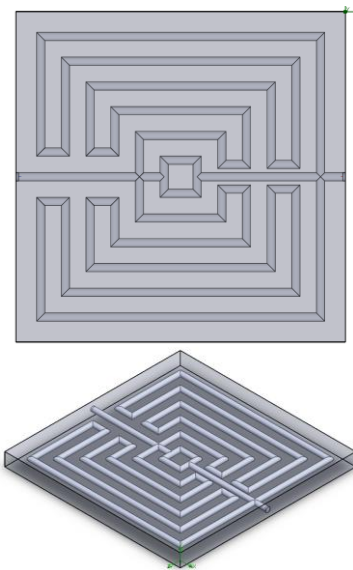




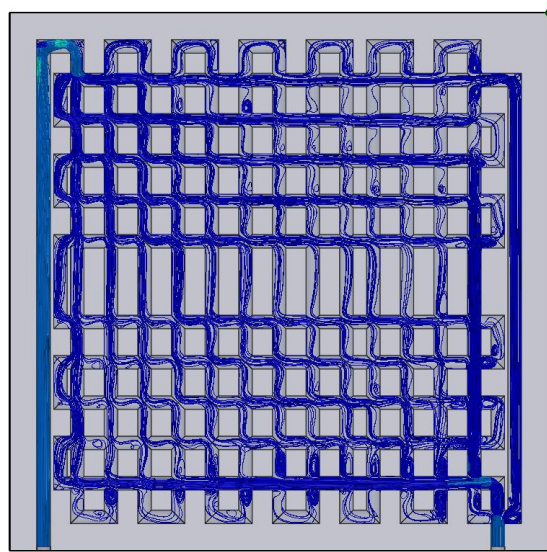
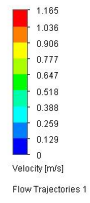
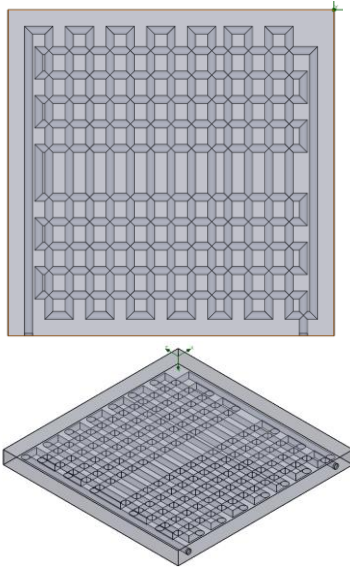
Concept 3



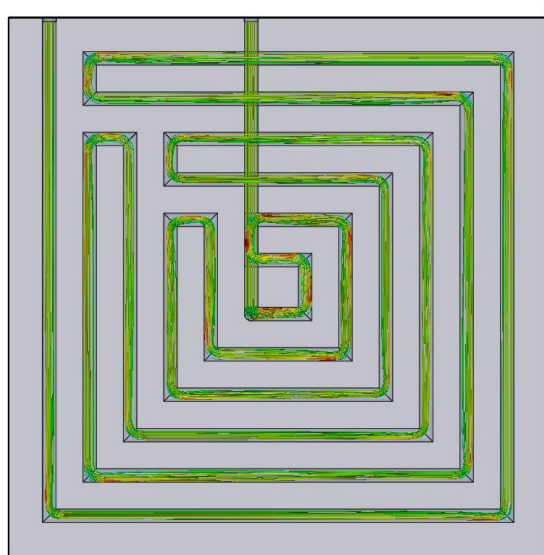
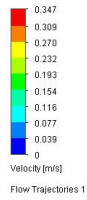
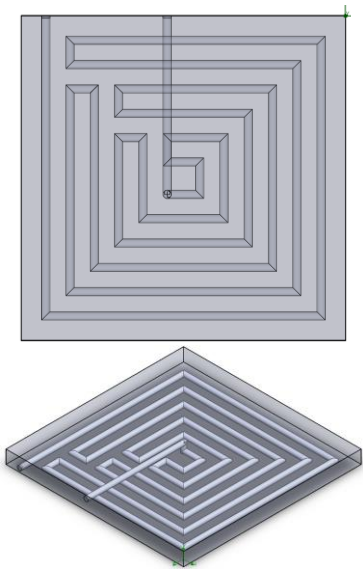
Concept 4



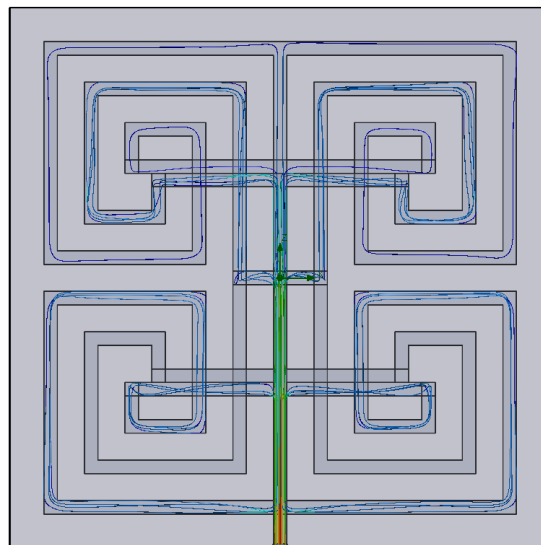
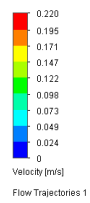
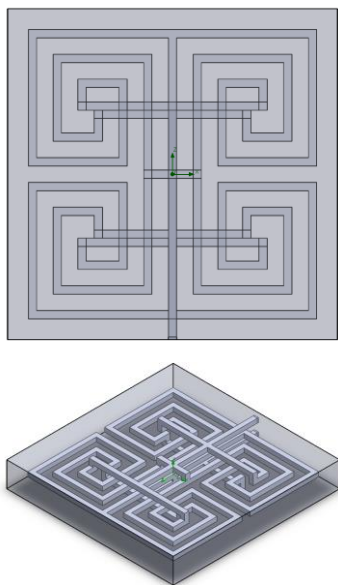
Concept 5



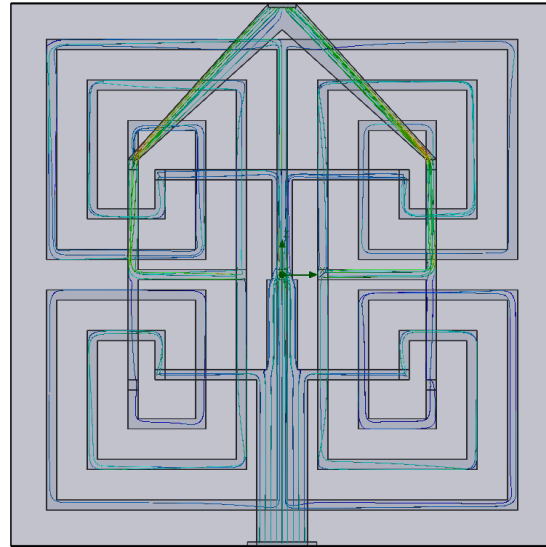
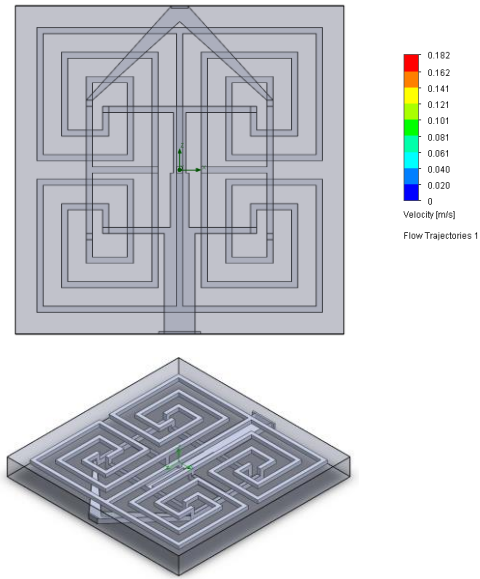
Concept 6



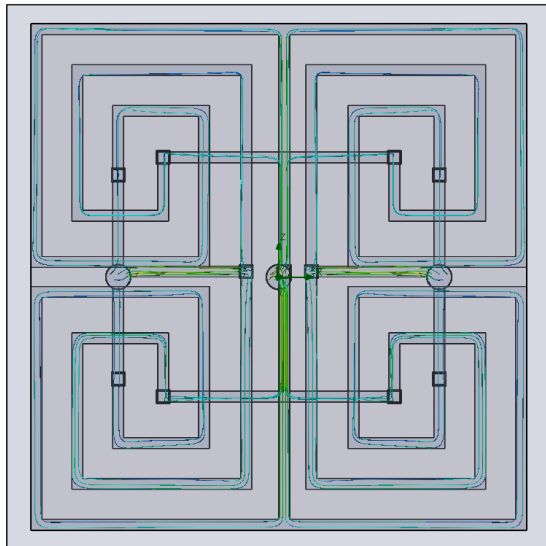
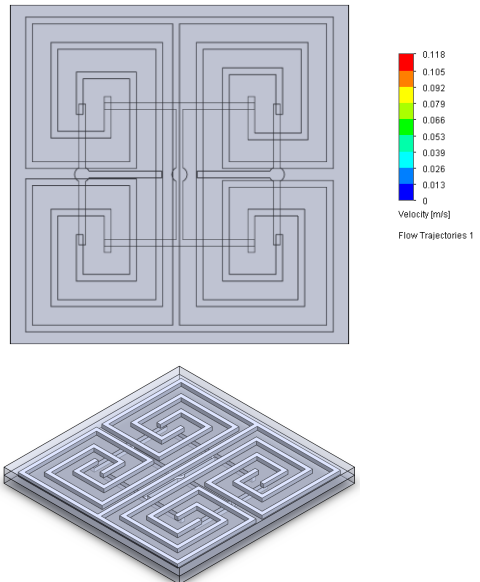
Concept 7



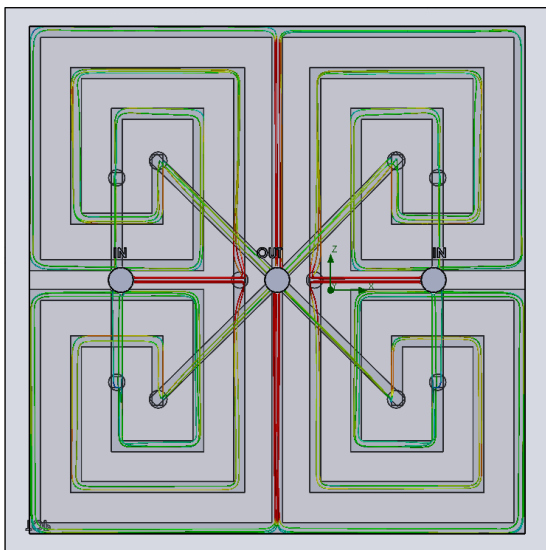
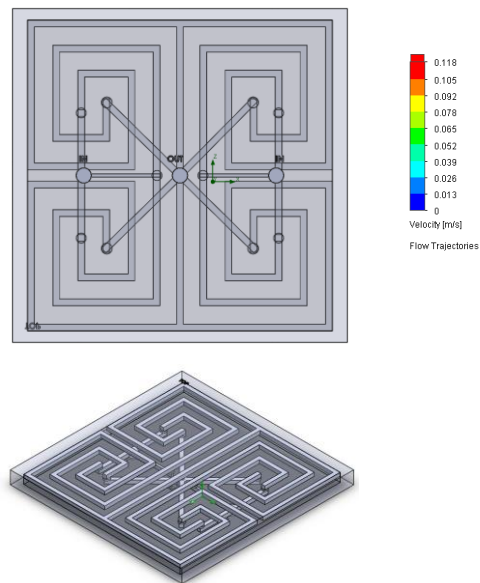
Concept 8



Concept 9



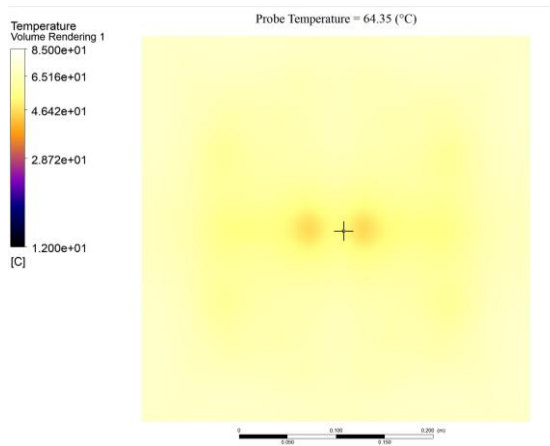
Concept 10



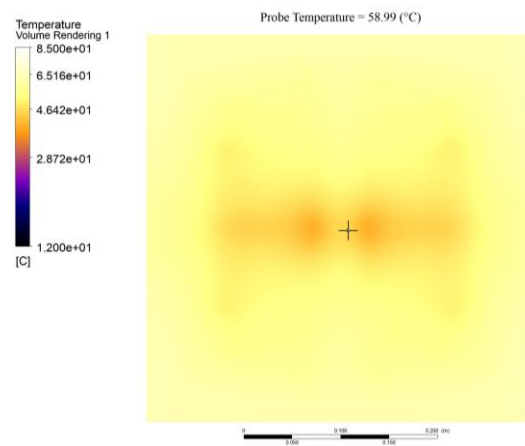
Concept 11

Appendix C

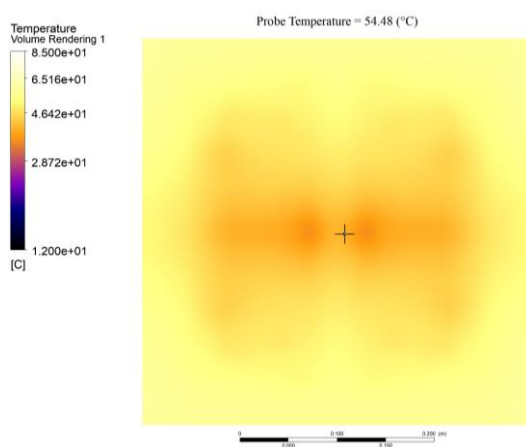
Simulation completed on Ansys with the final concept/cooling channel layout in the base to determine the shape of cooling on the top surface of the base.



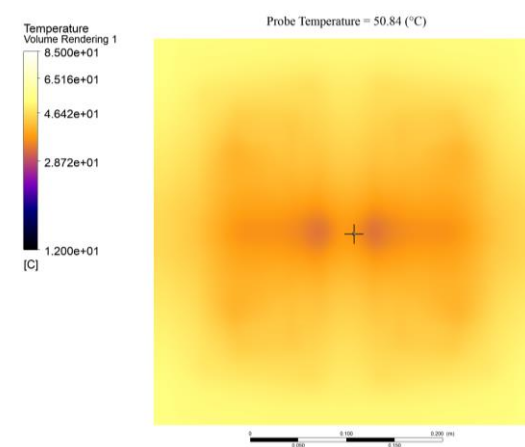
Time = 0 s; Temp = 64.4 °C



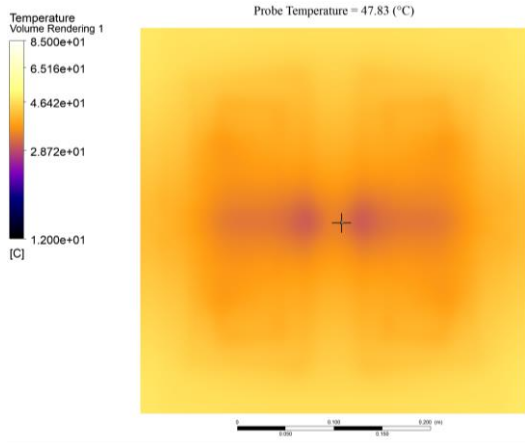
Time = 20 s; Temp = 59.0 °C



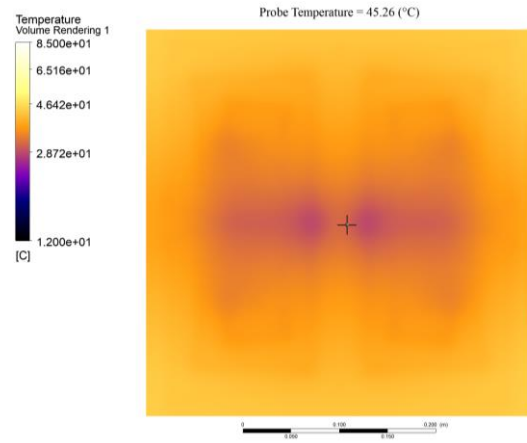
Time = 40 s; Temp = 54.5 °C



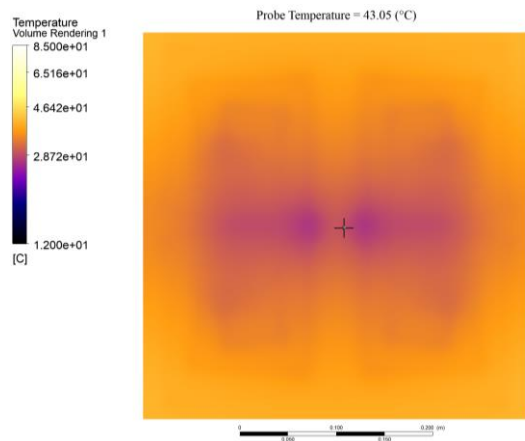
Time = 60 s; Temp = 50.8 °C



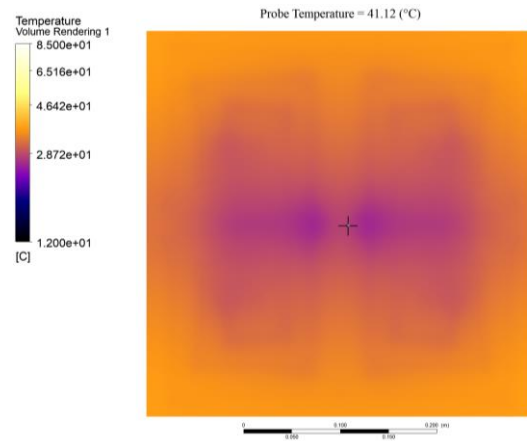
Time = 80 s; Temp = 47.8 °C



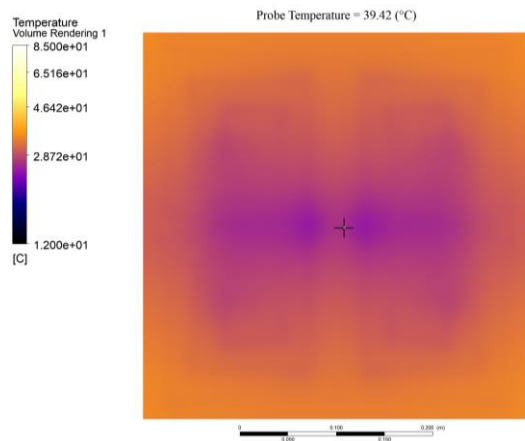
Time = 100 s; Temp = 45.3 °C



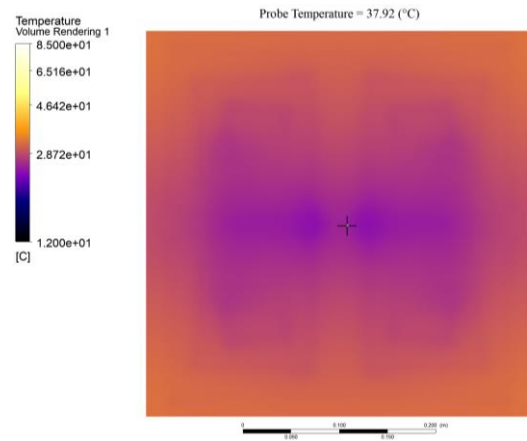
Time = 120 s; Temp = 43.0 °C



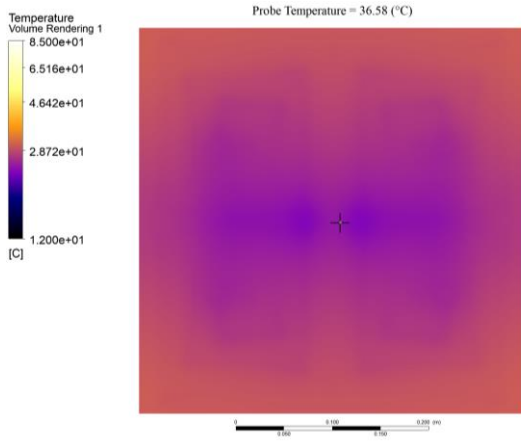
Time = 140 s; Temp = 41.1 °C



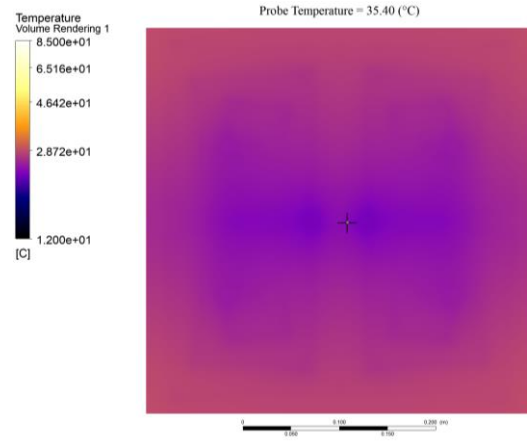
Time = 160 s; Temp = 39.4 °C



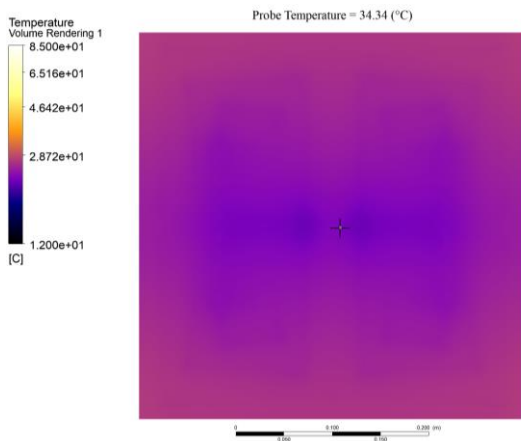
Time = 180 s; Temp = 37.9 °C



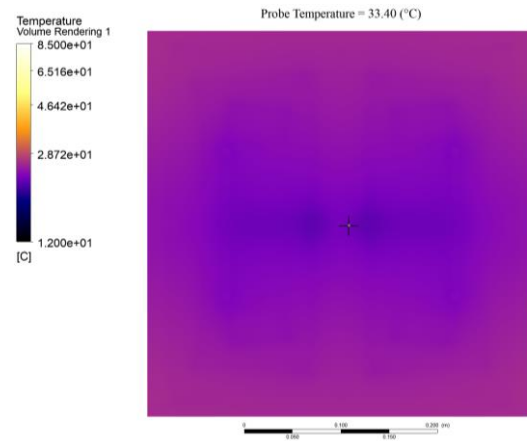
Time = 200 s; Temp = 36.6 °C



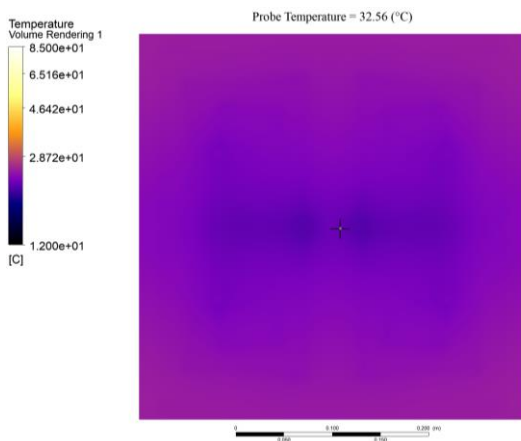
Time = 220 s; Temp = 35.4 °C



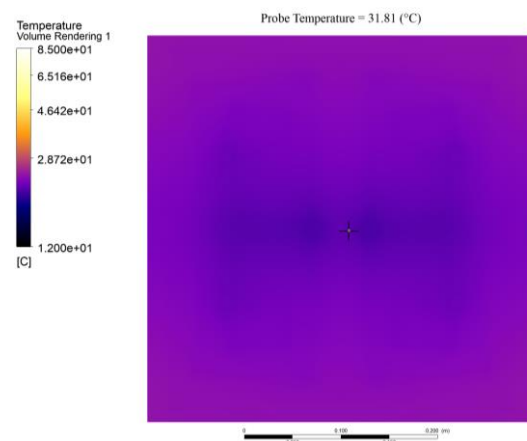
Time = 240 s; Temp = 34.3 °C



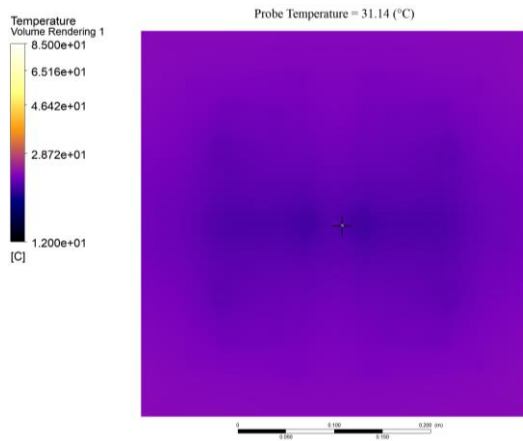
Time = 260 s; Temp = 33.4 °C



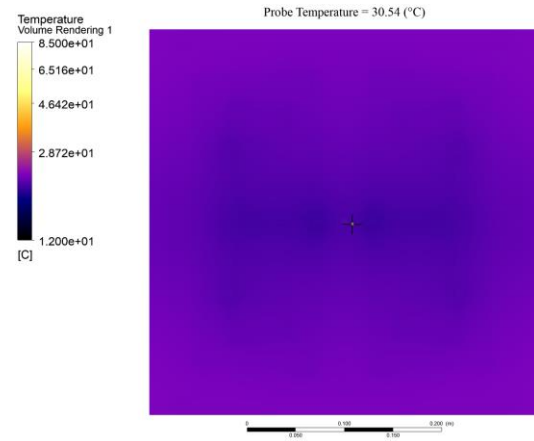
Time = 280 s; Temp = 32.6 °C



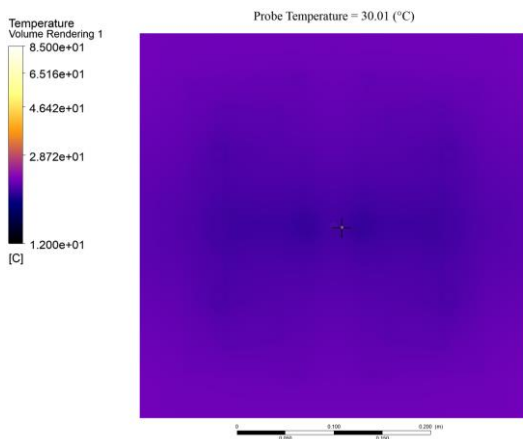
Time = 300 s; Temp = 31.8 °C



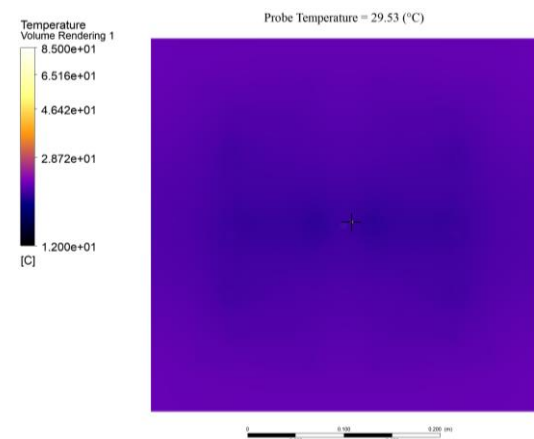
Time = 320 s; Temp = 31.1 °C



Time = 340 s; Temp = 30.5 °C



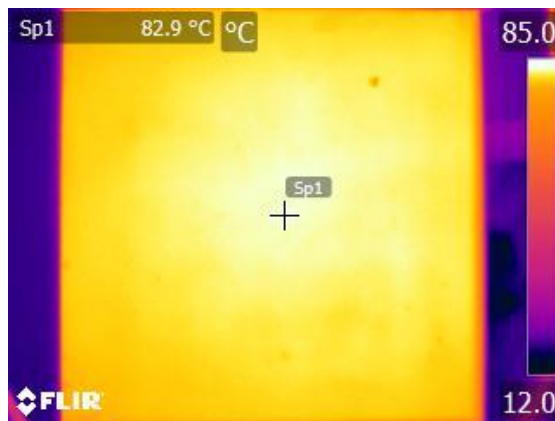
Time = 360 s; Temp = 30.0 °C



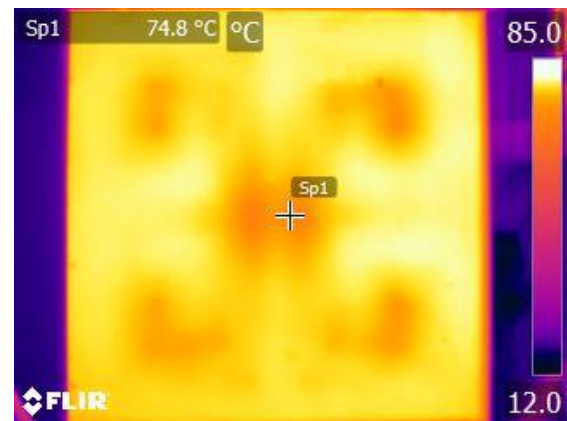
Time = 380 s; Temp = 29.5 °C

Appendix D

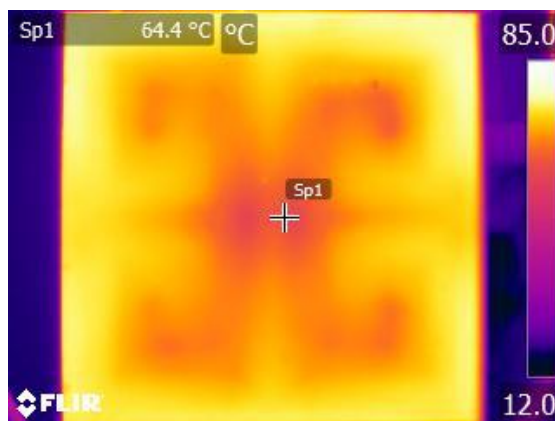
Infra-Red (IR) images of the final base design, taken at 20-second intervals with a FLIR E60 camera.



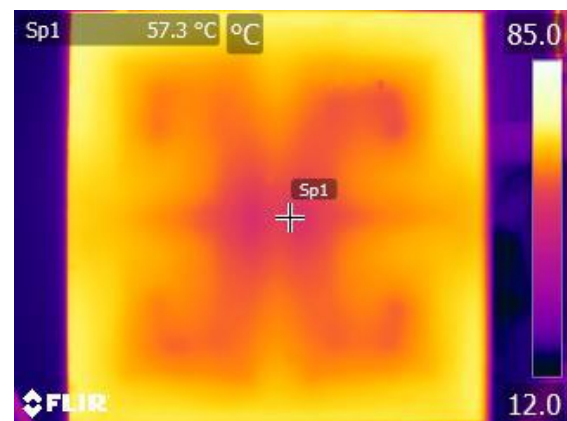
Time = 0 s; Temp = 82.9 °C



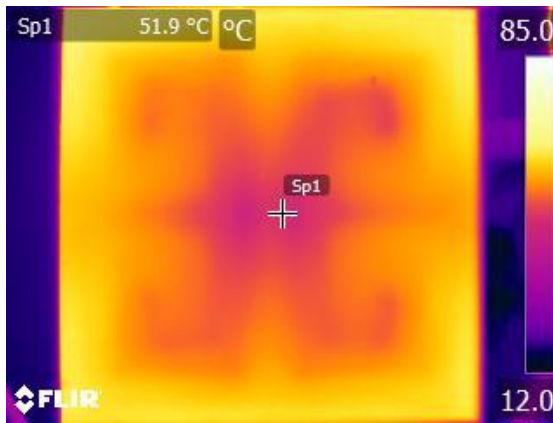
Time = 20 s; Temp = 74.8 °C



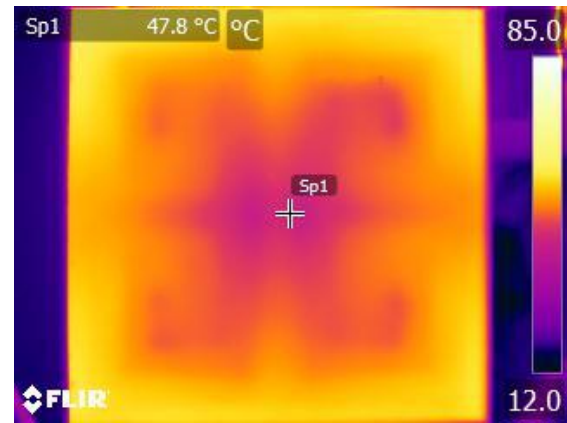
Time = 40 s; Temp = 64.4 °C



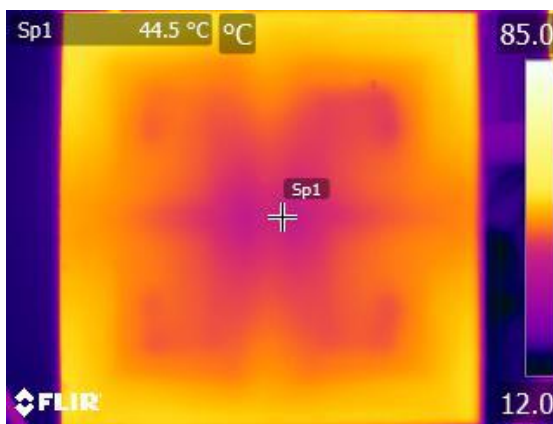
Time = 60 s; Temp = 57.3 °C



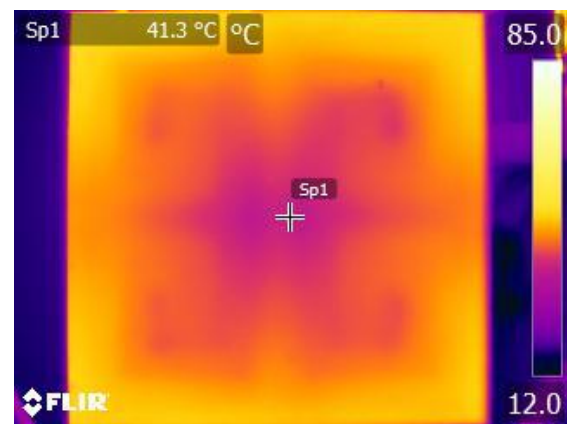
Time = 80 s; Temp = 51.9 °C



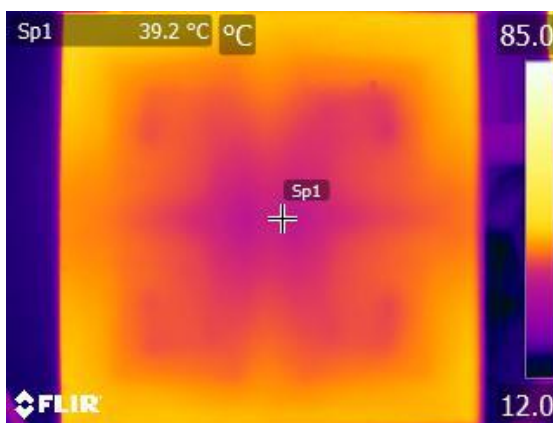
Time = 100 s; Temp = 47.8 °C



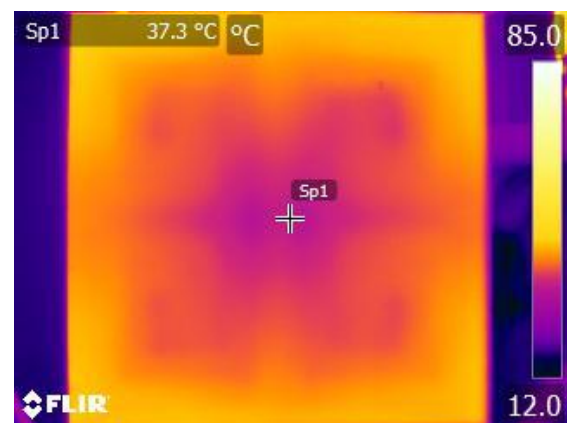
Time = 120 s; Temp = 44.5 °C



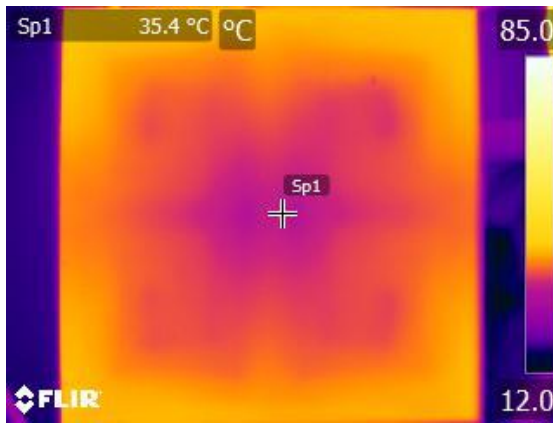
Time = 140 s; Temp = 41.3 °C



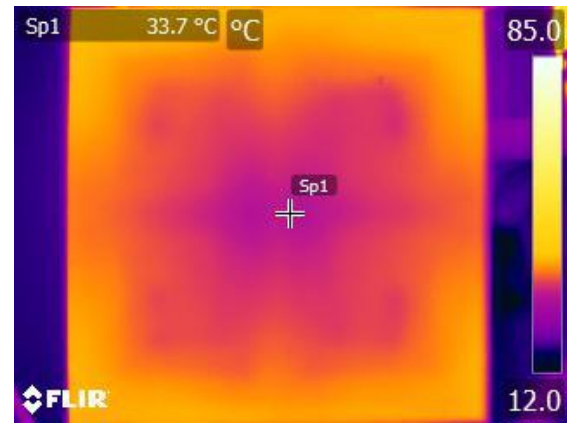
Time = 160 s; Temp = 39.2 °C



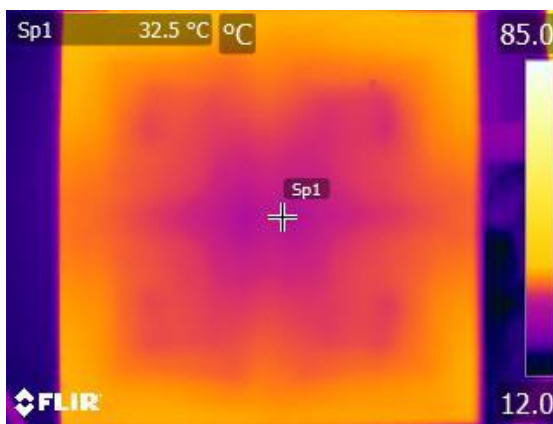
Time = 180 s; Temp = 37.3 °C



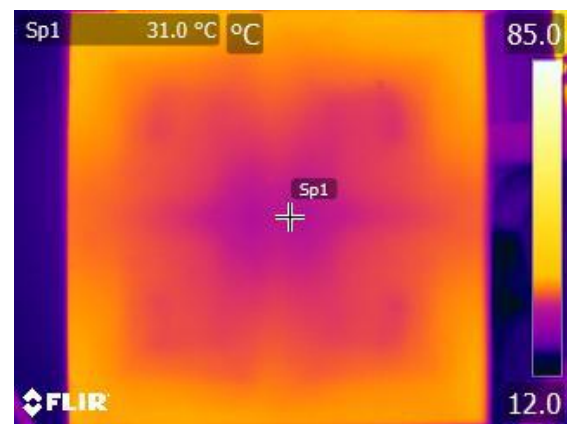
Time = 200 s; Temp = 35.4 °C



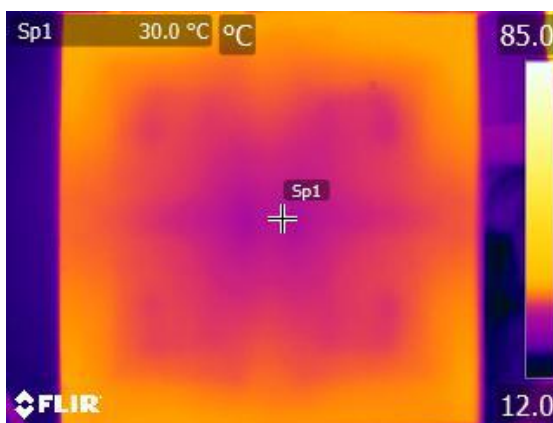
Time = 220 s; Temp = 33.7 °C



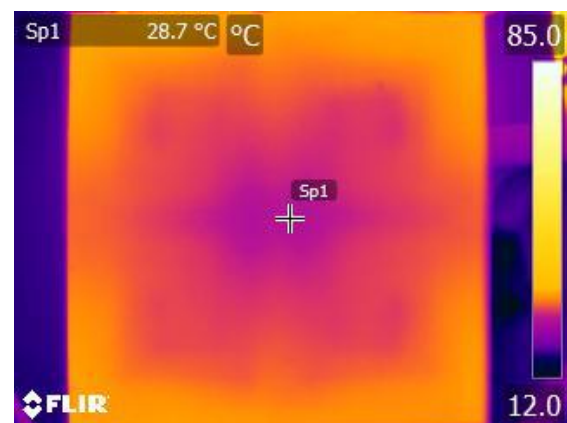
Time = 240 s; Temp = 32.5 °C



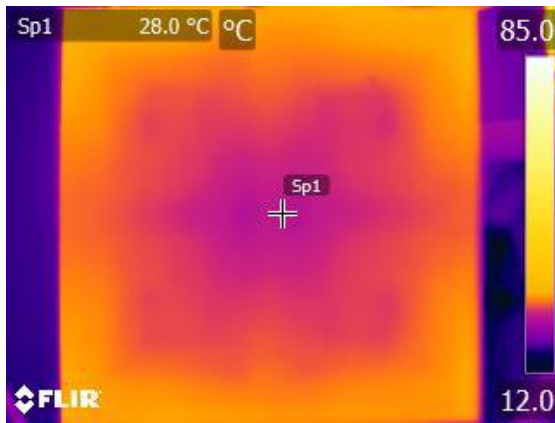
Time = 260 s; Temp = 31.0 °C



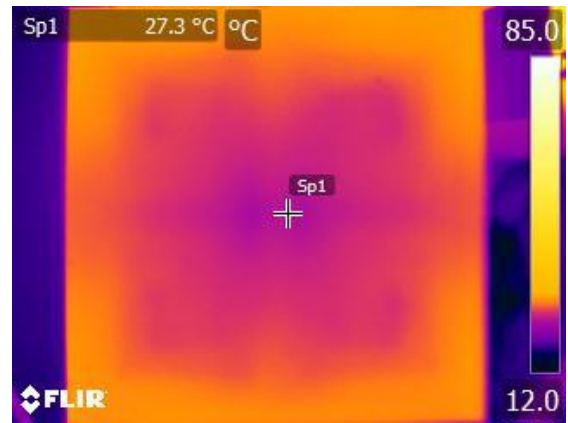
Time = 280 s; Temp = 30.0 °C



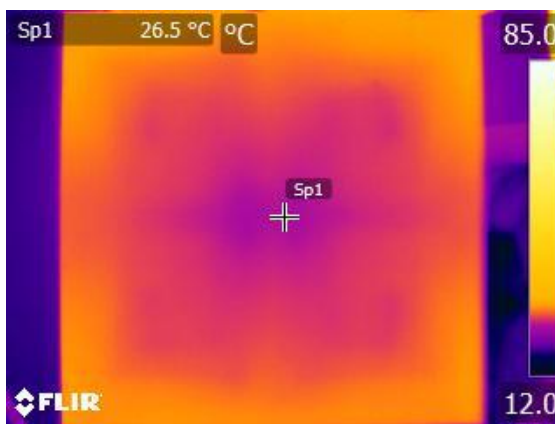
Time = 300 s; Temp = 28.7 °C



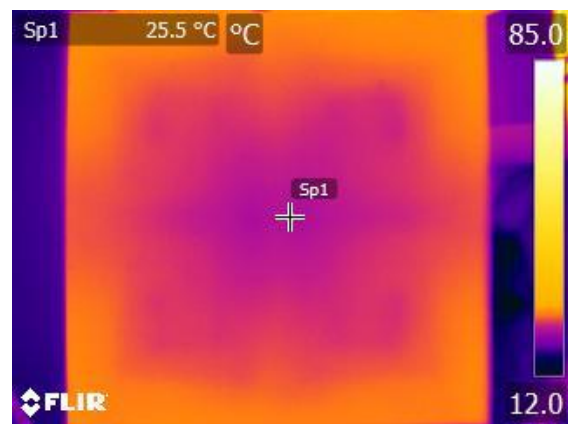
Time = 320 s; Temp = 28.0 °C



Time = 340 s; Temp = 27.3 °C



Time = 360 s; Temp = 26.5 °C



Time = 380 s; Temp = 25.5 °C

Appendix E

Jig and end-frame measurements before and after casting on the commercial Aktina jig. All dimensions are indicated in mm.

| 103 mm x 103 mm Jig size | | | | | | | |
|---------------------------|--------|----|--------|-----------|---|--------|--------------|
| 30 mm x 30 mm Portal size | | | | | | | |
| | Jig | | Frame | Expansion | | Portal | Border Width |
| A | 104.06 | AA | 104.61 | 0.55 | 1 | 30.16 | 36.95 |
| B | 104.3 | BB | 104.79 | 0.49 | 2 | 30.25 | 37.03 |
| C | 104.09 | CC | 104.45 | 0.36 | 3 | 30.2 | 36.95 |
| D | 104.26 | DD | 104.79 | 0.53 | 4 | 30.19 | 37.04 |
| E | 104.45 | EE | 104.95 | 0.5 | 5 | 30.22 | 37.12 |
| F | 104.3 | FF | 104.71 | 0.41 | 6 | 30.19 | 37.06 |
| | Jig | | Frame | Expansion | | Portal | Border Width |
| A | 104.13 | AA | 104.5 | 0.37 | 1 | 30.12 | 37.01 |
| B | 104.26 | BB | 104.7 | 0.44 | 2 | 30.19 | 37.04 |
| C | 104.11 | CC | 104.48 | 0.37 | 3 | 30.18 | 36.97 |
| D | 104.21 | DD | 104.68 | 0.47 | 4 | 30.16 | 37.03 |
| E | 104.37 | EE | 104.83 | 0.46 | 5 | 30.2 | 37.09 |
| F | 104.37 | FF | 104.8 | 0.43 | 6 | 30.2 | 37.09 |
| | Jig | | Frame | Expansion | | Portal | Border Width |
| A | 104.19 | AA | 104.42 | 0.23 | 1 | 30.12 | 37.04 |
| B | 104.5 | BB | 104.75 | 0.25 | 2 | 30.22 | 37.14 |
| C | 104.05 | CC | 104.39 | 0.34 | 3 | 30.19 | 36.93 |
| D | 104.23 | DD | 104.64 | 0.41 | 4 | 30.23 | 37.00 |
| E | 104.45 | EE | 104.72 | 0.27 | 5 | 30.21 | 37.12 |
| F | 104.18 | FF | 104.56 | 0.38 | 6 | 30.17 | 37.01 |
| 70 mm x 70 mm Portal size | | | | | | | |
| | Jig | | Frame | Expansion | | Portal | Border Width |
| A | 104.02 | AA | 104.3 | 0.28 | 1 | 70.16 | 16.93 |
| B | 104.3 | BB | 104.46 | 0.16 | 2 | 70.17 | 17.07 |
| C | 104.04 | CC | 104.18 | 0.14 | 3 | 70.23 | 16.91 |
| D | 104.22 | DD | 104.53 | 0.31 | 4 | 70.36 | 16.93 |
| E | 104.45 | EE | 104.57 | 0.12 | 5 | 70.38 | 17.04 |
| F | 104.3 | FF | 104.54 | 0.24 | 6 | 70.38 | 16.96 |
| | Jig | | Frame | Expansion | | Portal | Border Width |
| A | 104.12 | AA | 104.93 | 0.81 | 1 | 70.22 | 16.95 |

| | | | | | | | |
|----------|--------|-----------|--------|-------------|----------|-------|-------|
| B | 104.29 | BB | 104.81 | 0.52 | 2 | 70.22 | 17.04 |
| C | 104.72 | CC | 104.8 | 0.08 | 3 | 70.25 | 17.24 |
| D | 104.2 | DD | 104.5 | 0.3 | 4 | 70.36 | 16.92 |
| E | 104.46 | EE | 104.76 | 0.3 | 5 | 70.36 | 17.05 |
| F | 104.36 | FF | 104.52 | 0.16 | 6 | 70.36 | 17.00 |

| Jig | | Frame | | Expansion | Portal | | Border Width |
|------------|--------|--------------|--------|------------------|---------------|-------|---------------------|
| A | 104.28 | AA | 104.54 | 0.26 | 1 | 70.21 | 17.04 |
| B | 104.4 | BB | 104.65 | 0.25 | 2 | 70.23 | 17.09 |
| C | 104.27 | CC | 104.4 | 0.13 | 3 | 70.23 | 17.02 |
| D | 104.4 | DD | 104.77 | 0.37 | 4 | 70.38 | 17.01 |
| E | 104.47 | EE | 104.76 | 0.29 | 5 | 70.36 | 17.06 |
| F | 104.55 | FF | 104.78 | 0.23 | 6 | 70.37 | 17.09 |

Solid End-Frame

| Jig | | Frame | | Expansion | Portal | | Border Width |
|------------|--------|--------------|--------|------------------|---------------|---|---------------------|
| A | 104.08 | AA | 104.54 | 0.46 | 1 | 0 | 52.04 |
| B | 104.39 | BB | 104.75 | 0.36 | 2 | 0 | 52.20 |
| C | 104.12 | CC | 104.4 | 0.28 | 3 | 0 | 52.06 |
| D | 104.43 | DD | 104.69 | 0.26 | 4 | 0 | 52.22 |
| E | 104.65 | EE | 104.8 | 0.15 | 5 | 0 | 52.33 |
| F | 104.46 | FF | 104.81 | 0.35 | 6 | 0 | 52.23 |

150 mm x 150 mm Jig size

90 mm x 90 mm Portal size

| Jig | | Frame | | Expansion | Portal | | Border Width |
|------------|--------|--------------|--------|------------------|---------------|-------|---------------------|
| A | 151.42 | AA | 152.39 | 0.97 | 1 | 90.14 | 30.64 |
| B | 151.3 | BB | 151.97 | 0.67 | 2 | 90.19 | 30.56 |
| C | 150.88 | CC | 151.81 | 0.93 | 3 | 90.21 | 30.34 |
| D | 150.81 | DD | 151.63 | 0.82 | 4 | 90.12 | 30.35 |
| E | 151.07 | EE | 151.81 | 0.74 | 5 | 90.09 | 30.49 |
| F | 151.12 | FF | 152.13 | 1.01 | 6 | 90.13 | 30.50 |

| Jig | | Frame | | Expansion | Portal | | Border Width |
|------------|--------|--------------|--------|------------------|---------------|-------|---------------------|
| A | 151.71 | AA | 152.3 | 0.59 | 1 | 90.08 | 30.82 |
| B | 151.3 | BB | 151.85 | 0.55 | 2 | 90.1 | 30.60 |
| C | 151.29 | CC | 151.72 | 0.43 | 3 | 90.1 | 30.60 |
| D | 151.03 | DD | 151.62 | 0.59 | 4 | 90.09 | 30.47 |
| E | 151.29 | EE | 151.83 | 0.54 | 5 | 90.11 | 30.59 |
| F | 151.37 | FF | 152.01 | 0.64 | 6 | 90.16 | 30.61 |

| Jig | | Frame | | Expansion | Portal | | Border Width |
|------------|--------|--------------|--------|------------------|---------------|-------|---------------------|
| A | 151.76 | AA | 152.41 | 0.65 | 1 | 90.19 | 30.79 |
| B | 151.4 | BB | 152.01 | 0.61 | 2 | 90.2 | 30.60 |
| C | 151.02 | CC | 151.85 | 0.83 | 3 | 90.25 | 30.39 |
| D | 151.15 | DD | 151.77 | 0.62 | 4 | 90.11 | 30.52 |

| | | | | | | | |
|------------------------------------|--------|--------------|--------|------------------|---------------|--------|---------------------|
| E | 151.51 | EE | 151.84 | 0.33 | 5 | 90.14 | 30.69 |
| F | 151.4 | FF | 152.12 | 0.72 | 6 | 90.2 | 30.60 |
| 120 mm x 120 mm Portal size | | | | | | | |
| Jig | | Frame | | Expansion | Portal | | Border Width |
| A | 151.66 | AA | 152.21 | 0.55 | 1 | 120.11 | 15.78 |
| B | 151.36 | BB | 151.75 | 0.39 | 2 | 120.06 | 15.65 |
| C | 151.25 | CC | 151.62 | 0.37 | 3 | 120.08 | 15.59 |
| D | 151.3 | DD | 151.57 | 0.27 | 4 | 119.99 | 15.66 |
| E | 151.45 | EE | 151.64 | 0.19 | 5 | 120.02 | 15.72 |
| F | 151.42 | FF | 151.93 | 0.51 | 6 | 120.05 | 15.69 |
| 120 mm x 120 mm Portal size | | | | | | | |
| Jig | | Frame | | Expansion | Portal | | Border Width |
| A | 151.41 | AA | 152.32 | 0.91 | 1 | 120.08 | 15.67 |
| B | 151.35 | BB | 152.01 | 0.66 | 2 | 120.11 | 15.62 |
| C | 151.38 | CC | 151.77 | 0.39 | 3 | 120.06 | 15.66 |
| D | 151.25 | DD | 151.77 | 0.52 | 4 | 120.04 | 15.61 |
| E | 151.63 | EE | 151.82 | 0.19 | 5 | 120.14 | 15.75 |
| F | 151.44 | FF | 152.07 | 0.63 | 6 | 120.17 | 15.64 |
| 120 mm x 120 mm Portal size | | | | | | | |
| Jig | | Frame | | Expansion | Portal | | Border Width |
| A | 151.86 | AA | 152.39 | 0.53 | 1 | 120.02 | 15.92 |
| B | 151.64 | BB | 151.94 | 0.3 | 2 | 120 | 15.82 |
| C | 151.64 | CC | 151.9 | 0.26 | 3 | 119.96 | 15.84 |
| D | 151.39 | DD | 151.87 | 0.48 | 4 | 119.96 | 15.72 |
| E | 151.69 | EE | 151.83 | 0.14 | 5 | 120.03 | 15.83 |
| F | 151.72 | FF | 152.15 | 0.43 | 6 | 120 | 15.86 |
| Solid End-Frame | | | | | | | |
| Jig | | Frame | | Expansion | Portal | | Border Width |
| A | 151.68 | AA | 152.41 | 0.73 | 1 | 0 | 75.84 |
| B | 151.36 | BB | 152.05 | 0.69 | 2 | 0 | 75.68 |
| C | 151.14 | CC | 151.82 | 0.68 | 3 | 0 | 75.57 |
| D | 151.29 | DD | 151.8 | 0.51 | 4 | 0 | 75.65 |
| E | 151.37 | EE | 152.01 | 0.64 | 5 | 0 | 75.69 |
| F | 151.55 | FF | 152.16 | 0.61 | 6 | 0 | 75.78 |
| 200 mm x 200 mm Jig size | | | | | | | |
| 130 mm x 130 mm Portal size | | | | | | | |
| Jig | | Frame | | Expansion | Portal | | Border Width |
| A | 199.39 | AA | 200.09 | 0.7 | 1 | 130.14 | 34.63 |
| B | 199.29 | BB | 200.08 | 0.79 | 2 | 130.12 | 34.59 |
| C | 199.36 | CC | 200.32 | 0.96 | 3 | 130.09 | 34.64 |
| D | 198.54 | DD | 199.31 | 0.77 | 4 | 130.1 | 34.22 |
| E | 199.11 | EE | 199.83 | 0.72 | 5 | 130.07 | 34.52 |
| F | 199.34 | FF | 199.86 | 0.52 | 6 | 130.07 | 34.64 |

| Jig | | Frame | | Expansion | Portal | | Border Width |
|------------------------------------|--------|-------|--------|-----------|--------|--------|--------------|
| A | 199.31 | AA | 200 | 0.69 | 1 | 130.17 | 34.57 |
| B | 199.35 | BB | 199.76 | 0.41 | 2 | 130.12 | 34.62 |
| C | 199.53 | CC | 200.19 | 0.66 | 3 | 130.09 | 34.72 |
| D | 198.43 | DD | 199.27 | 0.84 | 4 | 130.13 | 34.15 |
| E | 199.17 | EE | 199.59 | 0.42 | 5 | 130.13 | 34.52 |
| F | 199.09 | FF | 199.75 | 0.66 | 6 | 130 | 34.55 |
| 170 mm x 170 mm Portal size | | | | | | | |
| Jig | | Frame | | Expansion | Portal | | Border Width |
| A | 199.4 | AA | 200.02 | 0.62 | 1 | 130.14 | 34.63 |
| B | 199.36 | BB | 199.94 | 0.58 | 2 | 130.08 | 34.64 |
| C | 199.43 | CC | 200.28 | 0.85 | 3 | 130.07 | 34.68 |
| D | 198.7 | DD | 199.38 | 0.68 | 4 | 130.16 | 34.27 |
| E | 199.19 | EE | 199.88 | 0.69 | 5 | 130.09 | 34.55 |
| F | 199.31 | FF | 199.85 | 0.54 | 6 | 130.04 | 34.64 |
| 170 mm x 170 mm Portal size | | | | | | | |
| Jig | | Frame | | Expansion | Portal | | Border Width |
| A | 198.83 | AA | 199.85 | 1.02 | 1 | 169.8 | 14.52 |
| B | 199.06 | BB | 199.44 | 0.38 | 2 | 169.69 | 14.69 |
| C | 199.07 | CC | 199.84 | 0.77 | 3 | 169.7 | 14.69 |
| D | 198.6 | DD | 198.97 | 0.37 | 4 | 169.85 | 14.38 |
| E | 198.81 | EE | 199.24 | 0.43 | 5 | 169.81 | 14.50 |
| F | 198.91 | FF | 199.62 | 0.71 | 6 | 169.82 | 14.55 |
| 170 mm x 170 mm Portal size | | | | | | | |
| Jig | | Frame | | Expansion | Portal | | Border Width |
| A | 199.29 | AA | 199.94 | 0.65 | 1 | 170.07 | 14.61 |
| B | 199.5 | BB | 199.53 | 0.03 | 2 | 169.88 | 14.81 |
| C | 199.76 | CC | 200.05 | 0.29 | 3 | 169.98 | 14.89 |
| D | 198.41 | DD | 199.1 | 0.69 | 4 | 170.13 | 14.14 |
| E | 199.33 | EE | 199.08 | -0.25 | 5 | 170.52 | 14.41 |
| F | 199.42 | FF | 199.62 | 0.2 | 6 | 170.05 | 14.69 |
| 170 mm x 170 mm Portal size | | | | | | | |
| Jig | | Frame | | Expansion | Portal | | Border Width |
| A | 199.3 | AA | 199.82 | 0.52 | 1 | 169.68 | 14.81 |
| B | 199.42 | BB | 199.58 | 0.16 | 2 | 169.88 | 14.77 |
| C | 199.37 | CC | 199.93 | 0.56 | 3 | 169.87 | 14.75 |
| D | 198.53 | DD | 199.23 | 0.7 | 4 | 169.98 | 14.28 |
| E | 198.99 | EE | 199.18 | 0.19 | 5 | 169.96 | 14.52 |
| F | 199.17 | FF | 199.6 | 0.43 | 6 | 169.97 | 14.60 |
| Solid End-Frame | | | | | | | |
| Jig | | Frame | | Expansion | Portal | | Border Width |
| A | 199.12 | AA | 199.91 | 0.79 | 1 | 0 | 99.56 |
| B | 199.04 | BB | 199.96 | 0.92 | 2 | 0 | 99.52 |
| C | 199.12 | CC | 199.99 | 0.87 | 3 | 0 | 99.56 |

| | | | | | | | |
|----------|--------|-----------|--------|-------------|----------|---|-------|
| D | 198.17 | DD | 199.12 | 0.95 | 4 | 0 | 99.09 |
| E | 199.03 | EE | 199.62 | 0.59 | 5 | 0 | 99.52 |
| F | 199.06 | FF | 199.72 | 0.66 | 6 | 0 | 99.53 |

Jig and end-frame measurements before and after casting on the new jig. All dimensions displayed in mm.

| 90 mm x 90 mm Jig size | | | | | | | |
|---------------------------|-------|-----------|-------|-------------|----------|-------|--------------|
| 30 mm x 30 mm Portal size | | | | | | | |
| Jig | | Frame | | Expansion | Portal | | Border Width |
| A | 89.22 | AA | 89.37 | 0.15 | 1 | 30.14 | 29.54 |
| B | 89.28 | BB | 89.43 | 0.15 | 2 | 30.15 | 29.57 |
| C | 89.29 | CC | 89.5 | 0.21 | 3 | 30.15 | 29.57 |
| D | 90.2 | DD | 90.57 | 0.37 | 4 | 30.14 | 30.03 |
| E | 90.17 | EE | 90.42 | 0.25 | 5 | 30.14 | 30.02 |
| F | 90.27 | FF | 90.44 | 0.17 | 6 | 30.14 | 30.07 |
| Jig | | Frame | | Expansion | Portal | | Border Width |
| A | 89.2 | AA | 89.32 | 0.12 | 1 | 30.15 | 29.53 |
| B | 89.2 | BB | 89.35 | 0.15 | 2 | 30.14 | 29.53 |
| C | 89.22 | CC | 89.38 | 0.16 | 3 | 30.14 | 29.54 |
| D | 90.37 | DD | 90.61 | 0.24 | 4 | 30.14 | 30.12 |
| E | 90.23 | EE | 90.47 | 0.24 | 5 | 30.14 | 30.05 |
| F | 90.31 | FF | 90.51 | 0.2 | 6 | 30.14 | 30.09 |
| Jig | | Frame | | Expansion | Portal | | Border Width |
| A | 89.21 | AA | 89.44 | 0.23 | 1 | 30.14 | 29.54 |
| B | 89.21 | BB | 89.62 | 0.41 | 2 | 30.13 | 29.54 |
| C | 89.23 | CC | 89.58 | 0.35 | 3 | 30.13 | 29.55 |
| D | 90.23 | DD | 90.64 | 0.41 | 4 | 30.11 | 30.06 |
| E | 90.25 | EE | 90.57 | 0.32 | 5 | 30.13 | 30.06 |
| F | 90.2 | FF | 90.53 | 0.33 | 6 | 30.13 | 30.04 |
| 60 mm x 60 mm Portal size | | | | | | | |
| Jig | | Frame | | Expansion | Portal | | Border Width |
| A | 90.31 | AA | 90.57 | 0.26 | 1 | 59.68 | 15.32 |
| B | 90.3 | BB | 90.52 | 0.22 | 2 | 59.63 | 15.34 |
| C | 90.33 | CC | 90.52 | 0.19 | 3 | 59.56 | 15.39 |
| D | 89.27 | DD | 89.56 | 0.29 | 4 | 60.02 | 14.63 |
| E | 89.27 | EE | 89.48 | 0.21 | 5 | 60.04 | 14.62 |
| F | 89.26 | FF | 89.52 | 0.26 | 6 | 60.01 | 14.63 |
| Jig | | Frame | | Expansion | Portal | | Border Width |
| A | 88.86 | AA | 89.14 | 0.28 | 1 | 59.64 | 14.61 |

| | | | | | | | |
|----------------------------------|--------|-----------|--------|-------------|----------|-------|-------|
| B | 89.05 | BB | 89.18 | 0.13 | 2 | 59.61 | 14.72 |
| C | 88.83 | CC | 89.19 | 0.36 | 3 | 59.57 | 14.63 |
| D | 90.51 | DD | 90.66 | 0.15 | 4 | 60.03 | 15.24 |
| E | 90.42 | EE | 90.6 | 0.18 | 5 | 60.03 | 15.20 |
| F | 90.45 | FF | 90.57 | 0.12 | 6 | 60.02 | 15.22 |
| Jig | | | | | | | |
| A | 89.03 | AA | 89.37 | 0.34 | 1 | 59.65 | 14.69 |
| B | 89.02 | BB | 89.4 | 0.38 | 2 | 59.59 | 14.72 |
| C | 89.06 | CC | 89.47 | 0.41 | 3 | 59.55 | 14.76 |
| D | 90.44 | DD | 90.56 | 0.12 | 4 | 60.01 | 15.22 |
| E | 90.36 | EE | 90.42 | 0.06 | 5 | 60.01 | 15.18 |
| F | 90.48 | FF | 90.59 | 0.11 | 6 | 60.01 | 15.24 |
| Solid End-Frame | | | | | | | |
| A | 89.05 | AA | 89.35 | 0.3 | 1 | 0 | 44.53 |
| B | 89.07 | BB | 89.36 | 0.29 | 2 | 0 | 44.54 |
| C | 89.21 | CC | 89.36 | 0.15 | 3 | 0 | 44.61 |
| D | 90.49 | DD | 90.72 | 0.23 | 4 | 0 | 45.25 |
| E | 90.43 | EE | 90.71 | 0.28 | 5 | 0 | 45.22 |
| F | 90.4 | FF | 90.75 | 0.35 | 6 | 0 | 45.20 |
| 130 mm x 130 mm Jig size | | | | | | | |
| 70 mm x 70 mm Portal size | | | | | | | |
| A | 130.12 | AA | 130.43 | 0.31 | 1 | 70.22 | 29.95 |
| B | 130.08 | BB | 130.55 | 0.47 | 2 | 70.24 | 29.92 |
| C | 130.22 | CC | 130.56 | 0.34 | 3 | 70.22 | 30.00 |
| D | 129.03 | DD | 129.21 | 0.18 | 4 | 70.34 | 29.35 |
| E | 129.08 | EE | 129.43 | 0.35 | 5 | 70.34 | 29.37 |
| F | 129.11 | FF | 129.38 | 0.27 | 6 | 70.34 | 29.39 |
| Jig | | | | | | | |
| A | 130.2 | AA | 130.43 | 0.23 | 1 | 70.21 | 30.00 |
| B | 130.2 | BB | 130.41 | 0.21 | 2 | 70.21 | 30.00 |
| C | 130.22 | CC | 130.43 | 0.21 | 3 | 70.25 | 29.99 |
| D | 129 | DD | 129.37 | 0.37 | 4 | 70.34 | 29.33 |
| E | 129.08 | EE | 129.34 | 0.26 | 5 | 70.36 | 29.36 |
| F | 129.17 | FF | 129.29 | 0.12 | 6 | 70.31 | 29.43 |
| Jig | | | | | | | |
| A | 129.09 | AA | 129.19 | 0.1 | 1 | 70.15 | 29.47 |
| B | 129.1 | BB | 129.22 | 0.12 | 2 | 70.16 | 29.47 |
| C | 129.02 | CC | 129.26 | 0.24 | 3 | 70.16 | 29.43 |
| D | 130.17 | DD | 130.36 | 0.19 | 4 | 70.27 | 29.95 |

| | | | | | | | |
|----------------------------------|--------|--------------|--------|------------------|---------------|-------|---------------------|
| E | 130.14 | EE | 130.38 | 0.24 | 5 | 70.27 | 29.94 |
| F | 130.11 | FF | 130.26 | 0.15 | 6 | 70.25 | 29.93 |
| 90 mm x 90 mm Portal size | | | | | | | |
| Jig | | Frame | | Expansion | Portal | | Border Width |
| A | 129.1 | AA | 129.18 | 0.08 | 1 | 90.13 | 19.49 |
| B | 129.11 | BB | 129.27 | 0.16 | 2 | 90.11 | 19.50 |
| C | 129.08 | CC | 129.23 | 0.15 | 3 | 90.13 | 19.48 |
| D | 130.13 | DD | 130.39 | 0.26 | 4 | 90.07 | 20.03 |
| E | 130.19 | EE | 130.36 | 0.17 | 5 | 90.01 | 20.09 |
| F | 130.06 | FF | 130.28 | 0.22 | 6 | 90.06 | 20.00 |
| 90 mm x 90 mm Portal size | | | | | | | |
| Jig | | Frame | | Expansion | Portal | | Border Width |
| A | 129.11 | AA | 129.14 | 0.03 | 1 | 90.07 | 19.52 |
| B | 129.11 | BB | 129.23 | 0.12 | 2 | 90.1 | 19.51 |
| C | 129.08 | CC | 129.24 | 0.16 | 3 | 90.09 | 19.50 |
| D | 130.19 | DD | 130.21 | 0.02 | 4 | 90.08 | 20.06 |
| E | 130.2 | EE | 130.26 | 0.06 | 5 | 90.1 | 20.05 |
| F | 130.17 | FF | 130.27 | 0.1 | 6 | 90.04 | 20.07 |
| 90 mm x 90 mm Portal size | | | | | | | |
| Jig | | Frame | | Expansion | Portal | | Border Width |
| A | 129.14 | AA | 129.19 | 0.05 | 1 | 90.08 | 19.53 |
| B | 129.15 | BB | 129.2 | 0.05 | 2 | 90.12 | 19.52 |
| C | 129.09 | CC | 129.13 | 0.04 | 3 | 90.13 | 19.48 |
| D | 130.15 | DD | 130.29 | 0.14 | 4 | 90.1 | 20.03 |
| E | 130.19 | EE | 130.26 | 0.07 | 5 | 90.11 | 20.04 |
| F | 130.07 | FF | 130.25 | 0.18 | 6 | 90.12 | 19.98 |
| Solid End-Frame | | | | | | | |
| Jig | | Frame | | Expansion | Portal | | Border Width |
| A | 129.16 | AA | 129.27 | 0.11 | 1 | 0 | 64.58 |
| B | 129.12 | BB | 129.3 | 0.18 | 2 | 0 | 64.56 |
| C | 129.11 | CC | 129.41 | 0.3 | 3 | 0 | 64.56 |
| D | 130.17 | DD | 130.55 | 0.38 | 4 | 0 | 65.09 |
| E | 130.16 | EE | 130.58 | 0.42 | 5 | 0 | 65.08 |
| F | 130.16 | FF | 130.58 | 0.42 | 6 | 0 | 65.08 |
| 170 mm x 170 mm Jig size | | | | | | | |
| 90 mm x 90 mm Portal size | | | | | | | |
| Jig | | Frame | | Expansion | Portal | | Border Width |
| A | 169.01 | AA | 169.32 | 0.31 | 1 | 90.13 | 39.44 |
| B | 168.95 | BB | 169.38 | 0.43 | 2 | 90.11 | 39.42 |
| C | 168.84 | CC | 169.3 | 0.46 | 3 | 90.13 | 39.36 |
| D | 170.48 | DD | 170.94 | 0.46 | 4 | 90.07 | 40.21 |
| E | 170.5 | EE | 170.89 | 0.39 | 5 | 90.01 | 40.25 |
| F | 170.48 | FF | 170.75 | 0.27 | 6 | 90.06 | 40.21 |

| Jig | | Frame | | Expansion | Portal | | Border Width |
|------------------------------------|--------|-----------|--------|-------------|----------|--------|--------------|
| A | 169.2 | AA | 169.28 | 0.08 | 1 | 90.08 | 39.56 |
| B | 169.06 | BB | 169.35 | 0.29 | 2 | 90.1 | 39.48 |
| C | 168.93 | CC | 169.28 | 0.35 | 3 | 90.12 | 39.41 |
| D | 170.28 | DD | 170.67 | 0.39 | 4 | 90.06 | 40.11 |
| E | 170.38 | EE | 170.75 | 0.37 | 5 | 90.11 | 40.14 |
| F | 170.27 | FF | 170.57 | 0.3 | 6 | 90.11 | 40.08 |
| 130 mm x 130 mm Portal size | | | | | | | |
| Jig | | Frame | | Expansion | Portal | | Border Width |
| A | 169.07 | AA | 169.22 | 0.15 | 1 | 90.07 | 39.50 |
| B | 168.95 | BB | 169.27 | 0.32 | 2 | 90.1 | 39.43 |
| C | 168.83 | CC | 169.1 | 0.27 | 3 | 90.12 | 39.36 |
| D | 170.47 | DD | 170.84 | 0.37 | 4 | 90.08 | 40.20 |
| E | 170.46 | EE | 170.75 | 0.29 | 5 | 90.09 | 40.19 |
| F | 170.47 | FF | 170.73 | 0.26 | 6 | 90.11 | 40.18 |
| 130 mm x 130 mm Portal size | | | | | | | |
| Jig | | Frame | | Expansion | Portal | | Border Width |
| A | 169.05 | AA | 169.17 | 0.12 | 1 | 130.08 | 19.49 |
| B | 168.92 | BB | 169.09 | 0.17 | 2 | 130.03 | 19.45 |
| C | 168.78 | CC | 168.96 | 0.18 | 3 | 130.04 | 19.37 |
| D | 170.46 | DD | 170.72 | 0.26 | 4 | 130.1 | 20.18 |
| E | 170.47 | EE | 170.7 | 0.23 | 5 | 130.03 | 20.22 |
| F | 170.47 | FF | 170.66 | 0.19 | 6 | 130.01 | 20.23 |
| 130 mm x 130 mm Portal size | | | | | | | |
| Jig | | Frame | | Expansion | Portal | | Border Width |
| A | 169.16 | AA | 169.23 | 0.07 | 1 | 130.1 | 19.53 |
| B | 169.06 | BB | 169.25 | 0.19 | 2 | 130.03 | 19.52 |
| C | 168.91 | CC | 169.09 | 0.18 | 3 | 129.99 | 19.46 |
| D | 170.34 | DD | 170.67 | 0.33 | 4 | 130.09 | 20.13 |
| E | 170.33 | EE | 170.69 | 0.36 | 5 | 130.01 | 20.16 |
| F | 170.43 | FF | 170.66 | 0.23 | 6 | 129.98 | 20.23 |
| 130 mm x 130 mm Portal size | | | | | | | |
| Jig | | Frame | | Expansion | Portal | | Border Width |
| A | 169.2 | AA | 169.39 | 0.19 | 1 | 130.08 | 19.56 |
| B | 169.08 | BB | 169.31 | 0.23 | 2 | 130.08 | 19.50 |
| C | 168.91 | CC | 169.16 | 0.25 | 3 | 130.04 | 19.44 |
| D | 170.37 | DD | 170.73 | 0.36 | 4 | 130.05 | 20.16 |
| E | 170.35 | EE | 170.69 | 0.34 | 5 | 130 | 20.18 |
| F | 170.34 | FF | 170.59 | 0.25 | 6 | 129.96 | 20.19 |
| Solid End-Frame | | | | | | | |
| Jig | | Frame | | Expansion | Portal | | Border Width |
| A | 169.16 | AA | 169.44 | 0.28 | 1 | 0 | 84.58 |
| B | 169.03 | BB | 169.49 | 0.46 | 2 | 0 | 84.52 |
| C | 169.07 | CC | 169.46 | 0.39 | 3 | 0 | 84.54 |

| | | | | | | | |
|----------|--------|-----------|--------|-------------|----------|---|-------|
| D | 170.4 | DD | 170.84 | 0.44 | 4 | 0 | 85.20 |
| E | 170.42 | EE | 170.82 | 0.4 | 5 | 0 | 85.21 |
| F | 170.41 | FF | 170.75 | 0.34 | 6 | 0 | 85.21 |

Appendix F

Temperature measurements taken during the cooling rate experiment.

Readings in tables below are given for every minute.

| Fast Cool on New Jig | | |
|----------------------|-----------|-------------|
| Time (0) | Heat (°C) | Time (Min) |
| 0 | 71.091723 | 0 |
| 60.550463 | 66.792556 | 1.009174383 |
| 120.594897 | 65.299815 | 2.00991495 |
| 180.056298 | 65.404281 | 3.0009383 |
| 240.92878 | 63.373518 | 4.015479667 |
| 300.880209 | 59.023867 | 5.01467015 |
| 360.86664 | 50.929084 | 6.014444 |
| 419.981022 | 45.1186 | 6.9996837 |
| 480.967509 | 40.088975 | 8.01612515 |
| 540.858935 | 36.16885 | 9.014315583 |
| 600.773362 | 33.267448 | 10.01288937 |
| 660.591784 | 31.335603 | 11.00986307 |
| 720.384204 | 29.917485 | 12.0064034 |
| 780.184624 | 28.799423 | 13.00307707 |
| 840.670083 | 28.015329 | 14.01116805 |
| 900.624513 | 27.145943 | 15.01040855 |
| 960.677948 | 26.283182 | 16.01129913 |
| 1020.594374 | 25.741369 | 17.00990623 |
| 1080.444798 | 24.977491 | 18.0074133 |
| 1140.041207 | 24.664109 | 19.00068678 |
| 1200.870686 | 25.201736 | 20.01451143 |
| 1260.765112 | 26.963783 | 21.01275187 |
| 1320.830547 | 29.263629 | 22.01384245 |
| 1380.67497 | 32.006065 | 23.0112495 |
| 1440.541394 | 35.002579 | 24.00902323 |

| | | |
|-------------|-----------|-------------|
| 1500.44682 | 38.041402 | 25.007447 |
| 1560.317245 | 41.312256 | 26.00528742 |
| 1620.246673 | 44.212142 | 27.00411122 |
| 1680.1671 | 47.373164 | 28.002785 |
| 1740.432547 | 50.371996 | 29.00720912 |
| 1800.373975 | 53.017359 | 30.00623292 |
| 1860.368407 | 56.098818 | 31.00614012 |
| 1920.460844 | 59.72723 | 32.00768073 |
| 1980.35327 | 63.373518 | 33.00588783 |
| 2025.924876 | 66.144711 | 33.7654146 |

| Slow Cool on New Jig | | |
|----------------------|-----------|-------------|
| Time (0) | Heat (°C) | Time (Min) |
| 0 | 70.11383 | 0 |
| 59.891426 | 70.234494 | 0.998190433 |
| 119.892858 | 70.234494 | 1.9982143 |
| 179.957293 | 70.967889 | 2.999288217 |
| 239.990727 | 70.721608 | 3.99984545 |
| 299.889153 | 70.844519 | 4.99815255 |
| 359.724575 | 70.967889 | 5.995409583 |
| 419.548997 | 71.340797 | 6.992483283 |
| 480.372476 | 71.216025 | 8.006207933 |
| 540.466913 | 71.091723 | 9.007781883 |
| 600.253333 | 70.844519 | 10.00422222 |
| 660.461776 | 70.355601 | 11.00769627 |
| 720.244196 | 70.721608 | 12.00406993 |
| 780.047616 | 70.599154 | 13.0007936 |
| 839.72303 | 70.234494 | 13.99538383 |
| 899.782465 | 69.993604 | 14.99637442 |
| 959.643889 | 69.873814 | 15.99406482 |
| 1019.619319 | 69.39894 | 16.99365532 |
| 1079.564748 | 69.517022 | 17.9927458 |
| 1140.399227 | 68.930769 | 19.00665378 |

| | | |
|-------------|-----------|-------------|
| 1199.883629 | 68.469099 | 19.99806048 |
| 1259.942065 | 67.564504 | 20.99903442 |
| 1319.799488 | 66.57522 | 21.99665813 |
| 1379.861924 | 64.885137 | 22.99769873 |
| 1439.828354 | 63.176915 | 23.99713923 |
| 1500.390818 | 61.362931 | 25.00651363 |
| 1560.40825 | 59.994628 | 26.00680417 |
| 1620.457685 | 59.023867 | 27.00762808 |
| 1680.430115 | 57.825338 | 28.00716858 |
| 1740.47655 | 56.992984 | 29.0079425 |
| 1800.44198 | 55.858684 | 30.00736633 |
| 1860.212398 | 55.225841 | 31.00353997 |
| 1919.968816 | 54.680793 | 31.99948027 |
| 1980.336269 | 53.689069 | 33.00560448 |
| 2039.898676 | 52.943447 | 33.99831127 |
| 2099.784101 | 52.21202 | 34.99640168 |
| 2159.761532 | 51.636641 | 35.99602553 |
| 2219.732962 | 50.78908 | 36.99554937 |
| 2280.37043 | 50.302903 | 38.00617383 |
| 2339.881834 | 49.754395 | 38.99803057 |
| 2399.931268 | 49.079041 | 39.99885447 |
| 2459.802693 | 48.480597 | 40.99671155 |
| 2519.642115 | 47.631122 | 41.99403525 |
| 2579.572543 | 47.437506 | 42.99287572 |
| 2640.385021 | 46.861899 | 44.00641702 |
| 2700.364452 | 46.293919 | 45.0060742 |
| 2760.393886 | 45.733273 | 46.00656477 |
| 2820.205307 | 45.1186 | 47.00342178 |
| 2880.162736 | 44.814417 | 48.00271227 |
| 2940.116165 | 44.512279 | 49.00193608 |
| 3000.085595 | 43.854562 | 50.00142658 |
| 3060.165032 | 43.206102 | 51.00275053 |
| 3120.147463 | 43.089162 | 52.00245772 |

| | | |
|-------------|-----------|-------------|
| 3179.980885 | 42.624279 | 52.99968142 |
| 3239.935314 | 42.163886 | 53.9989219 |
| 3299.907744 | 41.821452 | 54.9984624 |
| 3359.640161 | 41.312256 | 55.99400268 |
| 3419.60259 | 40.808236 | 56.9933765 |
| 3479.521017 | 40.364416 | 57.99201695 |
| 3539.620455 | 40.198974 | 58.99367425 |
| 3600.498937 | 39.760375 | 60.00831562 |
| 3660.427365 | 39.542454 | 61.00712275 |
| 3720.091777 | 39.217253 | 62.00152962 |
| 3779.616182 | 38.786718 | 62.99360303 |
| 3839.627614 | 38.466054 | 63.99379357 |
| 3900.451093 | 38.200264 | 65.00751822 |
| 3960.435524 | 37.830289 | 66.00725873 |
| 4019.509903 | 37.515099 | 66.99183172 |
| 4080.29738 | 37.462738 | 68.00495633 |
| 4140.26981 | 37.045563 | 69.00449683 |
| 4200.06823 | 36.734643 | 70.00113717 |
| 4259.881652 | 36.5798 | 70.99802753 |
| 4319.624068 | 36.117679 | 71.99373447 |
| 4380.49355 | 36.066551 | 73.00822583 |
| 4440.439979 | 35.608324 | 74.00733298 |
| 4500.086391 | 35.456337 | 75.00143985 |
| 4559.972816 | 35.052835 | 75.99954693 |
| 4619.949246 | 34.801946 | 76.9991541 |
| 4679.63066 | 34.552033 | 77.99384433 |
| 4739.560087 | 34.552033 | 78.99266812 |
| 4799.512517 | 34.104582 | 79.99187528 |
| 4860.325995 | 34.203754 | 81.00543325 |
| 4920.177418 | 34.055052 | 82.00295697 |
| 4980.112847 | 33.807946 | 83.00188078 |
| 5040.212284 | 33.660115 | 84.00353807 |
| 5100.044706 | 33.169627 | 85.0007451 |

| | | |
|-------------|-----------|-------------|
| 5159.994135 | 33.071942 | 85.99990225 |
| 5219.921563 | 32.731101 | 86.99869272 |
| 5280.128006 | 27.009295 | 88.00213343 |
| 5295.350877 | 25.786434 | 88.25584795 |

| Slow Cool on Commercial Rubber Jig | | |
|------------------------------------|-----------|-------------|
| Time (0) | Heat (°C) | Time (Min) |
| 0 | 70.11383 | 0 |
| 59.776419 | 68.814749 | 0.99627365 |
| 119.788851 | 67.342128 | 1.99648085 |
| 180.663334 | 66.467076 | 3.011055567 |
| 239.639707 | 66.683713 | 3.993995117 |
| 300.202171 | 66.251824 | 5.003369517 |
| 360.570624 | 66.359278 | 6.0095104 |
| 420.12803 | 66.57522 | 7.002133833 |
| 480.577488 | 66.57522 | 8.0096248 |
| 540.090892 | 67.011307 | 9.001514867 |
| 600.55935 | 67.564504 | 10.0093225 |
| 660.639786 | 67.676248 | 11.0106631 |
| 720.438207 | 67.564504 | 12.00730345 |
| 780.29463 | 67.788367 | 13.0049105 |
| 840.044048 | 67.676248 | 14.00073413 |
| 899.957474 | 67.453132 | 14.99929123 |
| 960.010909 | 67.453132 | 16.00018182 |
| 1019.794329 | 67.011307 | 16.99657215 |
| 1079.642752 | 67.011307 | 17.99404587 |
| 1140.410228 | 67.121218 | 19.00683713 |
| 1199.790624 | 66.792556 | 19.9965104 |
| 1260.548099 | 67.011307 | 21.00913498 |
| 1320.340519 | 67.011307 | 22.00567532 |
| 1379.826922 | 66.683713 | 22.99711537 |
| 1440.145372 | 67.231491 | 24.00242287 |
| 1500.058799 | 66.792556 | 25.00097998 |

| | | |
|-------------|-----------|-------------|
| 1560.835275 | 66.683713 | 26.01392125 |
| 1620.288675 | 66.144711 | 27.00481125 |
| 1680.284107 | 66.251824 | 28.00473512 |
| 1740.171532 | 66.251824 | 29.00285887 |
| 1799.908949 | 65.614184 | 29.99848248 |
| 1860.626422 | 65.404281 | 31.01044037 |
| 1919.903812 | 64.885137 | 31.99839687 |
| 1980.612284 | 63.373518 | 33.01020473 |
| 2040.527712 | 62.401528 | 34.0087952 |
| 2100.519143 | 61.084969 | 35.00865238 |
| 2160.579578 | 59.55008 | 36.00965963 |
| 2219.758963 | 57.994129 | 36.99598272 |
| 2280.617444 | 56.502555 | 38.01029073 |
| 2340.564872 | 54.913413 | 39.00941453 |
| 2400.637309 | 53.91563 | 40.01062182 |
| 2459.640683 | 52.943447 | 40.99401138 |
| 2520.517165 | 52.21202 | 42.00861942 |
| 2580.480595 | 51.210586 | 43.00800992 |
| 2640.390022 | 50.719262 | 44.00650037 |
| 2700.391453 | 49.686353 | 45.00652422 |
| 2760.170873 | 49.21322 | 46.00284788 |
| 2820.333314 | 49.012116 | 47.00555523 |
| 2880.429751 | 48.217375 | 48.00716252 |
| 2940.417182 | 47.501946 | 49.00695303 |
| 3000.317609 | 47.244771 | 50.00529348 |
| 3059.919018 | 46.67174 | 50.9986503 |
| 3120.070458 | 46.168707 | 52.0011743 |
| 3179.89888 | 45.857242 | 52.99831467 |
| 3239.934314 | 45.302109 | 53.99890523 |
| 3299.875742 | 44.935843 | 54.99792903 |
| 3359.903176 | 44.512279 | 55.99838627 |
| 3419.683595 | 44.272011 | 56.99472658 |
| 3479.654025 | 43.913966 | 57.99423375 |

| | | |
|-------------|-----------|-------------|
| 3540.570509 | 43.440861 | 59.00950848 |
| 3600.275924 | 43.206102 | 60.00459873 |
| 3660.143348 | 42.740073 | 61.00238913 |
| 3719.952769 | 42.566488 | 61.99921282 |
| 3779.9392 | 42.393531 | 62.99898667 |
| 3839.938632 | 42.049473 | 63.9989772 |
| 3899.655048 | 41.764613 | 64.9942508 |
| 3960.491527 | 41.312256 | 66.00819212 |
| 4020.518961 | 41.087619 | 67.00864935 |
| 4080.389385 | 40.696916 | 68.00648975 |
| 4140.543825 | 40.419682 | 69.00906375 |
| 4200.514256 | 40.198974 | 70.00857093 |
| 4260.188669 | 39.924415 | 71.00314448 |
| 4320.133097 | 39.814998 | 72.00221828 |
| 4379.922517 | 39.542454 | 72.99870862 |
| 4439.774941 | 39.163246 | 73.99624902 |
| 4499.890379 | 38.894028 | 74.99817298 |
| 4559.861809 | 38.894028 | 75.99769682 |
| 4619.678231 | 38.679619 | 76.99463718 |
| 4679.795669 | 38.412793 | 77.99659448 |
| 4739.687094 | 38.359584 | 78.9947849 |
| 4800.590578 | 38.041402 | 80.00984297 |
| 4860.409 | 37.72503 | 81.00681667 |
| 4920.311426 | 37.830289 | 82.00519043 |
| 4980.085845 | 37.462738 | 83.00143075 |
| 5040.164281 | 37.253772 | 84.00273802 |
| 5100.014704 | 37.201649 | 85.00024507 |
| 5159.981134 | 36.941738 | 85.99968557 |
| 5219.786555 | 36.786348 | 86.99644258 |
| 5279.708982 | 36.786348 | 87.9951497 |
| 5339.677412 | 36.476797 | 88.99462353 |
| 5400.536893 | 36.322625 | 90.00894822 |
| 5460.557326 | 36.16885 | 91.00928877 |

| | | |
|-------------|-----------|-------------|
| 5520.41775 | 36.015467 | 92.0069625 |
| 5580.339177 | 35.913426 | 93.00565295 |
| 5639.715574 | 35.55762 | 93.99525957 |
| 5699.992021 | 35.405757 | 94.99986702 |
| 5760.482481 | 35.456337 | 96.00804135 |
| 5819.969883 | 35.203845 | 96.99949805 |
| 5880.363338 | 35.052835 | 98.00605563 |
| 5939.981747 | 34.852046 | 98.99969578 |
| 6001.75228 | 34.601938 | 100.0292047 |
| 6060.382634 | 34.751886 | 101.0063772 |
| 6119.699027 | 34.203754 | 101.9949838 |
| 6179.771463 | 34.005558 | 102.9961911 |
| 6241.196976 | 33.758633 | 104.0199496 |
| 6299.703323 | 33.807946 | 104.9950554 |
| 6362.416909 | 33.365406 | 106.0402818 |
| 6419.672184 | 33.365406 | 106.9945364 |
| 6479.976633 | 33.120768 | 107.9996106 |
| 6540.377088 | 32.974393 | 109.0062848 |
| 6574.526041 | 32.974393 | 109.575434 |

Appendix G

Images taken of the solid end-frames cast in the commercial rubber Aktina jig for the density comparison experiment.



Bottom surface of slow-cast end-frame 1



Top surface of slow-cast end-frame 1



Bottom surface of slow-cast end-frame 2



Top surface of slow-cast end-frame 2



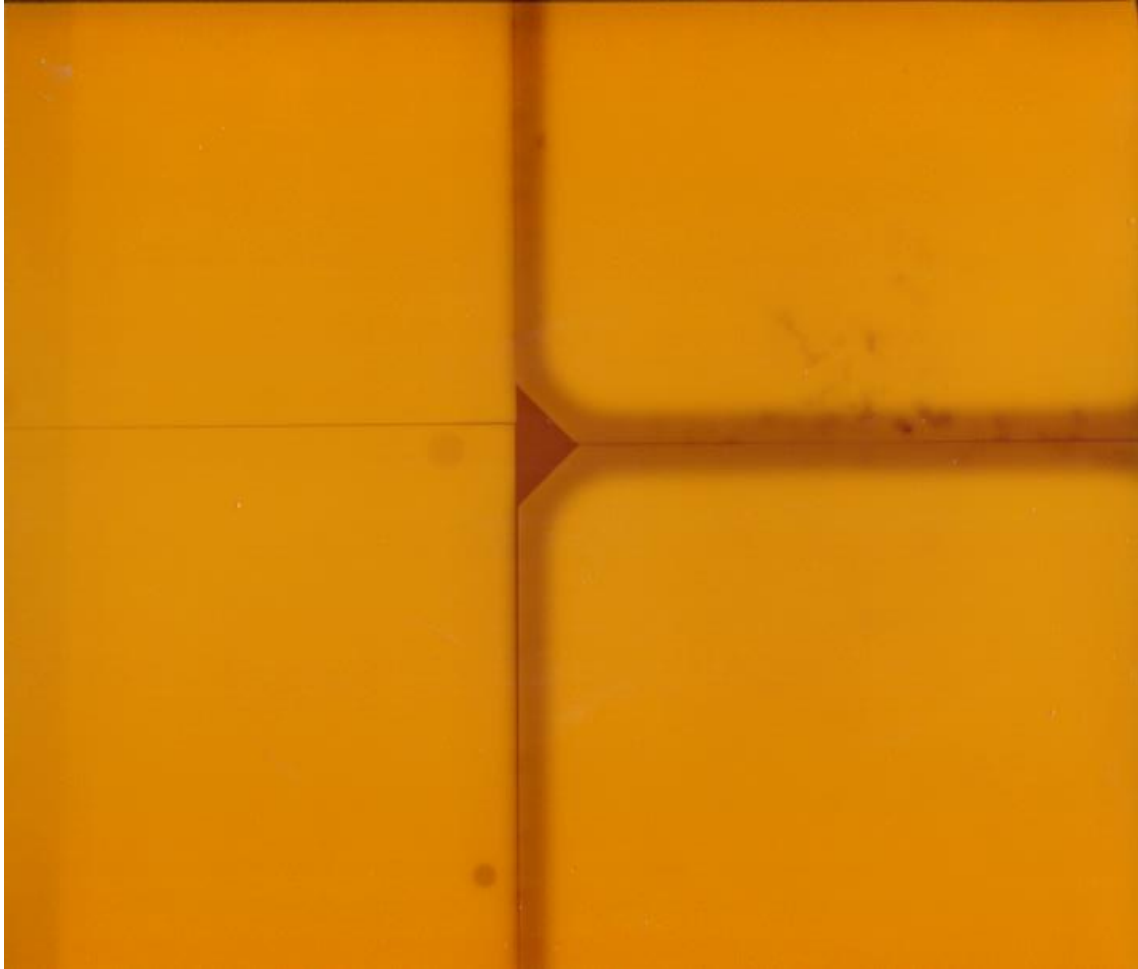
Bottom surface of slow-cast end-frame 3



Top surface of slow-cast end-frame 2

Appendix H

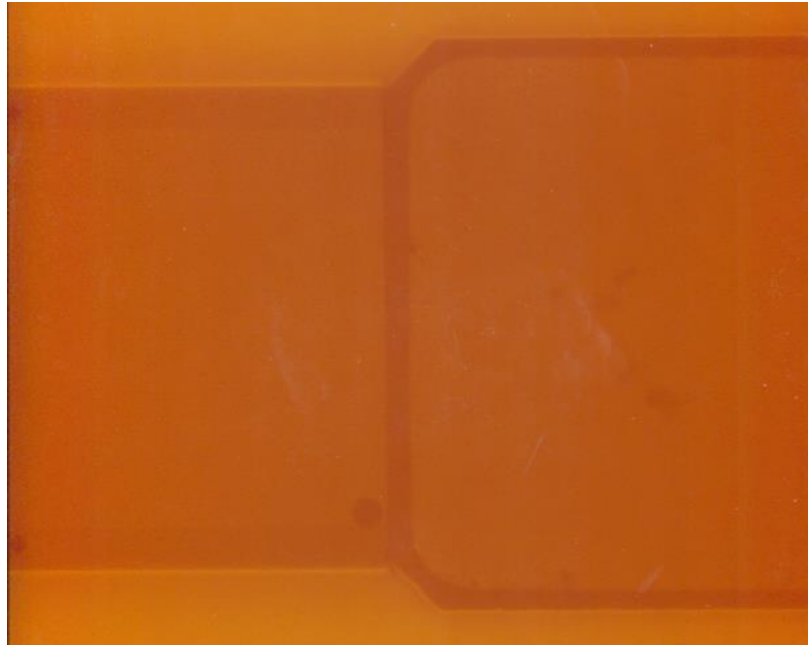
Scanned Gafchromic film of radiated end-frames using electron radiation



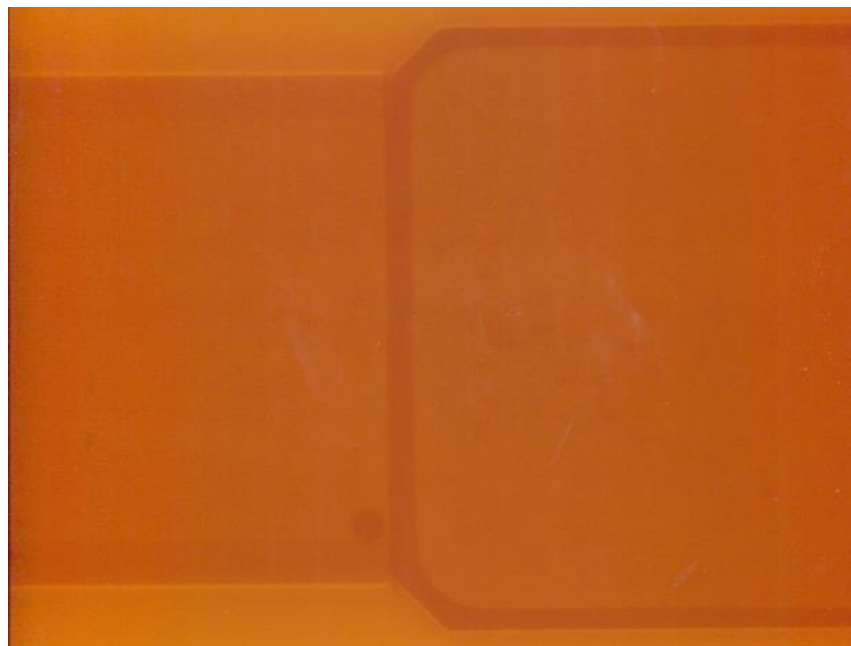
Gafchromic film of two fast-cooled end-frames (Left) and two slow-cooled end-frames (Right) radiated with electron radiation.

Appendix I

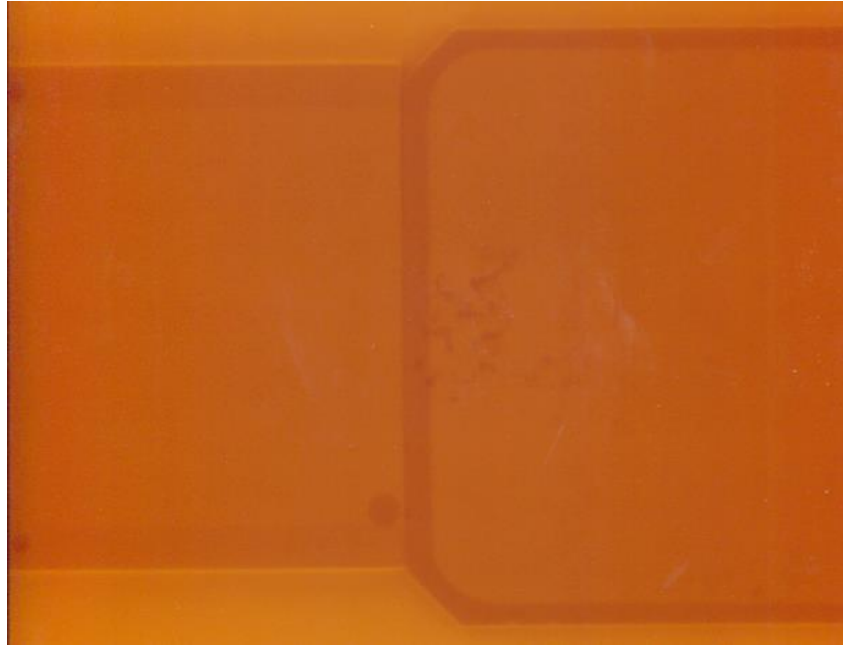
Scanned Gafchromic films of radiated end-frames using photon radiation



Gafchromic film of a fast-cooled end-frame (Left) and a slow-cooled end-frame (Right) of Set 1 radiated with photon radiation.



Gafchromic film of a fast-cooled end-frame (Left) and a slow-cooled end-frame (Right) of Set 2 radiated with photon radiation.



Gafchromic film of a fast-cooled end-frame (Left) and a slow-cooled end-frame (Right) of Set 1 radiated with photon radiation.